ISOLATION AND STRUCTURE ELUCIDATION OF ANTIPROLIFERATIVE NATURAL PRODUCTS FROM MADAGASCAR

by

Brian Thacher Murphy

Dissertation submitted to the Faculty of Virginia Polytechnic Institute and State University in partial fulfillment of the requirements for the degree of

Doctor of Philosophy

In

Chemistry

David G. I. Kingston, Chair

Paul R. Carlier

Harry W. Gibson

Judy Riffle

James M. Tanko

November 7, 2007

Blacksburg, Virginia

Keywords: Chemistry; Cancer; Natural Products; Biodiversity

ABSTRACT

ISOLATION AND STRUCTURE ELUCIDATION OF ANTIPROLIFERATIVE NATURAL PRODUCTS FROM MADAGASCAR

Brian Thacher Murphy

As part of an ongoing search for bioactive natural products from the endemic rainforests and surrounding ocean in Madagascar, a total of four extracts were comprehensively studied and were found to contain novel and/or bioactive compounds. The following dissertation discusses the isolation, structure elucidation, and bioactivity studies of these isolates.

The following compounds from plants of Madagascar's rainforest are discussed in the order they were studied: flavonoids and long-chain compounds from *Schizolaena hystrix*, a cyclohexene derivative and butenolides from *Artabotrys madagascariensis*, and limonoids from *Malleastrum* sp. From the Malagasy marine ascidian *Tridemnum* sp. collected in the Indian Ocean, the identification as well as the potential biosynthetic origin of polyketide derived bistramides is reported.

In an attempt to explore other facets of natural products chemistry, the second part of this dissertation discusses the process of designing potential anticancer agents based on the scaffold of a natural product. The biomolecular target of these studies is an enzyme that is overexpressed in tumor cells, namely Cdc25B, whose inhibition catalyzes cell cycle arrest at the G2/M transition of the cell cycle. Several analogs of a potent Cdc25B inhibitor were synthesized and tested in the enzyme-based assay.

ACKNOWLEDGEMENTS

Firstly, the author is grateful to members of his committee for enduring a student with such an awkward classroom presence, and for allowing said author to express his sense of humor despite struggling through some difficult classes. More so, a special gratitude must be extended to two gentlemen in particular that allowed for a great deal of the technical and professional training received by the candidate. Dr. Shugeng Cao provided sound guidance through difficult research problems, and his daily presence provided a platform to transition from an eager student into a patient researcher. And a special thank you is extended to Dr. David G. I. Kingston, who continues to teach aspects of chemistry previously unknown to the author: elegance and professionalism. Instead of giving up on a struggling student in year one, he allowed for that student to prove himself in the laboratory. The knowledge and wisdom of a man who seems to have all of the answers is everything that I hoped it would be coming to Virginia Tech, and it will surely be missed.

Finally, a humble author wishes to recognize those who are the coauthors of this dissertation. Though the title page may boast one name, the current work would not have been possible without an international collaboration of scientists. Behind every chemical structure lies those who made an arduous journey through the forest to collect and identify a plant, those who performed initial extractions on the plant, those who assayed plant samples for bioactivity, and those who organized the transport and distribution of such plants. Each participant is a splinter in a rung of a continually growing ladder, whose ascension seeks only to preserve the well-being of our fellow man against a force

that operates without regard for racial, social, or national boundaries; it debilitates without prejudice and without mercy. Each scientific advance, albeit an accidental discovery or an unexpected failure, contributes ever so slightly to the body of knowledge that may be used by another to create a piece of the ladder's next rung. Therefore, it is with ineffable privilege that the author of this work extends his gratitude to those who dedicate themselves to this greater cause, the fight against disease. In alphabetical order:

Mamisoa Andrianjafy, Rabodo Andriantsiferana, A. Belalahy, Chris Birkinshaw, Peggie Brodie, Caleb Foster, John S. Lazo, Jean Maharavo, R. Mananjara, James S. Miller, Andrew Norris, Tom Olson, Ende Pan, Etienne Rakotobe, Stephan Rakotonandrasana, Andrianmalala Rakotondrafara, Sennen Randrianasolo, Randrianjafisoa, Lucien M. Randrianjanaka, Vincent E. Rasamison, Fidisoa Ratovoson, Jeremie Razafitsalama, Carla Slebodnick, Edward M. Suh, Karen TenDyke, among others.

TABLE OF CONTENTS

		Page
LIST OF FIGURES		xi
LIST OF SCHEMES		xiii
LIST OF TABLES		xiv
I.	INTRODUCTION: NATURAL PRODUCTS DRUG DISCOVERY	1
1.1	Introduction	1
1.1.1	Potential Drugs from Natural Products	1
1.1.2	International Cooperative Biodiversity Group (ICBG) Program	5
References		6
II.	ANTIPROLIFERATIVE FLAVANONES AND LONG-CHAIN COMPOUNDS OF *SCHIZOLAENA HYSTRIX* (SARCOLAENCEAE) FROM THE MADAGASCAR RAINFOREST	9
2.1	Introduction	9
2.1.1	Previous Investigations of *Schizolaena hystrix*	9
2.1.2	Chemical investigations of *Schizolaena hystrix*	10
2.1.3	Previous Investigations of Flavonoids	11
2.2	Results and Discussion	14

2.2.1 Isolation of Compounds from *Schizolaena hystrix* 14

2.2.2 Structure Elucidation of Schizolaenone A (**2.1**) 17

2.2.3 Structure Elucidation of Schizolaenone B (**2.2**) 20

2.2.4 Structure Elucidation of Schizolaenone C (**2.3**) 21

2.2.5 Structure Elucidation of 4'-O-Methylbonnanione A (**2.4**) 21

2.2.6 Structure Elucidation of 3*S*-Acetoxy-eicosanoic Acid Ethyl Ester (**2.11**) 22

2.2.7 Structure Elucidation of 3*S*-Acetoxy-doeicosanoic Acid (**2.13**) 24

2.2.8 Identification of Known Compounds from *Schizolaena hystrix* 25

2.2.9. Evaluation of Antiproliferative Activity of Compounds from *Schizolaena hystrix* 25

2.3 Experimental Section 26

References 34

III. ANTIPROLIFERATIVE COMPOUNDS OF *ARTABOTRYS MADAGASCARIENSIS* FROM THE MADAGASCAR RAINFOREST 37

3.1 Introduction 37

3.1.1 Previous Investigations of *Artabotrys madagascariensis* 37

3.1.2 Chemical Investigation of *Artabotrys madagascariensis* 38

3.2 Results and Discussion 39

3.2.1 Isolation of Compounds from *A. madagascariensis* 39

3.2.2. Structure Elucidation of Artabotrene (**3.1**) 40

3.2.3. Identification of Known Compounds from *A. Madagascariensis* 44

3.2.4. Antiproliferative Evaluation of Compounds from *A. madagascariensis.* 46

3.3 Experimental Section 46

References 51

IV. ANTIPROLIFERATIVE LIMONOIDS OF A *MALLEASTRUM SP*. FROM THE MADAGASCAR RAINFOREST 55

4.1 Introduction 55

4.1.1 Previous Investigations of *Malleastrum* sp. 55

4.1.2 Chemical Investigation of *Malleastrum* sp. 55

4.1.3 Previous Investigations of Limonoids 56

4.2 Results and Discussion 58

4.2.1 Isolation of Compounds from *Malleastrum* sp. 58

4.2.2 Structure Elucidation of Malleastrone A (**4.1**) 59

4.2.3 Structure Elucidation of Malleastrone B (**4.2**) 64

4.2.4 Structure Elucidation of Malleastrone C (**4.3**) 66

4.2.5. Evaluation of the Antiproliferative Activities of Compounds from *Malleastrum* sp. 68

4.2.6 Biosynthetic History of Limonoids 69

4.3 Experimental Section 70

References 74

V. ANTIPROLIFERATIVE BISTRAMIDES FROM THE ASCIDIAN *TRIDIDEMNUM* SP. 78

5.1 Introduction 78

5.1.1 Previous Investigations of *Tridemnum* species 78

5.1.2 Previous Investigations of Bistramides 80

5.1.3 Bioactive Properties of Bistramides 81

5.1.4 Chemical Investigation of a *Tridemnum* sp. 84

5.2 Results and Discussion 84

5.2.1 Isolation of Compounds from a *Tridemnum* sp. 84

5.2.2 Structure Confirmation of Bistramide A (**5.1**) 89

5.2.3 Structure Elucidation of Bistramide D (**5.2**) 89

5.2.4 Antiproliferative Activity of (**5.1**) 94

5.2.5 Biosynthetic Studies and the Future of the *Tridemnum* Genus 94

5.3 Experimental Section 97

References 104

VI. MISCELLANEOUS PLANTS STUDIED 113

6.1 Introduction 113

6.1.1 Investigation of *Ravensara floribunda* (MG 1916) 113

6.1.2 Investigation of *Plagioscyphus* sp. (MG 2157) 114

6.1.3 Investigation of *Pemphis acidula* (MG 2317) 115

6.1.4 Investigation of *Xylopia* sp. (MG 1834, 1835) 115

6.1.5 Investigation of *Polyscias* sp. (MG 0870) 116

6.1.6 Investigation of *Rhopalocarpus macrorhamnofolias* (MG 1813) 116

6.1.7 Investigation of *Potameia* sp. (MG 1848, 1849) 117

6.1.8 Investigation of *Rothmannia* sp. (MG 1891, 1893) 117

6.1.9 Investigation of *Terminalia* sp. (MG 2182) 118

References 118

VII. SYNTHESIS AND BIOACTIVITIES OF SIMPLIFIED ADOCIAQUINONE B AND NAPHTHOQUINONE DERIVATIVES AGAINST CDC25B PHOSPHATASE 119

7.1 Introduction 119

7.1.1 Role of Cdc25B in Regulation of the Cell Cycle 119

7.2 Results and Discussion 121

7.2.1 Synthesis of Cdc25B Inhibitors 121

7.2.2 Bioactivity 123

7.2.3 Discussion 123

7.3 Experimental Section 127

References 131

VIII. GENERAL CONCLUSIONS 138

APPENDIX 141

VITA 167

LIST OF FIGURES

Figure 1.1.	Structure of paclitaxel, epothilone D, and discodermolide	2
Figure 1.2.	Structure of dolastatin-10 and synthadotin	3
Figure 1.3	Structure of curacin A (**1.5**) and **1.6**.	4
Figure 2.1.	Compounds of *Schizolaena hystrix*	11
Figure 2.2.	Flavonol antioxidants	12
Figure 2.3.	Prenylated flavones from *Artocarpus elasticus*	13
Figure 2.4.	Prenylated flavonoids from hops	13
Figure 2.5.	Select 2D correlations of schizolaenone A (**2.1**)	20
Figure 2.6.	Select 2D correlations of **2.11**	23
Figure 2.7.	Mass spectral analysis of **2.11**	24
Figure 3.1.	Compounds of *Artabotrys madagascariensis*	38
Figure 3.2.	HMBC spectrum of artabotrene (**3.1**)	42
Figure 3.3.	Select 2D NMR correlations of artabotrene (**3.1**)	43
Figure 3.4.	Select 2D NMR correlations of melodorinol (**3.2**)	45
Figure 3.5.	Select 2D NMR correlations of polycarpol (**3.4**)	45
Figure 4.1.	Compounds of *Malleastrum* sp.	56
Figure 4.2.	Structures of bioactive limonoids	57
Figure 4.3.	Select 2D NMR correlations of malleastrone A (**4.1**)	61
Figure 4.4.	Crystal structure of malleastrone A (**4.1**)	62
Figure 4.5.	1D TOCSY spectrum of malleastrone B (**4.2**)	65
Figure 4.6.	Crystal structure and select ROESY correlations	

	of Malleastrone B (**4.2**)	66
Figure 4.7.	Select A-ring 2D NMR correlations of malleastrone C (**4.3**)	67
Figure 4.8.	COSY spectrum of malleastrone C (**4.3**)	68
Figure 4.9.	Structure of euphane	69
Figure 5.1.	Structure of didemnin B	79
Figure 5.2.	Structures of bistramides A, D, and K	81
Figure 5.3.	Crystal structure of bistramide A-actin complex	83
Figure 5.4.	Select 2D NMR correlations of C12-C19 of **5.2**	91
Figure 5.5.	Select 2D NMR correlations of C31-C40 of **5.2**	91
Figure 5.6.	Spiroketal-containing marine metabolites	97
Figure 5.7.	Semi-preparative HPLC chromatogram of fraction G @ 239 nm	100
Figure 5.8.	Semi-preparative HPLC chromatogram of fraction U @ 239 nm	102
Figure 7.1.	CDK-cyclin complexes and the cell cycle	120
Figure 7.2.	Cdc25B dephosphorylation mechanism.	120
Figure 7.3.	Structures of potent Cdc25B inhibitors	121
Figure 7.4.	Structures of Cdc25B-inhibiting quinones	122
Figure 7.5.	Proposed mechanism for formation of **7.12**	124
Figure 7.6.	DA3003-1 and JUN1111	126
Figure 7.7.	Crystal structure of **7.12**.	129

LIST OF SCHEMES

Scheme 2.1.	Separation of aqueous methanol fraction of *Schizolaena hystrix*	15
Scheme 2.2.	Second separation of aqueous methanol fraction of *Schizolaena hystrix*	16
Scheme 2.3.	Separation of the hexanes fraction of *Schizolaena hystrix*	17
Scheme 3.1.	Isolation of compounds from *A. madagascariensis*	40
Scheme 4.1.	Separation of aqueous methanol fraction of *Malleastrum* sp.	59
Scheme 5.1.	Separation of the DCM fraction of a *Trididemnum* sp.	86
Scheme 5.2.	Second separation of the DCM fraction of a *Trididemnum* sp.	87
Scheme 7.1	Synthesis of Cdc25B inhibiting quinones.	122

LIST OF TABLES

Table 2.1.	NMR Spectral Data of Flavanones **2.1-2.4**	19
Table 2.2.	Antiproliferative Activity of Compounds **2.1-2.14**	26
Table 3.1.	NMR Spectral Data of Artabotrene (**3.1**) in $CDCl_3$	44
Table 3.2.	Antiproliferative Data of Compounds **3.1**-**3.4**	46
Table 4.1.	NMR Spectral Data of Limonoids **4.1**-**4.3** in $CDCl_3$	63
Table 4.2.	Antiproliferative Data of Compounds **4.1-4.3**	69
Table 5.1.	^{13}C NMR Spectral Data of Bistramide A (**5.1**) in $CDCl_3$	88
Table 5.2.	^{13}C NMR Spectral Data of **5.2** in CD_3OD and bistramide A in $CDCl_3$	93
Table 7.1.	Biological Activities of Compounds **7.2 – 7.13** (μM)	123
Table 8.1.	Summary of Natural Products Isolated	140

I. Introduction: Natural Products Drug Discovery

1.1 Introduction

The term "cancer" refers to more than 100 diseases, particularly represented by rapid production of abnormal cells that have the ability to affect any part of the body. This disease exerts its fatal effects through the process of metastasis, or the spreading of these new cells to other parts of the body. The World Health Organization (WHO) estimated that of the 58 million deaths in 2005, 7.6 million (13%) resulted from cancer.[1] Lung, stomach, and breast cancer are the most fatal of cancers, resulting in approximately 1.3, 1.0, and 0.5 million deaths per year, respectively.[1]

The Kingston research group at Virginia Tech focuses on combating cancer by two different means: 1) employing chemical synthesis to improve the activity and biological compatibility of the tubulin interacting drugs paclitaxel (Taxol®), epothilone D, and discodermolide, and 2) using separation techniques to isolate new therapeutic agents from natural products of plant and marine origin.

1.1.1 Potential Drugs from Natural Products

Paclitaxel is a taxane diterpenoid isolated from the bark of the Pacific yew tree, *Taxus brevifolia* Nutt. (Taxaceae).[2] Since its approval as an anticancer drug by the Food and Drug Administration in 1992, it has been used to treat several different types of cancer including ovarian, breast, and lung.[3,4] The story of taxol is the embodiment of a successful natural products isolation program, and has been the justification and guiding inspiration for the multitude of natural product drug discovery initiatives in the period

since. Some of the recent advances of bioactive components from plants, microbial species, and marine organisms will briefly be discussed according to the means by which they act on cancer. The Harbor Branch Media Lab has compiled a well organized list of the following data under sponsorship from the National Sea Grant Program.[5]

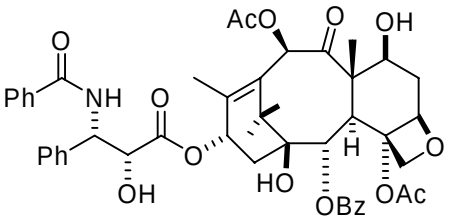

1.1. Taxol

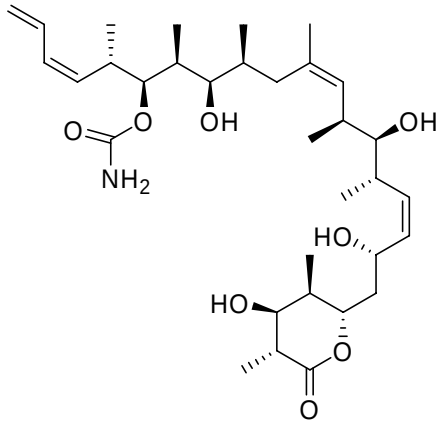

1.2. (+)-Discodermolide

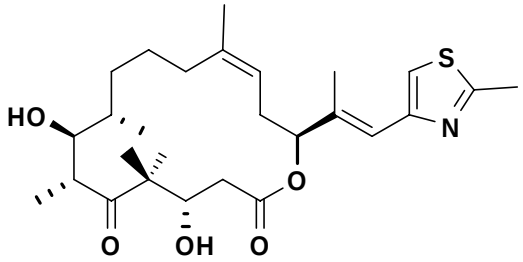

1.3. Epothilone D

Figure 1.1. *Structures of paclitaxel, epothilone D, and discodermolide*

Like paclitaxel, discodermolide targets tubulin by stabilizing microtubules, halting cell division, and thus triggering cell cycle arrest.[6,7] It is a polyketide lactone isolated from the sponge *Discodermia dissolute* (Porifera) of the Bahamas.[8] The drug

was is in Phase I clinical trials for the treatment of lung, pancreatic, and several other paclitaxel-resistant cancers, but unfortunately toxicity issues caused it to be withdrawn.

Other promising microtubule agents include the linear peptide dolastatins. Originally thought to come from the Indian Ocean sea mollusk *Dollabella auricularia*, it was later found that these metabolites were actually a product of a symbiotic cyanobacterium (*Symploca* sp.) *D. auricularia*.[9,10] Dolastatin-10 was shown to inhibit tubulin formation and affected tubulin-dependent guanosine triphosphate hydrolysis.[11] It was discontinued from Phase II clinical trials as a single agent, however a synthetic analog of the structurally similar dolastatin-15, synthadotin, is orally active and currently in Phase II clinical trials for non-small cell lung cancer and also hormone refractory prostate cancer.[12]

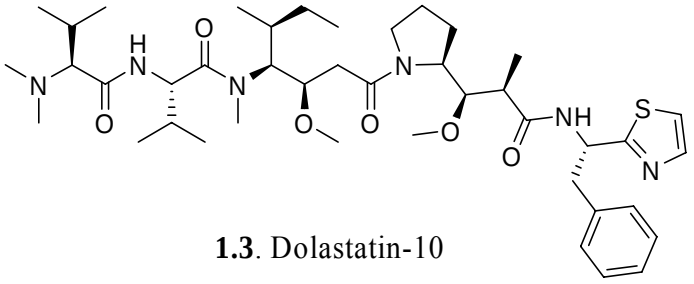

1.3. Dolastatin-10

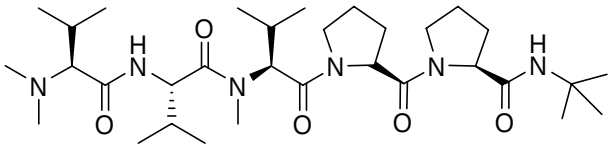

1.4. Synthadotin

Figure 1.2. *Structure of dolastatin-10 and synthadotin*

Curacin A is another example of a tubulin polymerization inhibitor. Originally isolated from the Curaçao marine cyanobacterium *Lyngbya majuscule* (Cyanophyta) by

Gerwick et al.,[13] it was proposed that this polyketide derivative was of mixed polyketide/non-ribosomal peptide origin.[14] It exerts its biological activity by binding to the colchicines site on tubulin thus blocking cell cycle progression.[15] Its *in vitro* antiproliferative and cytotoxic activity was directed toward breast, renal, and colon cancer cell lines.[16] However, the poor water solubility of this compound prevented successful *in vivo* results. This prompted many synthetic studies, and a more hydrophilic analog that retained curacin A's potent activity was prepared (**1.6**).[17] Preclinical evaluation of these potential drugs is currently underway.

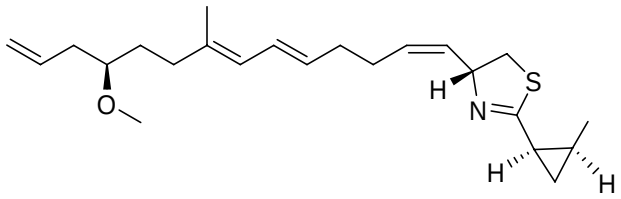

1.5. Curacin A

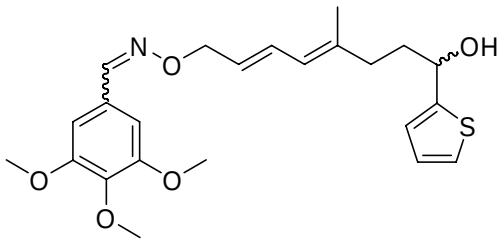

1.6.

Figure 1.3. *Structure of curacin A (**1.5**) and **1.6**.*

Curacin A is simply another example of the extraction of novel bioactive agents from natural sources and their development to combat various diseases.

1.1.2 International Cooperative Biodiversity Group (ICBG) program

The ICBG is a program of the National Institutes of Health (NIH), the Biological Sciences Directorate of the National Science Foundation (NSF), and the Foreign Agricultural Service and Forest Service of the USDA. The nine participating branches of the NIH include the Fogarty International Center, the National Cancer Institute, the National Institute of Allergy and Infectious Diseases, and the National Heart, Blood, and Lung Institute. In 2003, the program gave out six awards of approximately $600,000 each per year.[18]

Focused on expanding the interactions between drug development, biodiversity, and economic growth, the ICBG has collected over 5,000 species of plants, animals and fungi in Latin America, Africa, Asia and some Pacific islands.[18] Screening these samples against various diseases guides the process of drug discovery. An incentive for participating countries is to reap the direct benefit of any drug isolated from their region, subsequently encouraging further preservation of their biodiversity.

The current thesis presents work that was only made possible through a joint international effort of scientists. The bioactive plants that will be discussed were collected by botanists from the Missouri Botanical Garden and the Centre National d'Application des Recherches Pharmaceutiques in Madagascar. The bioactive marine organism to be discussed was collected by Centre National de Recherches sur l'Environnement and Centre National de Recherches Oceanographiques. Preliminary extraction of these plants and organisms took place at some of the aforementioned institutions, while biological testing was conducted at Virginia Tech and Eisai Research Institute.

References

1. *World Health Organization*, URL http://www.who.int
2. Wani, M. C.; Taylor, H. L.; Wall, M. E.; Coggon, P.; McPhail, A. T. The isolation and structure of taxol, a novel antileukemic and antitumor agent from *Taxus brevifolia*. *J. Am. Chem. Soc.* **1971**, *93*, 2325-2327.
3. Eisenhauer, E. A.; Vermorken, J. B. The taxoids. Comparative clinical pharmacology and therapeutic potential. *Drugs* **1998**, *55*, 5-30.
4. Kingston, D. G. I. Recent advances in the chemistry of taxol. *J. Nat. Prod.* **2000**, *63*, 726-734.
5. *Harbor Branch Medial Lab,* URL http://www.marinebiotech.org
6. Hung, D. T.; Chen, J.; Schreiber, S. L. Syntheses of discodermolides useful for investigating microtubule binding and stabilization. *Chem. Biol.* **1996**, *3*, 287-293.
7. ter Haar, E.; Kowalski, R. J.; Hamel, E.; Lin, C. M.; Longley, R. E.; Gunasekera, S. P.; Rosenkranz, H. S.; Day, B. W. Discodermolide, a cytotoxic marine agent that stabilizes microtubules more potently than taxol. *Biochemistry* **1996**, *35*, 243-250.
8. (a) Gunasekera, S. P.; Gunasekera, M.; Longley, R. E.; Schulte, G. K. Discodermolide: a new bioactive polyhydroxylated lactone from the marine sponge *Discodermia dissoluta*. *J. Org. Chem.* **1990**, *55*, 4912-4915. (b) Correction, *J. Org. Chem.* **1991**, *56*, 1346.

9. Pettit, G. R.; Kamano, Y.; Herald, C. L.; Tuinman, A. A.; Boettner, F. E.; Kizu, H.; Schmidt, J. M.; Baczynskyj, L.; Tomer, K. B.; Bontems, R. J. The isolation and structure of a remarkable marine animal antineoplastic constituent: dolastatin 10. *J. Am. Chem. Soc.* **1987**, *109*, 6883-6885.

10. Harrigan, G. G.; Luesch, H.; Yoshida, W. Y.; Moore, R. E.; Nagle, D. G.; Paul, V. J.; Mooberry, S. L.; Corbett, T. H.; Valeriote, F. A. Symplostatin 1: A dolastatin 10 analogue from the marine cyanobacterium *Symploca hydnoides*. *J. Nat. Prod.* **1998**, *61*, 1075-1077.

11. Bai, R. L.; Pettit, G. R.; Hamel, E. Binding of dolastatin 10 to tubulin at a distinct site for peptide antimitotic agents near the exchangeable nucleotide and vinca alkaloid sites. *J. Biol. Chem.* **1990**, *265*, 17141-17149.

12. Newman, D. J.; Cragg, G. M. Marine natural products and related compounds in clinical and advanced preclinical trials. *J. Nat. Prod.* **2004**, *67*, 1216-1238.

13. Gerwick, W. H.; Proteau, P. J.; Nagle, D. G.; Hamel, E.; Blokhin, A.; Slate, D. L. Structure of curacin A, a novel antimitotic, antiproliferative, and brine shrimp toxic natural product from the marine cyanobacterium *Lyngbya majescula*. *J. Org. Chem.* **1994**, *59*, 1243-1245.

14. Chang, Z.; Sitachitta, N.; Rossi, J. V.; Roberts, M. A.; Flatt, P. M.; Jia, J. Sherman, D. H.; Gerwick, W. H. Biosynthetic pathway and gene cluster analysis of curacin A, an antitubulin natural product from the tropical marine cyanobacterium *Lyngbya majuscule*. *J. Nat. Prod.* **2004**, *67*, 1356-1367.

15. Blokhin, A. V.; Yoo, H. D.; Geralds, R. S.; Nagle, D. G.; Gerwick, W. H. Hamel, E. Characterization of the interaction of the marine cyanobacterial natural product curacin A with the colchicine site of tubulin and initial structure-activity studies with analogues. *Mol. Pharmacol.* **1995**, *48*, 523-531.

16. Verdier-Pinard, P.; Lai, J. Y.; Yoo, H. D.; Yu,J. R.; Marquez, B.; Nagle, D. G.; Nambu, M.; White, J. D.; Falck, J. R.; Gerwick, W. H.; Day, B. Structure-activity analysis of the interaction of curacin A, the potent colchicine site antimitotic agent, with tubulin and effects of analogs on the growth of MCF-7 breast cancer cells. *Mol. Pharmacol.* **1998**, *53*, 62-76.

17. Wipf, P.; Reeves, J. T.; Balachandran, R.; Day, B. W. Synthesis and biological evaluation of structurally highly modified analogues of the antimitotic natural product curacin A. *J. Med. Chem.* **2002**, *45*, 1901-1917.

18. *U.S. National Institutes of Health, Fogarty International Center, ICBG*, URL http://www.fic.nih.gov/programs/research_grants/icbg/index.htm

II. Antiproliferative Flavanones and Long-chain Compounds of *Schizolaena hystrix* (Sarcolaenaceae) from the Madagascar Rainforest [1, 2]

2.1 Introduction

Bioassay-guided fractionation of an ethanol extract of a Madagascar collection of *Schizolaena hystrix* afforded four new flavanones, schizolaenones A-C, and 4'-*O*-methylbonnanione A, as well as the six known flavonoids. In addition, two new long-chain compounds, 3*S*-acetoxy-eicosanoic acid ethyl ester, and 3*S*-acetoxy-doeicosanoic acid, were isolated along with two known long-chain moieties. Structures were elucidated using various methods of 1- and 2-D NMR spectroscopy in conjunction with mass spectrometry. All of the isolates were tested for antiproliferative activity against the A2780 human ovarian cancer cell line and displayed weak activity. This chapter is an expanded version of two published papers on this plant species.[1,2]

2.1.1 Previous Investigations of the Schizolaena hystrix

Indigenous to the humid forests of Anjanaharibe-Sud (Antsiranana) to Fort Carnot (Fianarantsoa) in Madagascar, *S. hystrix* is a 14-35 m tall tree brandishing large, leathery leaves.[3] Lowry et al. reported eighteen species belonging to the genus *Schizolaena*, eight of which were reported for the first time.[3] The family Sarcolaenceae is the largest of the nine vascular plant families endemic to Madagascar and comprises nine genera with about 50 species. The only past chemical investigation of *S. hystrix* was a fatty acid analysis, which revealed the presence of fatty acids predominantly of the 16:0, 18:1Δ9, and 18:2Δ9, 12-types.[4] There are no other published reports on the chemical constituents

of *S. hystrix*, and since many of the species of *Schizolaena* have only recently been discovered, there have been few attempts to characterize the chemistry of this genus.

2.1.2 Chemical Investigation of Schizolaena hystrix

In our continuing search for biologically active natural products from tropical rainforests as part of an International Cooperative Biodiversity Group (ICBG) program, we obtained an extract from *Schizolaena hystrix* of the family Sarcolaenaceae. The ethanol extract of the fruit of *S. hystrix* was found to be active in the A2780 human ovarian cancer cell assay, with an IC_{50} value of 10 μg/mL. Bioassay-guided fractionation of this extract led to the isolation of four new prenylated and geranyl substituted flavanones, schizolaenones A-C (**2.1**-**2.3**), and 4'-*O*-methylbonnanione A (**2.4**), as well as six known flavonoids, nymphaeol A (**2.5**), bonannione A (**2.6**), bonanniol A (**2.7**), diplacol (**2.8**), macarangaflavanone B (**2.9**), and 3'-prenylaringenin (**2.10**). Two new and two known long-chain compounds, 3*S*-acetoxy-eicosanoic acid ethyl ester (**2.11**), 3*S*-acetoxy-doeicosanoic acid (**2.13**), 3*S*-acetoxy-eicosanoic acid (**2.12**), and 1-hydroxy-dodecan-2-one (**2.14**) were also isolated from the plant. The isolation and structure elucidation of the novel compounds, as well as the antiproliferative activity of all of the isolates will be discussed.

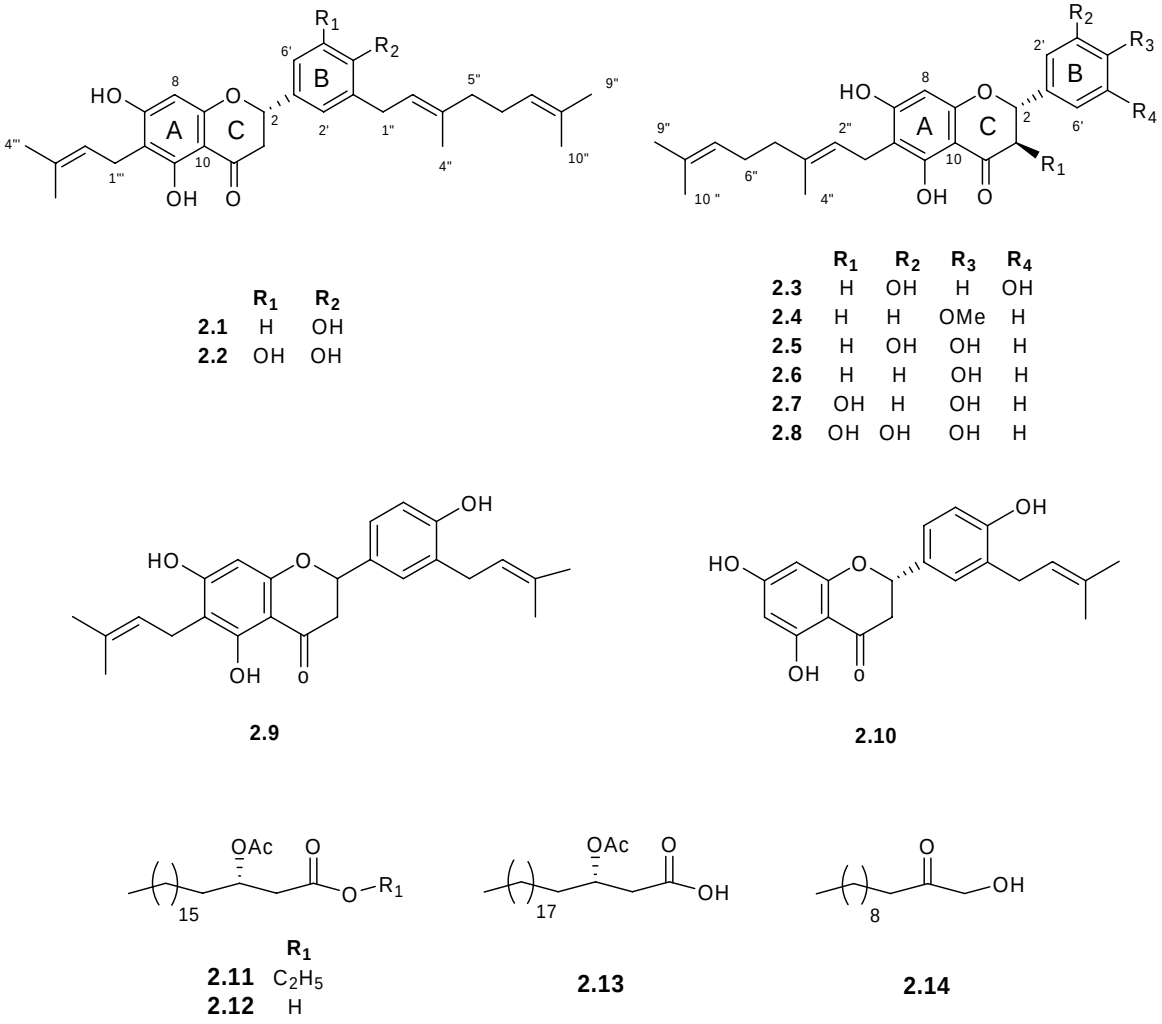

Figure 2.1. *Compounds of Schizolaena hystrix.*

2.1.3 Previous Investigations of Flavonoids

Flavonoids are a class of polyaromatic molecules derived from a combination of acetate and shikimate biosynthetic pathways, and are extremely abundant in nature.[5] Among the beneficial properties reported in the literature are anticancer, anti-inflammatory, and antioxidant activities. Regarding the latter, flavonoids are well known protectors against cardiovascular disease, due to their ability to scavenge reactive oxygen species, namely hydroxyl and superoxide free radicals.[6] Two such examples are the

flavonols quercetin (**2.15**) and kaempferol (**2.16**), which are common constituents of various fruits, red wine, and tea.

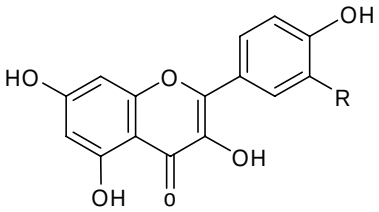

	R
2.15	OH
2.16	H

Figure 2.2. *Flavonol antioxidants.*

A specific subclass of flavonoids known as prenylated flavonoids is well characterized in a review by Botta et al.[7] It is postulated that the range of diverse bioactivities can be attributed to the addition of C_5 and C_{10} units on the aromatic rings, thus increasing the molecule's lipophilicity and affinity to biological membranes.[7] In recent years, studies on the families Leguminosae and Moraceae have yielded the greatest number of novel prenylated metabolites.

Cidade et al. reported two new prenylated flavones, artocarpesin (**2.17**) and artelastin (**2.18**), and four known prenylated flavonoids from the wood of *Artocarpus elasticus*. Each isolate displayed *in vitro* cytotoxicity against various tumor cell lines, with **2.18** exhibiting the greatest inhibitory activity.[8]

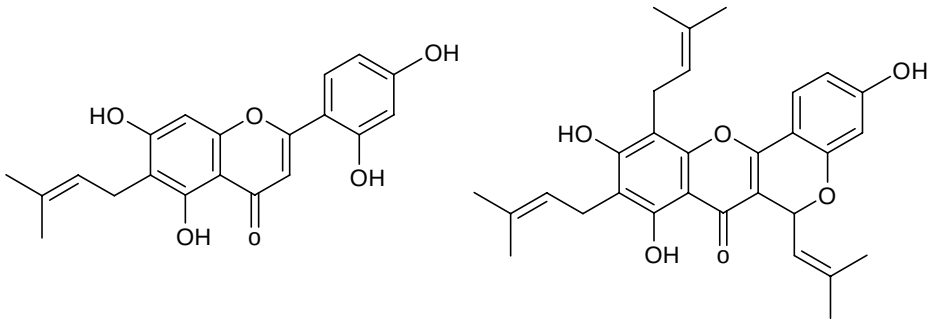

2.17. Artocarpesin **2.18.** Artelastin

Figure 2.3. *Prenylated flavones from Artocarpus elasticus.*

Further antiproliferative and cytotoxic studies were carried out by Miranda et al.[9] Six prenylated flavonoids from hops (*Humulus lupulus*) were isolated and evaluated for antiproliferative activity against human breast (MCF-7), colon (HT-29), and ovarian (A2780) cancer cell lines *in vitro*. Xanthohumol (**2.19**) and isoxanthohumol (**2.20**) caused a dose-dependant decrease in the growth of all of the cancer cells. Xanthohumol in particular exhibited an IC_{50} value of 0.52 μM against the A2780 cell line.

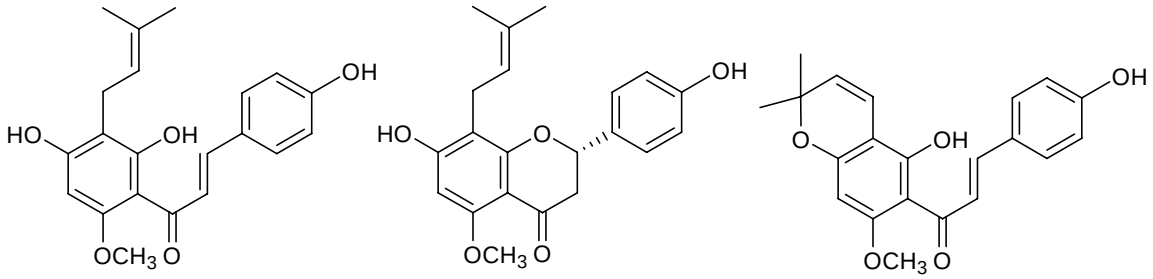

2.19. Xanthohumol **2.20.** Isoxanthohumol **2.21.** Xanthohumol B

Figure 2.4. *Prenylated flavonoids from hops.*

2.2 Results and Discussion

2.2.1 Isolation of Compounds from Schizolaena hystrix

Fourteen compounds were isolated from the fruits of *Schizolaena hystrix* by employing bioassay-guided fractionation, as shown in Schemes 2.1-2.3. The crude plant extract was suspended between hexanes and 90% aqueous methanol to yield two separate fractions. The aqueous methanol fraction was found to be active, thus it was further separated using preparative reversed-phase C-18 HPLC. An isocratic flow of 87% aqueous methanol afforded 10 fractions, three of which were pure flavanones: fractions E (**2.5**, 19 mg), F (**2.6**, 32 mg), and J (**2.1**, 95 mg). Preparative TLC using a cyano bonded phase silica gel on two separate HPLC fractions afforded the flavanol N (**2.7**, 13 mg), and the flavanones O (**2.9**, 1.9 mg), and S (**2.2**, 13 mg). Semi-preparative reversed-phase HPLC was employed to purify the flavanone **2.2**, affording 4 mg of pure compound.

The hexanes fraction from the liquid-liquid partitioning also displayed weak antiproliferative activity, thus it was chromatographed using solid phase extraction (SPE) on a diol column. A step-gradient of hexanes to chloroform was employed to yield two weakly active fractions. There was no improvement in activity, thus the most abundant fractions were further separated (A and B). Cyano bonded phase and silica preparative TLC afforded the long chain compounds G (**2.11**, 3.4 mg), L (**2.13**, 4.3 mg), and M (**2.12**, 2.8 mg).

In a second attempt to isolate compounds with greater bioactivity from *S. hystrix*, an additional 650 mg of crude ethanol plant extract was subjected to liquid-liquid partitioning as described above. The aqueous methanol fraction was chromatographed over an open C-18 column, and the resultant active fraction (8) was separated using

preparative RP-C18 HPLC. The two most bioactive fractions (15 and 17), as well as the second most abundant fraction (12) were further separated. Fraction 15 was purified by semi-preparative HPLC on a cyano bonded phase column using hexanes and chloroform as the eluent to yield fraction 34 (**2.8**, 2.5 mg). Preparative silica TLC of 17 afforded the long-chain alcohol (**2.14**, 2.0 mg), and the novel flavanone (**2.3**, 11 mg). Fraction 12 was subjected to semi-preparative amino HPLC using 4:1 chloroform:methanol as the eluent. Fraction 24 was a prenylated flavanone (**2.10**, 8.3 mg).

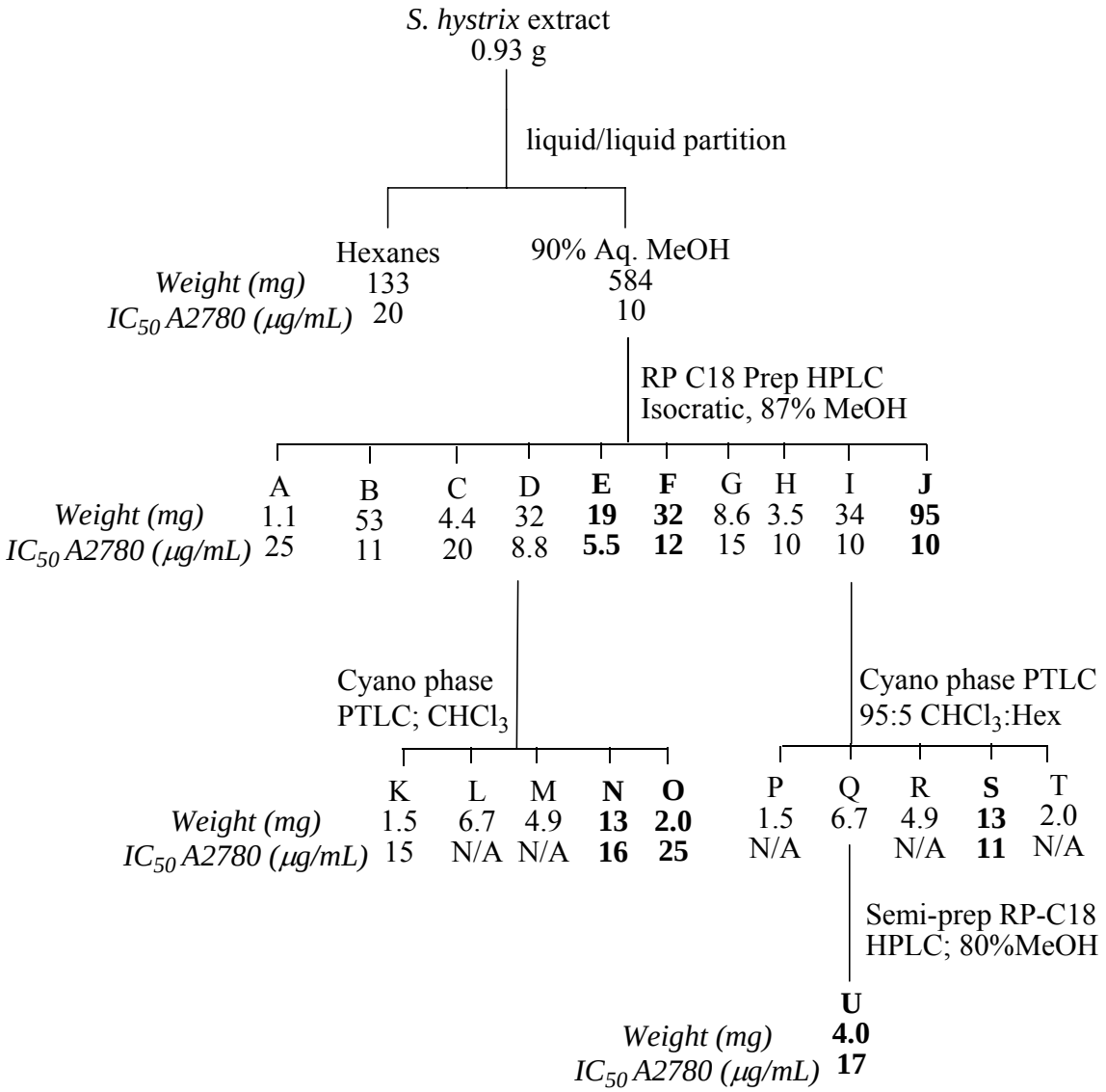

Scheme 2.1. *Separation of aqueous methanol fraction of Schizolaena hystrix*.

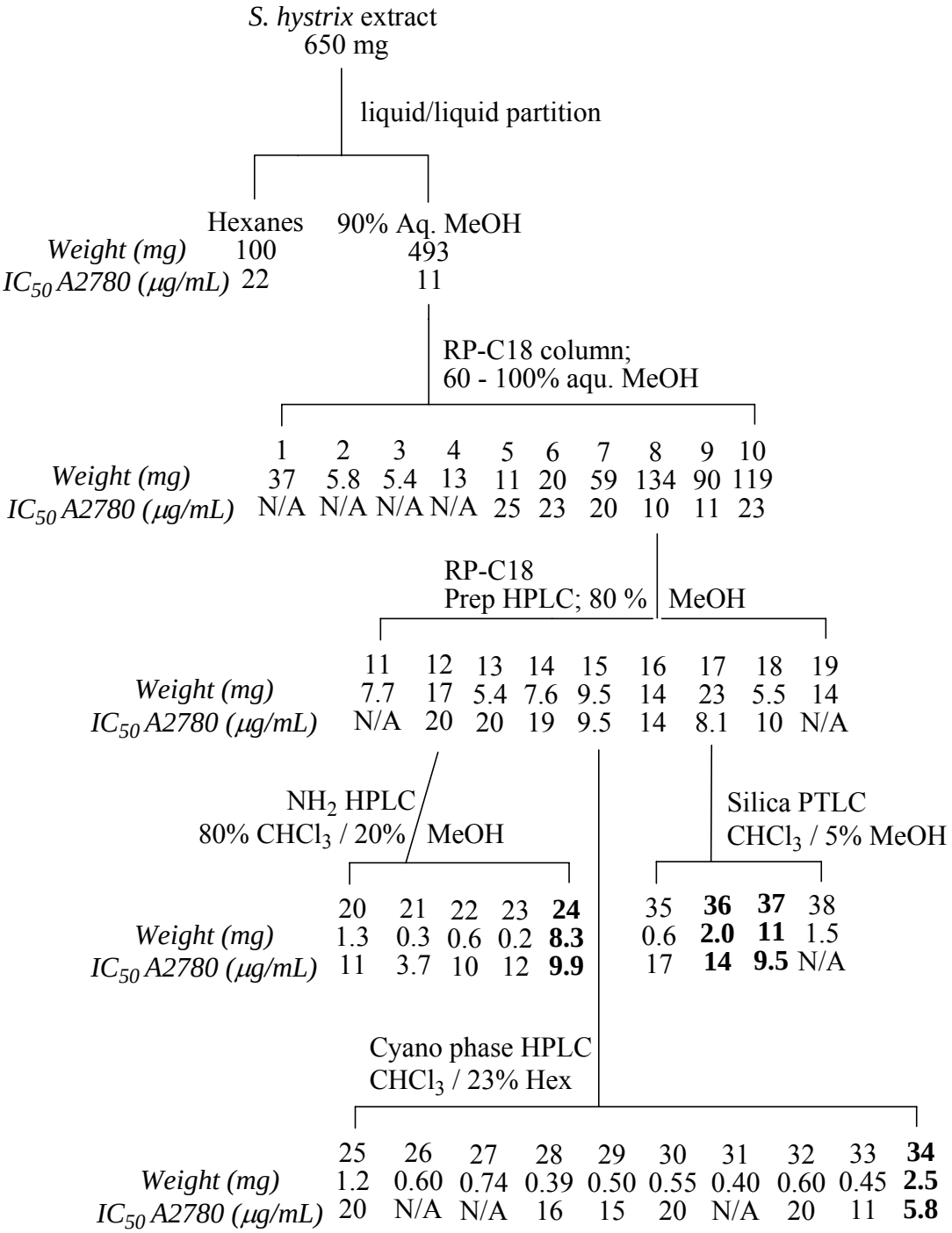

Scheme 2.2. Second *separation of aqueous methanol fraction of Schizolaena hystrix*.

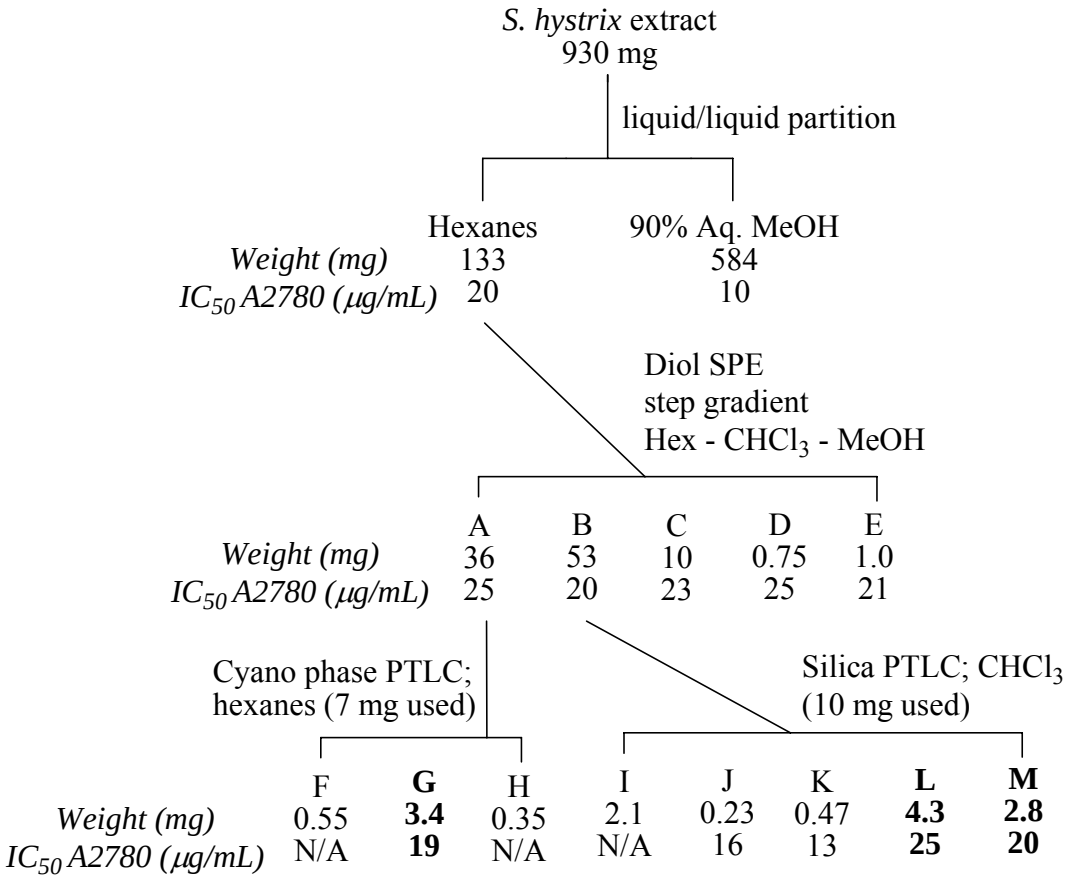

Scheme 2.3. *Separation of hexanes fraction of Schizolaena hystrix.*

*2.2.2. Structure Elucidation of Schizolaenone A (**2.1**)*

Schizolaenone A (**2.1**) was obtained as a light yellow amorphous solid. Positive-ion HRFABMS analysis gave a pseudomolecular ion at *m/z* 477.2592, which suggested a formula of $C_{30}H_{37}O_5$ ($[M+1]^+$). The ^1H NMR spectrum of **2.1** showed the presence of one chelated hydroxyl group (δ_H 12.4, s, 5-OH), one methylene α to the carbonyl (δ_H 3.09, dd, J = 13.0, 17.0 Hz, H_{ax}-3 and δ_H 2.77, dd, J = 3.0, 17.0 Hz, H_{eq}-3), and one oxymethine (δ_H 5.30, dd, J = 3.0, 13.0 Hz, H-2) (Table 2.1). These data suggested that **2.1** possess a flavanone skeleton. The observation of one doublet (δ_H 6.84, d, J = 8.0 Hz,

H-5'), one doublet of doublets (δ_H 7.19, dd, J = 2.0, 8.0 Hz, H-6'), and one broad singlet (δ_H 7.18, br s, H-2') implied the B-ring substitution pattern as shown for **2.1**. In addition, the coupling constants of the B ring protons illustrated an ABX-type spin system. Prenyl and geranyl substituents gave rise to three olefinic (δ_H 5.03, m; δ_H 5.26, m; and δ_H 5.32, m), four methylene (δ_H 2.07, m; δ_H 2.09, m; δ_H 3.37, d, J = 4.0 Hz; δ_H 3.39, d, J = 3.6 Hz), and four methyl signals, representing a total of five methyl groups (δ_H 1.81, 1.78, 1.78, 1.67, and 1.59, all s). The HMBC spectrum of **2.1** revealed correlations of H-2' (δ_H 7.18, s) with C-4' (δ_C 155.2) and C-1" (δ_C 130.3), and thus indicated the presence of the geranyl substituent on the B ring. Geranyl methyl protons H_3-9" (δ_H 1.67, s) and H_3-10" (δ_H 1.59, s) both showed correlations to olefinic carbons C-7" (δ_C 124.0) and C-8" (δ_C 132.5), and H_3-4" (δ_H 1.81, s) showed a correlation with C-3" (δ_C 140.1). Furthermore, the olefinic prenyl proton H-2"' (δ_H 5.32, m) displayed correlations to C-6 (δ_C 107.0), while H_3-4″ and H_3-5"' (δ_H 1.78, s) correlated with C-2"' (δ_C 121.6) and C-3"' (δ_C 135.8). The chelated OH-5 proton (δ_H 12.4, s) correlated with three quaternary carbons (C-5, C-6, and C-10 at δ_C 161.5, 107.0, and 103.3). The lone A ring proton H-8 (δ_H 5.99, s) showed correlations with four of the six aromatic A ring carbons (C-7, C-9, C-6, and C-10 at δ_C 164.4, 161.5, 107.0 and 103.3). These correlations confirmed the proposed structure of **2.1**. The absolute configuration of schizolaenone A was determined to be 2*S* by analysis of its circular dichroism (CD) spectrum and comparison with literature values.[10]

Table 2.1. NMR Spectral Data of Flavanones **2.1-2.4** [a]

	2.1 [f]		**2.2** [f]		**2.3** [g]		**2.4** [f]	
position	^{13}C[b]	^{1}H[b,c] (*J*, Hz)	^{13}C[b]	^{1}H[b,c] (*J*, Hz)	^{13}C[b]	^{1}H[b,c] (*J*, Hz)	^{13}C[b]	^{1}H[b,c] (*J*, Hz)
2	79.4	5.30 dd (3.0, 13.0)	79.2	5.27 dd (2.5, 10.0)		5.24 dd (3.2, 12.8)	79.0	5.34 dd (2.8, 13.0)
3ax	43.7	3.09 dd (13.0, 17.0)	43.5	3.04 dd (10.0, 13.0)		3.05 dd (12.8, 16.8)	43.4	3.09 dd (13.0, 17.0)
3eq		2.77 dd (3.0, 17.0)		2.75 dd (2.5, 13.0)		2.68 dd (3.2, 16.8)		2.78 dd (2.8, 17.0)
4	196.6		196.5		197.8		196.3	
5	161.5		161.3		162.4		161.3	
6	107.0		107.2		109.7		106.9	
7	164.4		164.3		165.9		164.2	
8	96.0	5.99 s	95.9	5.98 s	95.4	5.94 s	95.8	5.99 s
9	161.5		161.4		162.5		161.3	
10	103.3		103.1		103.2		103.1	
1'	130.9		130.8		131.9		130.7	
2'	128.6	7.18[e] br s	119.8	6.73 d (2.0)	119.2 [d]	6.91 s [d]	127.9	7.38 d (8.8)
3'	127.6		127.8		146.8		114.4	6.95 d (8.8)
4'	155.2		142.8		116.2 [d]	6.78 s [d]	160.2	
5'	116.4	6.84 d (8.0)	144.3		146.5		114.4	6.95 d (8.8)
6'	126.1	7.19 dd (2.0, 8.0)	111.5	6.86 d (2.0)	114.7[d]	6.78 s [d]	127.9	7.38 d (8.8)
1"	30.3	3.39 d (3.6)	29.9	3.37 d (6.5)	21.8	3.21 d (7.2)	29.8	3.37 d (7.2)
2"	121.6[d]	5.26[d] m	121.6[d]	5.25[d] m	123.9	5.19 m	121.4	5.25 t
3"	140.1		139.6		135.2		139.8	
4"	16.6	1.81 s	16.4	1.80 s	16.2	1.74 s	16.5	1.80 s
5"	40.1	2.07 m	39.9	2.07 m	40.9	2.04 m	39.9	2.04 m
6"	26.7	2.09 m	26.6	2.10 m	27.7	1.94 m	26.5	2.07 m
7"	124.0	5.03 m	123.9	5.05 m	125.4	5.06 m	123.8	5.05 m
8"	132.5		132.3		132.0		132.3	
9"	26.0	1.67 s	25.9	1.67 s	25.8	1.62 s	25.8	1.67 s
10"	18.1	1.59 s	17.9	1.59 s	17.7	1.56 s	18.0	1.59 s
1"'	21.4	3.37 d (4.0)	21.3	3.35 d (7.0)				
2"'	121.6[d]	5.32[d] m	121.5[d]	5.32[d] m				
3"'	135.8		135.6					
4"'	26.2	1.78 s	26.0	1.78 s				
5"'	18.3	1.78 s	18.1	1.78 s				
MeO-4'							55.5	3.83 s
HO-5		12.4 s		12.4 s				12.4 s

[a] Assignments based on COSY, HMBC, HSQC. [b] Chemical shifts (δ) in ppm. [c] br s: broad singlet; d: doublet; m: multiplet. [d] Values are interchangeable. [e] Signal overlapped with H-6′. [f] in $CDCl_3$. [g] in CD_3OD.

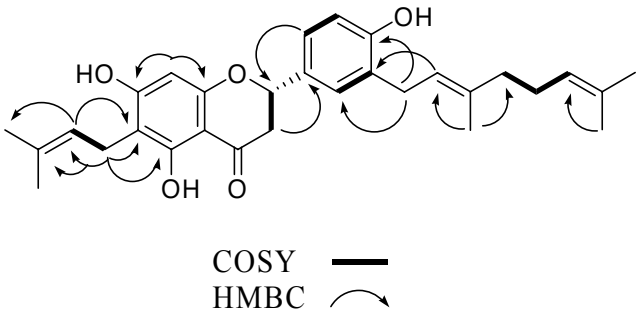

Figure 2.5. *Select 2D correlations of schizolaenone A (**2.1**).*

*2.2.3. Structure Elucidation of Schizolaenone B (**2.2**)*

Schizolaenone B (**2.2**) was obtained as a yellow amorphous solid. Positive-ion HRFABMS analysis gave a pseudomolecular ion at *m/z* 493.2569, which suggested a formula of $C_{30}H_{37}O_6$ ($[M+1]^+$). Compound **2.2** had very similar NMR and mass spectral data to those of **2.1**, suggesting their structural similarity. A sixteen mass unit difference in the HRFABMS as well as the absence of proton H-5' in the ^{1}H NMR spectrum of **2.2** indicated the presence of an extra B ring hydroxyl group to be the sole difference between **2.1** and **2.2**. The ^{1}H spectrum of **2.2** showed the presence of an aromatic proton in the A ring, a chelated hydroxyl proton, a methylene α to a carbonyl, an oxymethine, and the same signals for both prenyl and geranyl substituents as those of **2.1**. The B ring aromatic signals of H-2' (δ_H 6.73, d, J = 2.0 Hz) and H-6' (δ_H 6.86, d, J = 2.0 Hz) supported the proposed substitution pattern. The two B ring protons both showed HMBC correlations with C-2 (δ_C 79.2) and C-4' (δ_C 142.8), while an additional HMBC correlation indicated the proximity of H-2' (δ_H 6.73, d, J = 2.0 Hz) with C-1" (δ_C 29.9). The absolute configuration of schizolaenone B was determined to be 2*S*, as deduced upon analysis of its CD spectrum and comparison with literature values.[10]

*2.2.4. Structure Elucidation of Schizolaenone C (**2.3**)*

Schizolaenone C (**2.3**) was obtained as a light yellow amorphous solid. Positive-ion HRFABMS analysis gave a pseudomolecular ion at *m/z* 425.19638 ($[M+1]^+$), which suggested a formula of $C_{25}H_{28}O_6$. NMR and FABMS suggested this structure to be similar to that of **2.2**, though without a C_5H_9 prenyl substituent. The ^1H NMR spectrum of **2.3** in CD_3OD showed the presence of one methylene α to the carbonyl, and one oxymethine. When a ^1H NMR spectrum of **2.3** was taken in DMSO-d_6, one chelated hydroxyl proton was observed (δ_H 12.4, s, OH-5). The observation of two aromatic singlets in CD_3OD integrating to a total of three hydrogen atoms (δ_H 6.78, s, H-2' or H-6' and H-4'; δ_H 6.91, s, H-6' or H-2') in addition to key correlations in the HMBC spectrum of H-2' and H-6' to C-2 (δ_C 80.4), and H_{ax}-3 to C-1' (δ_C 131.9) implied the B-ring substitution pattern as shown for **2.3**. The HMBC spectrum of **2.3** correlated H-1" with C-5 (δ_C 162.4), C-6 (δ_C 109.7), and C-7 (δ_C 165.9), thus indicating the presence of the geranyl substituent on the A ring. The absolute configuration of Schizolaenone C was determined to be 2*S* by analysis of its CD spectrum and comparison with literature values.[10]

*2.2.5. Structure Elucidation of 4'-O-Methylbonnanione A (**2.4**)*

4'-*O*-methylbonnanione A (**2.4**) was obtained as a pale yellow solid. Positive-ion HRFABMS analysis gave a pseudomolecular ion at *m/z* 423.2139, which suggested a formula of $C_{26}H_{31}O_5$ ($[M+1]^+$). The basic flavanone skeleton was present in **2.4** as indicated in the ^1H spectrum by a downfield singlet (H-8, δ_H 5.99) and three characteristic doublets of doublets (δ_H 5.34, J = 2.8, 13.0 Hz, H-2; δ_H 3.09, J = 13.0, 17.0 Hz, H_{ax}-3 and

δ_H 2.78, *J* = 2.8, 17.0 Hz, H_{eq}-3). In addition, a pair of downfield doublets characteristic of *para*-substitution (δ_H 6.95, *J* = 8.8 Hz, H-3', 5' and δ_H 7.38, *J* = 8.8 Hz, H-2', 6'), a 3H singlet (δ_H 3.83, C-4'-OMe), a singlet for a chelated hydroxy proton (δ_H 12.4, 5-OH), and signals for a geranyl group were observed. The ^{1}H spectrum also shared features with those of bonannione A,[11] indicating nearly identical structures. HMBC data placed the geranyl substituent on the A ring, as H-1" (δ_H 3.37, d, *J* = 7.2 Hz) correlated with three nearby quaternary carbons (δ_C 161.3, C-5; δ_C 106.9, C-6; δ_C 164.2, C-7). Confirmation of **2.4** was finalized with correlations of aromatic protons H-2', 6' with C-2 (δ_C 79.0) and C-4' (δ_C 160.2), and H-3', 5' with C-1' (δ_C 130.7). The absolute configuration of 4'-*O*-methylbonnanione A was determined to be 2*S*, as deduced upon analysis of its CD spectrum and comparison with literature values.[10]

*2.2.6. Structure Elucidation of 3S-Acetoxy-eicosanoic Acid Ethyl Ester (**2.11**)*

3*S*-acetoxy-eicosanoic acid ethyl ester (**2.11**) was obtained as transparent oil. Positive-ion HRFABMS analysis gave a pseudomolecular ion at *m/z* 399.34839 ($[M+1]^+$), which suggested a molecular formula of $C_{24}H_{46}O_4$. The presence of acetoxy and ethyl moieties in **2.11** were suggested by abundant fragments at $[M + 1 - 59]^+$ (loss of $C_2H_3O_2$) and $[M + 1 - 28]^+$ (loss of C_2H_4) *via* a McLafferty-type rearrangement. In addition, the ^{13}C NMR spectrum of **2.11** in C_6D_6 displayed signals for two ester carbonyls (δ_C 169.6, C-1" and 170.0, C-1) as well as two sp^3-oxygenated carbons (δ_C 60.3, C-1' and 70.6, C-3). The ^{1}H NMR spectrum of **2.11** in C_6D_6 showed the presence of one oxymethine (δ_H 5.42, m, H-3), one oxygenated methylene (δ_H 3.95, m, H_2-1'), one methyl alpha to a carbonyl (δ_H 1.72, s, H_3-2"), one broad multiplet between δ_H 1.18-1.34 (30H, m, H_2-5

through 19), and two upfield methyl triplets (0.91, t, J = 6.6 Hz, H_3-20 and 0.96, t, J = 7.0 Hz, H_3-2'). These data inferred that **2.11** was a long-chain fatty acid ethyl ester with an acetoxy substituent. The COSY NMR spectrum displayed key connectivity between H_2-1' and H_3-2', as well as H-3 with both H_2-2 (δ_H 2.35, dd, J = 5.0, 15.2 Hz, H_α-2 and 2.46, dd, J = 7.6, 15.2 Hz, H_β-2), and H_2-4 (δ_H 1.46 and 1.53, each m). The final arrangement of **2.11** was fortified *via* HMBC correlations of H-1' with the carbonyl at C-1, and of H-3 with both carbonyl moieties C-1 and C-1", thus confirming the location of the acetoxy substituent at C-3 and subsequently establishing the precise position of the ester carbonyl of the fatty acid chain. These correlations confirmed the proposed structure of **2.11**. The absolute configuration of 3-acetoxy-eicosanoic acid ethyl ester was determined to be 3*S* by analysis of its optical rotation spectrum and comparison with literature values of similar 3-acetoxy fatty acid esters.[12]

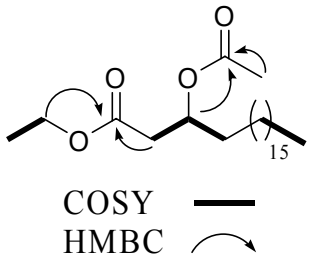

Figure 2.6. *Select 2D correlations of **2.11**.*

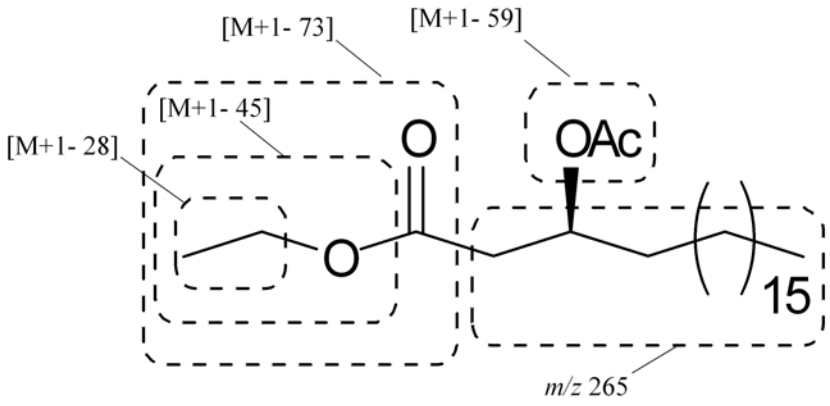

Figure 2.7. *Mass spectral analysis of **2.11**.*

*2.2.7. Structure Elucidation of 3S-Acetoxy-doeicosanoic Acid (**2.13**)*

3*S*-acetoxy-doeicosanoic acid (**2.13**) was obtained as transparent oil. Positive-ion HRFABMS analysis gave a pseudomolecular ion at *m/z* 399.34457 ($[M+1]^+$), which suggested a formula of $C_{24}H_{46}O_4$. Though the proposed molecular formula was identical to that of **2.11**, subtle differences in the ^1H and ^{13}C NMR spectra suggested a slightly different structure. The absence of the C-1' methylene and C-2' methyl signals, as in the ^1H spectrum of **2.11**, offered the proposition that the C_2H_5 moiety may not be present. In addition, the ^{13}C NMR spectrum of **2.13** showed the presence of only one sp^3-oxygenated carbon (δ_C 68.1, C-3) and signals representative of two methyl groups (δ_C 14.3, C-22 and 20.6, C-2"). The C-2' signal of the C_2H_5 moiety in **2.11** was clearly not present in the ^{13}C NMR spectrum of **2.13**. In comparison with **2.11**, the C-1 carbonyl signal (δ_C 175.7) underwent a slight downfield chemical shift, signaling the presence of a carboxylic acid in **2.13**. This proposition was further supported by the presence of two carbonyl peaks in the IR spectrum of **2.13**, the acid functionality at C-1 (1716 cm^{-1}) and the ester moiety at C-1" (1742 cm^{-1}). Finally, aside from the minor structural differences between **2.11** and

2.13, their respective COSY and HMBC NMR spectra displayed identical correlations, thus confirming the structure of **2.13**. The absolute configuration of 3-acetoxy-doeicosanoic acid was determined to be 3*S* by analysis of its OR data and comparison with literature values of similar 3-acetoxy fatty acid esters.[12]

2.2.8. Identification of Known Compounds from Schizolaena hystrix

Nymphaeol A (**2.5**), bonannione A (**2.6**), bonanniol A (**2.7**), diplacol (**2.8**), macarangaflavanone B (**2.9**), 3'-prenylaringenin (**2.10**), 3*S*-acetoxy-eicosanoic acid (**2.12**), and 1-hydroxy-dodecan-2-one (**2.14**) were all identified by analysis of 1- and 2-D NMR and mass spectra, as well as comparison to spectral data found in literature.[11, 13-19]

2.2.9. Evaluation of Antiproliferative Activity of Compounds from Schizolaena hystrix.

All of the isolates were tested against the A2780 human ovarian cancer cell line, as previously reported.[20] The results are shown in Table 2.2. All isolates displayed weak bioactivity with IC_{50} values ranging from 13-70 μM. Interestingly, nymphaeol A contains an extra B ring hydroxyl substituent compared with its counterpart, bonannione A, and was found to be about twice as active, with an IC_{50} value of 14 μM as compared to 32 μM for the latter compound.

Table **2.2.** Antiproliferative Activity of Compounds **2.1-2.14**[a]

compound	IC_{50} (μM)
schizolaenone A (**2.1**)	21
schizolaenone B (**2.2**)	22
Schizolaenone C (**2.3**)	21
4'-*O*-methylbonannione A (**2.4**)	40
nymphaeol A (**2.5**)	14
bonannione A (**2.6**)	32
bonanniol A (**2.7**)	64
diplacol (**2.8**)	13
Macarangaflavanone B (**2.9**)	43
3'-prenylaringenin (**2.10**)	29
3-acetoxy-eicosanoic acid ethyl ester (**2.11**)	48
3-acetoxy-eicosanoic acid (**2.12**)	54
3-acetoxy-doeicosanoic acid (**2.13**)	63
1-hydroxy-dodecan-2-one (**2.14**)	70

[a]Concentration of each compound that inhibited 50% of the growth of the A2780 human ovarian cell line according to the procedure described,[10] with actinomycin D (IC_{50} 1-3 ng/mL) as the positive control.

2.3 Experimental Section.

General Experimental Procedures. CD analysis was performed on a JASCO J-720 spectropolarimeter. IR and UV spectra were measured on MIDAC M-series FTIR and Shimadzu UV-1201 spectrophotometers, respectively. Melting point was taken using Buchi Melting Point B-540. NMR spectra were obtained on JEOL Eclipse 500, Varion Inova 400, and Varion Unity 400 spectrometers. Mass spectra were obtained on a JEOL JMS-HX-110 instrument. Chemical shifts are given in δ (ppm), and coupling constants (*J*) are reported in Hz. HPLC was performed using either Shimadzu LC-8A pumps coupled with a Varian Dynamax preparative C_{18} column (250 x 21.4 mm), or Shimadzu LC-10AT pumps coupled with a Varian Dynamax semi-preparative C_{18} column (250 x 10 mm). Both HPLC systems employed a Shimadzu SPD-M10A diode array detector.

Preparative TLC was performed on Merck HPTLC cyano (CN) plates (10 x 10 cm), 200 μm thickness.

Plant Material. The plant sample used was a collection of fruits of *Schizolaena hystrix* (Sarcolaenaceae), and duplicates of the voucher specimen (Rakotondrafara 225) are deposited at the Missouri Botanical Garden (MO), the Muséum National d'Histoire Naturelle, Paris (P), the Départment des Recherches Forestières et Pisicoles, Madagascar (TEF), and the Centre National d'Applications des Recherches Pharmaceutiques (CNARP), Madagascar. The collection was made in the province of Toamasina, 15-20 km SE of the village of Ambarifotsy, in forest adjacent to the Zahamena Protected Areas at 560 m in elevation on 30 May 2003 by A. Rakotondrafara**,** S. Randrianasolo, N.M. Andrianjafy, L.J. Razafitsalama, L.M. Randrianjanaka, A. Belalahy, Randrianjafisoa, and R. Mananjara.

Extract Preparation. The dried plant sample described above (336 g) was extracted with EtOH to give 27.3 g of extract designated MG 1938 (7.02 g).

Cell Growth Inhibition A**ssay.** The A2780 human ovarian cancer cell line antiproliferative assay was performed at Virginia Polytechnic Institute and State University as previously reported.[20]

Bioassay-guided Fractionation of Flavonoids from *S. hystrix*. Extract MG 1938 (0.93 g) was suspended in aqueous MeOH (MeOH-H_2O, 9:1, 350 mL) and extracted with

hexanes (2 x 150 mL). The aqueous MeOH fraction displayed antiproliferative activity (IC_{50} = 10 μg/mL), and was further chromatographed by preparative RP-C_{18} HPLC using MeOH-H_2O (87:13) to yield ten fractions (A-J). Fraction J was identified as **2.1** (t_R 27.9 min, 122 mg), while fractions E and F were identified as nymphaeol A (t_R 12.1 min, 42.6 mg) and bonannione A (t_R 14.5 min, 50.4 mg), respectively. Fraction D (20.6 mg, IC_{50} = 9.0 μg/mL) was further separated via preparative TLC on CN plates (95:5, $CHCl_3$-hexane) to afford bonanniol A (R_f 0.31, 2.7 mg) and macarangaflavanone B (R_f 0.56, 1.79 mg). Fraction I (70.4 mg, IC_{50} = 10 μg/mL) was separated using CN preparative TLC ($CHCl_3$-hexane, 95:5) to afford compound **2.2** (R_f 0.60, 13.5 mg), and fraction Q (R_f 0.85, 6.66 mg). Using a MeOH-H_2O system (85:15), fraction Q required chromatographic purification over semi-preparative RP-C_{18} HPLC to afford **2.4** (t_R 12.5 min, 1.99 mg).

An additional 650 mg of MG 1938 was separated using the aforementioned liquid-liquid partitioning technique. The aqueous MeOH fraction displayed antiproliferative activity (493 mg, IC_{50} = 11 μg/mL), and was therefore chromatographed over a RP-C18 flash column (30 g, 2.5 x 6.5 cm) using a step gradient of H_2O to MeOH in 10% increments to furnish 10 fractions (1-10). Fraction 8 (134 mg, 10 μg/mL) was further separated using an isocratic flow of 80% aqueous MeOH on a preparative RP-C18 HPLC column to furnish 9 fractions (11-19). Fraction 12 (t_R 9.7 min, 17.6 mg, IC_{50} = 20 μg/mL) was subjected to semi-preparative NH_2 HPLC (isocratic flow of $CHCl_3$-MeOH, 4:1) to afford 5 fractions (20-24), of which fraction 24 was identified as 3'-prenylaringenin (t_R 16.0 min, 8.3 mg, IC_{50} = 10 μg/mL). Fraction 15 (t_R 14.7 min, 9.5 mg, IC_{50} = 9.5 μg/mL) was separated via semi-preparative CN HPLC (isocratic flow of

$CHCl_3$-hexanes, 77:23) to yield 10 fractions (25-34), of which fraction 34 was a broad peak identified as diplacol (t_R 22.5 min, 2.5 mg, IC_{50} = 5.8 μg/mL). Fraction 18 (t_R 20.5 min, 23.5 mg, IC_{50} = 8.1 μg/mL) was chromatographed using Si PTLC ($CHCl_3$-MeOH, 95:5) to afford 4 fractions (35-38). Fractions 36 and 37 were identified as 1-hydroxy-dodecan-2-one (R_f 0.50, 2.0 mg) and **2.3** (R_f 0.33, 11.5 mg), respectively. The structures of the known compounds were identified by comparison of their spectral data with literature values.[11, 13-15, 17-19]

Bioassay-guided Fractionation of Long-chain Compounds from *S. hystrix*. The hexanes fraction from liquid-liquid partitioning displayed antiproliferative activity (133 mg, IC_{50} = 20 μg/mL), and was further chromatographed with diol Solid Phase Extraction (SPE) using a step gradient of hexane-$CHCl_3$-MeOH to yield five fractions (A-E). 10 mg of fraction A (35.8 mg, 25 μg/mL) was further chromatographed over CN PTLC plates (hexanes) to furnish 3 fractions (F-H). Fraction G was identified as **2.11** (R_f 0.51, 3.4 mg). 10 mg of fraction B (52.6 mg, 20 μg/mL) was separated over Si PTLC and eluted with hexanes to yield 5 fractions (I-M). Fraction L was identified as **2.13** (R_f 0.25, 4.3 mg), while fraction M was identified as **2.12** (R_f 0.06, 2.8 mg). The structures of the known compounds were identified by comparison of their spectral data with literature values.[16]

Schizolaenone A (2.1): yellow amorphous solid; $[\alpha]_D$ + 2.7° (*c* 0.44, MeOH); UV (MeOH) λ_{max} (log ε) 224 (2.25) nm, 293 (2.10) nm; IR ν_{max} 2966, 2920, 2853, 1633,

1597, 1447, 1149, 1085, 1063, 819 cm^{-1}; CD (MeOH, *c* 0.039) $[\theta]_{293}$ -24; ^{1}H and ^{13}C NMR, see Table 2.1; HRFABMS *m/z* 477.2592 $[M+1]^+$ (calcd for $C_{30}H_{37}O_5$, 477.2641).

Schizolaenone B (2.2): yellow amorphous solid; $[\alpha]_D$ -3.9° (*c* 0.53, MeOH); UV (MeOH) λ_{max} (log ε) 231 (2.18), 292 (2.15) nm; IR ν_{max} 2966, 2914, 2855, 1633, 1597, 1446, 1297, 1152, 1085, 1065 cm^{-1}; CD (MeOH, *c* 0.076) $[\theta]_{295}$ -2.2; ^{1}H and ^{13}C NMR, see Table 2.1; HRFABMS *m/z* 493.2569 $[M+1]^+$ (calcd for $C_{30}H_{37}O_6$, 493.2590).

Schizolaenone C (2.3): yellow amorphous solid; $[\alpha]_D$ -1.0° (*c* 0.20, MeOH); UV (MeOH) λ_{max} (log ε) 233 (4.10) nm, 288 (4.06) nm, 340 (3.55) nm; IR ν_{max} 3318, 2973, 2921, 1641, 1598, 1454, 1343, 1305, 1161, 1090 cm^{-1}; CD (MeOH, *c* 0.042) $[\theta]_{299}$ –6.5; ^{1}H NMR (DMSO-d_6): δ_H 1.52 (3H, s, H-10''), 1.59 (3H, s, H-9''), 1.68 (3H, s, H-4''), 1.88 (2H, m, H-6''), 1.97 (2H, m, H-5''), 2.65 (1H, dd, *J* = 3.0, 17.0 Hz, H_{eq}-3), 3.10 (2H, d, *J* = 7.5 Hz, H-1''), 3.13 (1H, dd, *J* = 12.5, 17.0 Hz, H_{ax}-3), 5.03 (1H, m, H-7''), 5.11 (1H, m, H-2''), 5.32 (1H, dd, *J* = 3.0, 12.5 Hz, H-2), 5.96 (1H, s, H-8), 6.72 (2H, br s, H-4', $^{6'\,a}$), 6.85 (1H, s, H-2' ^{a}), 12.4 (1H, s, OH-5) ppm, ^{a} values are interchangeable; ^{1}H and ^{13}C NMR (CD_3OD), see Table 2.1; HRFABMS *m/z* 425.19638 $[M+1]^+$ (calcd for $C_{25}H_{29}O_6$, 425.19642).

4'-*O*-Methylbonannione A (2.4): pale yellow solid, mp 133-136°C; $[\alpha]_D$ -3.2° (*c* 0.15, MeOH); UV (MeOH) λ_{max} (log ε) 296 (1.97) nm; IR ν_{max} 2922, 2851, 1627, 1582, 1458, 1312, 1295, 1252, 1173, 1089, 830 cm^{-1}; CD (MeOH, *c* 0.012) $[\theta]_{290}$ -3.6; ^{1}H and ^{13}C NMR, see Table 2.1; HRFABMS *m/z* 423.2139 $[M-1]^+$ (calcd for $C_{26}H_{31}O_5$, 423.2172).

Nymphaeol A (2.5): ^{1}H NMR (CD_3OD): δ_H 1.55 (3H, s, H-10''), 1.60 (3H, s, H-9''), 1.73 (3H, s, H-4''), 1.93 (2H, m, H-6''), 2.03 (2H, m, H-5''), 2.65 (1H, dd, *J* = 2.8, 17.2 Hz, H_{eq}-3), 3.04 (1H, dd, *J* = 12.8, 17.2 Hz, H_{ax}-3), 3.20 (2H, d, *J* = 6.8 Hz, H-1''), 5.05 (1H, br t, *J* = 6.8 Hz, H-7''), 5.17 (1H, br t, *J* = 6.0 Hz, H-2''), 5.23 (1H, dd, *J* = 2.8, 12.8 Hz, H-2), 5.93 (1H, s, H-8), 6.77 (2H, br s, H-5', 6'), 6.90 (1H, br s, H-2') ppm.

Bonnanione A (2.6): ^{1}H NMR (CD_3OD): δ_H 1.55 (3H, s, H-10''), 1.61 (3H, s, H-9''), 1.74 (3H, s, H-4''), 1.93 (2H, m, H-6''), 2.03 (2H, m, H-5''), 2.65 (1H, dd, *J* = 2.8, 17.2 Hz, H_{eq}-3), 3.07 (1H, dd, *J* = 12.8, 17.2 Hz, H_{ax}-3), 3.20 (2H, d, *J* = 7.2 Hz, H-1''), 5.05 (1H, br t, *J* = 7.2 Hz, H-7''), 5.18 (1H, br t, *J* = 6.8 Hz, H-2''), 5.32 (1H, dd, *J* = 2.8, 13.2 Hz, H-2), 5.92 (1H, s, H-8), 6.80 (2H, d, *J* = 8.4 Hz, H-3', 5'), 7.29 (2H, d, *J* = 8.8 Hz, H-2', 6') ppm.

Bonnaniol A (2.7): ^{1}H NMR ($CDCl_3$): δ_H 1.59 (3H, s, H-10''), 1.67 (3H, s, H-9''), 1.81 (3H, s, H-4''), 2.08 (4H, m, H-5'', 6''), 3.38 (2H, d, *J* = 7.6 Hz, H-1''), 4.53 (1H, d, *J* = 12 Hz, H-3), 4.99 (1H, d, *J* = 12 Hz, H-2), 5.03 (1H, m, H-7''), 5.25 (1H, br t, *J* = 6.8 Hz, H-2''), 6.00 (1H, s, H-8), 6.91 (2H, d, *J* = 8.4 Hz, H-3', 5'), 7.42 (2H, d, *J* = 8.8 Hz, H-2', 6') ppm.

Diplacol (2.8): ^{1}H NMR (CD_3OD): δ_H 1.55 (3H, s, H-10''), 1.61 (3H, s, H-9''), 1.74 (3H, s, H-4''), 1.95 (2H, m, H-6''), 2.03 (2H, m, H-5''), 3.21 (2H, d, *J* = 6.8 Hz, H-1''), 4.48 (1H, d, *J* = 11.6 Hz, H-3), 4.87 (1H, d, *J* = 11.6 Hz, H-2), 5.05 (1H, m, H-7''), 5.18 (1H,

m, H-2"), 5.91 (1H, s, H-8), 6.78 (1H, d, *J* = 7.6 Hz, H-5'), 6.83 (1H, d, *J* = 7.6 Hz, H-6'), 6.94 (1H, s, H-2') ppm.

Macarangaflavanone B (2.9): ^{1}H NMR ($CDCl_3$): δ_H 1.72 (6H, s, H-4"', 5"'), 1.78 (6H, s, H-4", 5"), 2.80 (1H, dd, *J* = 2.8, 17.2 Hz, H_{eq}-3), 3.05 (1H, dd, *J* = 12.8, 17.2 Hz, H_{ax}-3), 3.30 (2H, d, *J* = 6.0 Hz, H-1"'), 3.37 (2H, d, *J* = 6.0 Hz, H-1"), 5.21 (1H, m, H-2"'), 5.31 (1H, m, H-2"), 5.31 (1H, dd, *J* = 2.8, 12.8 Hz, H-2), 6.01 (1H, s, H-8), 6.84 (1H, d, *J* = 8.0 Hz, H-5'), 7.17 (1H, s, H-2'), 7.18 (1H, d, *J* = 8.0 Hz, H-6') ppm.

3'-Prenylaringenin (2.10): ^{1}H NMR ($CDCl_3$): δ_H 1.77 (6H, s, H-4", 5"), 2.75 (1H, dd, *J* = 2.8, 17.2 Hz, H_{eq}-3), 3.10 (1H, dd, *J* = 12.8, 17.2 Hz, H_{ax}-3), 3.37 (2H, d, *J* = 7.2 Hz, H-1"), 5.31 (1H, m, H-2"), 5.31 (1H, dd, *J* = 2.8, 12.8 Hz, H-2), 5.97 (1H, d, *J* = 2.0 Hz, H-6), 5.99 (1H, d, *J* = 2.0 Hz, H-8), 6.84 (1H, d, *J* = 8.8 Hz, H-5'), 7.17 (1H, s, H-2'), 7.18 (1H, d, *J* = 8.8 Hz, H-6') ppm.

3*S*-Acetoxy-eicosanoic Acid Ethyl Ester (2.11): transparent oil; $[\alpha]_D$ + 2.1° (*c* 0.20, $CHCl_3$); UV ($CHCl_3$) λ_{max} (log ε) 240 (1.94) nm; IR ν_{max} 2927, 2854, 1741, 1464, 1371, 1238 cm^{-1}; ^{1}H-NMR ($CDCl_3$): δ_H 0.86 (3H, t, *J* = 6.5 Hz, H-20), 0.86 (3H, t, *J* = 6.5 Hz, H-2'), 1.26-1.23 (30H, m, H-5 through 19), 1.58 (2H, m, H-4), 2.03 (3H, s, H-2"), 2.54 (2H, m, H-2), 4.14 (2H, q, *J* = 7.0, 14.0 Hz, H-1'), 5.21 (1H, m, H-3) ppm, ^{1}H-NMR (C_6D_6): δ_H 0.91 (3H, t, *J* = 6.6 Hz, H-20), 0.96 (3H, t, *J* = 7.0 Hz, H-2'), 1.18-1.34 (30H, m, H-5 through 19), 1.46 and 1.53 (2H, each m, H-4), 1.72 (3H, s, H-2"), 2.35 (1H, dd, *J* = 5.0, 15.2 Hz, H_{α}-2), 2.46 (1H, dd, *J* = 7.6, 15.2 Hz, H_{β}-2), 3.95 (2H, m, H-1'), 5.42 (1H,

m, H-3) ppm, and ^{13}C NMR (C_6D_6): 14.1 (C-2'), 14.3 (C-20), [23.0, 25.5, 29.7 x 2, 29.8, 29.9, 30.0, 30.1, 32.2 (C5-19)], 20.6 (C2''), 34.4 (C-4), 39.5 (C-2), 60.3 (C-1'), 70.6 (C-3), 169.6 (C-1''), 170.0 (C-1) ppm; HRFABMS *m/z* 399.3484 $[M+1]^+$ (calcd for $C_{24}H_{47}O_4$, *m/z* 399.3474).

3*S*-Acetoxy-eicosanoic Acid (2.12): transparent oil; ^{1}H-NMR (C_6D_6): δ_H 0.92 (3H, t, *J* = 6.4 Hz, H-20), 1.18-1.34 (30H, m, H-5 through 19), 1.50 (2H, m, H-4), 1.70 (3H, s, H-2''), 2.27 (1H, dd, *J* = 4.8, 15.6 Hz, H_α-2), 2.41 (1H, dd, *J* = 7.6, 15.6 Hz, H_β-2), 5.37 (1H, m, H-3) ppm; HRFABMS *m/z* 371.3157 $[M+1]^+$ (calcd for $C_{22}H_{43}O_4$, *m/z* 371.3161).

3*S*-Acetoxy-doeicosanoic Acid (2.13): transparent oil; $[\alpha]_D$ + 1.5° (*c* 0.13, $CHCl_3$); UV ($CHCl_3$) λ_{max} (log ε) 253 (2.88) nm; IR ν_{max} 2920, 2854, 1742, 1716, 1466, 1371, 1234 cm^{-1}; ^{1}H-NMR (C_6D_6): δ_H 0.92 (3H, t, *J* = 6.4 Hz, H-22), 1.14-1.34 (34H, m, H-5 through 21), 1.47 (2H, m, H-4), 1.70 (3H, s, H-2''), 2.27 (1H, dd, *J* = 4.8, 16 Hz, H_α-2), 2.42 (1H, dd, *J* = 7.6, 15.6 Hz, H_β-2), 5.37 (1H, m, H-3) ppm and ^{13}C NMR (C_6D_6): 14.3 (C-22), [23.0, 25.5, 29.7, 29.8, 29.9, 30.0 x 2, 30.1, 32.3 (C5-21)], 20.6 (C2''), 34.3 (C-4), 40.9 (C-2), 68.1 (C-3), 169.8 (C-1''), 175.7 (C-1) ppm; HRFABMS *m/z* 399.3446 $[M+1]^+$ (calcd for $C_{24}H_{47}O_4$, 399.3474).

1-Hydroxy-dodecan-2-one (2.14): ^{1}H-NMR ($CDCl_3$): δ_H 0.88 (3H, t, *J* = 6.8 Hz, H-11), 1.23-1.30 (14H, m, H-4 through 10), 1.63 (2H, m, H-3), 2.35 (2H, t, *J* = 8.0 Hz, H-2), 3.75 (2H, s, H-1') ppm; FABMS *m/z* 228.27 $[M+1]^+$ (calcd for $C_{14}H_{28}O_2$, *m/z* 228.37).

References

1. Murphy, B. T.; Cao, S.; Norris, A.; Miller, J. S.; Ratovoson, F.; Andriantsiferana, R.; Rasamison, V. E.; Kingston, D. G. I. Cytotoxic flavanones of *Schizolaena hystrix* of the Madagascar rainforest. *J. Nat. Prod*. **2005**, *68*, 417-419.
2. Murphy, B. T.; Cao, S.; Norris, A.; Miller, J. S.; Ratovoson, F.; Andriantsiferana, R.; Rasamison, V. E.; Kingston, D. G. I. Cytotoxic compounds of *Schizolaena hystrix* of the Madagascar rainforest. *Planta Med*. **2006**, *72*, 1235-1238.
3. Lowry, P. P.; Schatz, G. E.; Leroy, J.; Wolf, A. Endemic families of Madagascar. III. A synoptic revision of *Schizolaena* (Sarcolaenaceae). *Adansonia, sér 3* **1999**, *21*, 183-212.
4. Gaydou, E. M.; Ramanoelina, A. R. P. A survey of the Sarcolaenaceae for cyclopropene fatty acids. *Phytochemistry* **1983**, *22*, 1725-1728.
5. Dewick, P. M. Medicinal *Natural Products: A Biosynthetic Approach*; John Wiley and Sons Ltd.: Chichester, 2001.
6. Pietta, P. -G. Flavonoids as antioxidants. *J. Nat. Prod.* **2000**, *63*, 1035-1042.
7. Botta, B.; Vitali, A.; Menendez, P.; Misiti, D.; Monache, G. D. Prenylated flavonoids: pharmacology and biotechnology. *Curr. Med. Chem*. **2005**, *12*, 713-739.
8. Cidade, H. M.; Nacimento, M. S.; Pinto, M. M. M.; Kijjoa, A.; Silva, A. M. S.; Herz, W. Artelastocarpin and carpelastofuran, two new flavones, and cytotoxicities of prenyl flavonoids from *Artocarpus elasticus* against three cancer cell lines. *Planta Med*. **2001**, *67*, 867-870.

9. Miranda, C. L.; Stevens, J. F.; Helmrich, A.; Henderson, M. C.; Rodriguez, R. J.; Yang, Y. H.; Deinzer, M. L.; Barnes, D. W.; Buhler, D. R. Antiproliferative and cytotoxic effects of prenylated flavonoids from hops (*Humulus lupulus*) in human cancer cell lines. *Food Chem. Toxicol*. **1999**, *37*, 271-285.

10. Cao, S.; Schilling, J. K.; Miller, J. S.; Adriantsiferana, R.; Rasamison, V. E.; Kingston, D. G. I. Cytotoxic compounds from *Mundulea chapelieri* from the Madagascar rainforest. *J. Nat. Prod.* **2004**, *67*, 454-456.

11. Bruno, M.; Savona, G.; Lamartina, L.; Lentini, F. New flavonoids from *Bonannia graeca*. *Heterocycles* **1985**, *23*, 1147-1153.

12. Jakob, B.; Voss, G.; Gerlach, H. Synthesis of (*S*)- and (*R*)- 3-hydroxyhexadecanoic acid. *Tetrahedron: Asymmetry*, **1996**, *7*, 3255-62.

13. Wang, Y.; Tan, W.; Li, W. Z.; Li, Y. A facile synthetic approach to prenylated flavanones: first total syntheses of (±)-bonannione A and (±)-sophoraflavanone A. *J. Nat. Prod.* **2001**, *64*, 196-199.

14. Phillips, W. R.; Baj, N. J.; Gunatilaka, A. A. L.; Kingston, D. G. I. C-Geranyl compounds from *Mimulus clevelandii*. *J. Nat. Prod.,* **1996**, *59*, 495-497.

15. Schütz, B. A.; Wright, A. D.; Rali, T.; Sticher, O. Prenylated flavanones from leaves of *Macaranga pleiostemona*. *Phytochemistry*, **1995**, *40*, 1273-1277.

16. Seigler, D. Simpson, B. B.; Martin, C.; Neff, J. L. Free 3-acetoxy fatty acids in floral glands of *Krameria* species. *Phytochemistry*. **1978**, *17*, 995-996.

17. Lincoln, D. Leaf resin flavonoids of *Diplacus aurantiacus*. *Biochem. Syst. Ecol*. **1980**, *8*, 397-400.

18. Nkengfack, A. E.; Sanson, D. R.; Tempesta, M. S.; Fomum, Z. T. Two new flavonoids from *Erythrina eriotriocha*. **1989**, *52*, 320-324.

19. Meyer, C.; Lutz, A.; Spiteller, G. α-Hydroxy aldehyde derivatives as secondary products of the oxidation of plasmalogens. *Agnew. Chem. Int. Ed.* **1992**, *31*, 468-470.

20. Louie, K. G.; Behrens, B. C.; Kinsella, T. J.; Hamilton, T. C.; Grotzinger, K. R.; McKoy, W. M.; Winker, M. A.; Ozols, R. F. Radiation survival parameters of antineoplastic drug-sensitive and -resistant human ovarian cancer cell lines and their modification by buthionine sulfoximine. *Cancer Res.* **1985**, *45*, 2110–2115.

III. Antiproliferative Compounds of *Artabotrys madagascariensis* from the Madagascar Rainforest [1]

3.1 Introduction

Bioassay-guided fractionation of an ethanol extract of *Artabotrys madagascariensis* led to the isolation of a new oxygenated cyclohexene derivative, two butenolides, and a tetracyclic triperpene. The butenolides have been reported to have potent cytotoxicity (0.08-2.0 μg/mL) against a variety of tumor cell lines.[2] Structure elucidation was carried out by one and two-dimensional NMR spectroscopy, and the absolute configuration of compounds **3.1 - 3.3** was verified by analysis of their CD spectra and optical rotations. Two of the isolates, melodorinol (**3.2**) and acetylmelodorinol (**3.3**), were found to display antiproliferative activity against five different tumor cell lines with IC_{50} values ranging from 2.4 to 12 μM. This chapter is an expanded version of a published paper on this plant species.[1]

3.1.1 Previous Investigations of Artabotrys madagascariensis

Often referred to as the custard-apple family, Annonaceae is the largest family of Magnoliales, consisting of approximately 2300 species in 130 genera. To our knowledge, there are no known published reports on the chemistry of *A. madagascariensis* Miq, however a survey of the literature on the genus *Artabotrys* revealed a large number of chemical investigations. The genus *Artabotrys* contains approximately 100 species of lianas situated throughout the tropical areas of Africa, Asia, and the western Pacific.[3] From it have been isolated isoquinoline and cytotoxic aporphine alkaloids,[4,5] butyrolactones,[6] sesquiterpenes,[7] flavonol glycosides,[8] and the antimalarial

chemotherapeutic peroxides yingzhaosu A-D,[9-11] thus affirming the truly diverse structural repertoire of this genus.

3.1.2 Chemical Investigation of Artabotrys madagascariensis

In our continuing search for biologically active natural products from tropical rainforests as part of an International Cooperative Biodiversity Group (ICBG) program, we obtained an ethanol extract from *Artabotrys madagascariensis* of the family Annonaceae. Bioassay-guided fractionation of an ethanol extract of the leaves and fruits of *A. madagascariensis* led to the isolation of the novel compound artabotrene (**3.1**), two bioactive butenolides, melodorinol (**3.2**) and acetylmelodorinol (**3.3**), and the tetracyclic triterpene polycarpol (**3.4**). Structure elucidation was determined on the basis of one and two-dimensional NMR spectra, and absolute configuration was verified upon analysis of CD and optical rotation data.

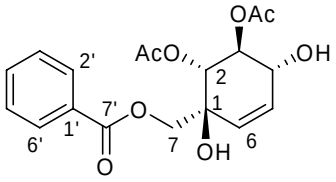

3.1

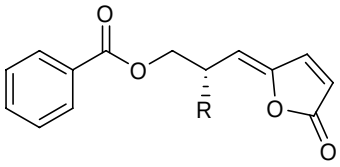

3.2 R = OH
3.3 R = OAc

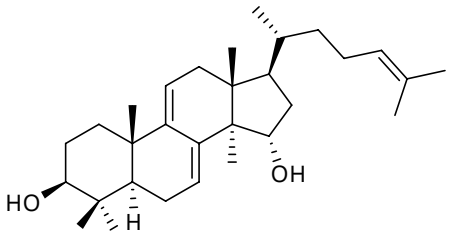

3.4

Figure 3.1. *Compounds of Artabotrys madagascariensis.*

3.2 Results and Discussion

3.2.1 Isolation of Compounds from A. madagascariensis

Four compounds were isolated from the leaves and fruits of *A. madagascariensis* by employing bioassay-guided fractionation, as shown in Scheme 3.1. The crude plant extract was suspended between hexanes and 90% aqueous methanol to yield two separate fractions. The aqueous methanol fraction was then diluted to 60% methanol and partitioned with chloroform. The organic chloroform layer was found to be active, thus it was further separated using silica gel flash column chromatography. Three fractions were produced from the flash column; the two least polar were found to be active (fractions A and B).

Fraction A was separated using preparative silica gel HPLC with chloroform as the eluent to afford six fractions, two of which were pure compounds: fraction F (**3.3**, 27 mg) and fraction G (**3.4**, 15 mg). Fraction B was also separated using preparative silica gel HPLC with chloroform to afford four fractions, two of which were pure compounds: fraction J (**3.2**, 3.8 mg) and fraction K (**3.1**, 0.5 mg).

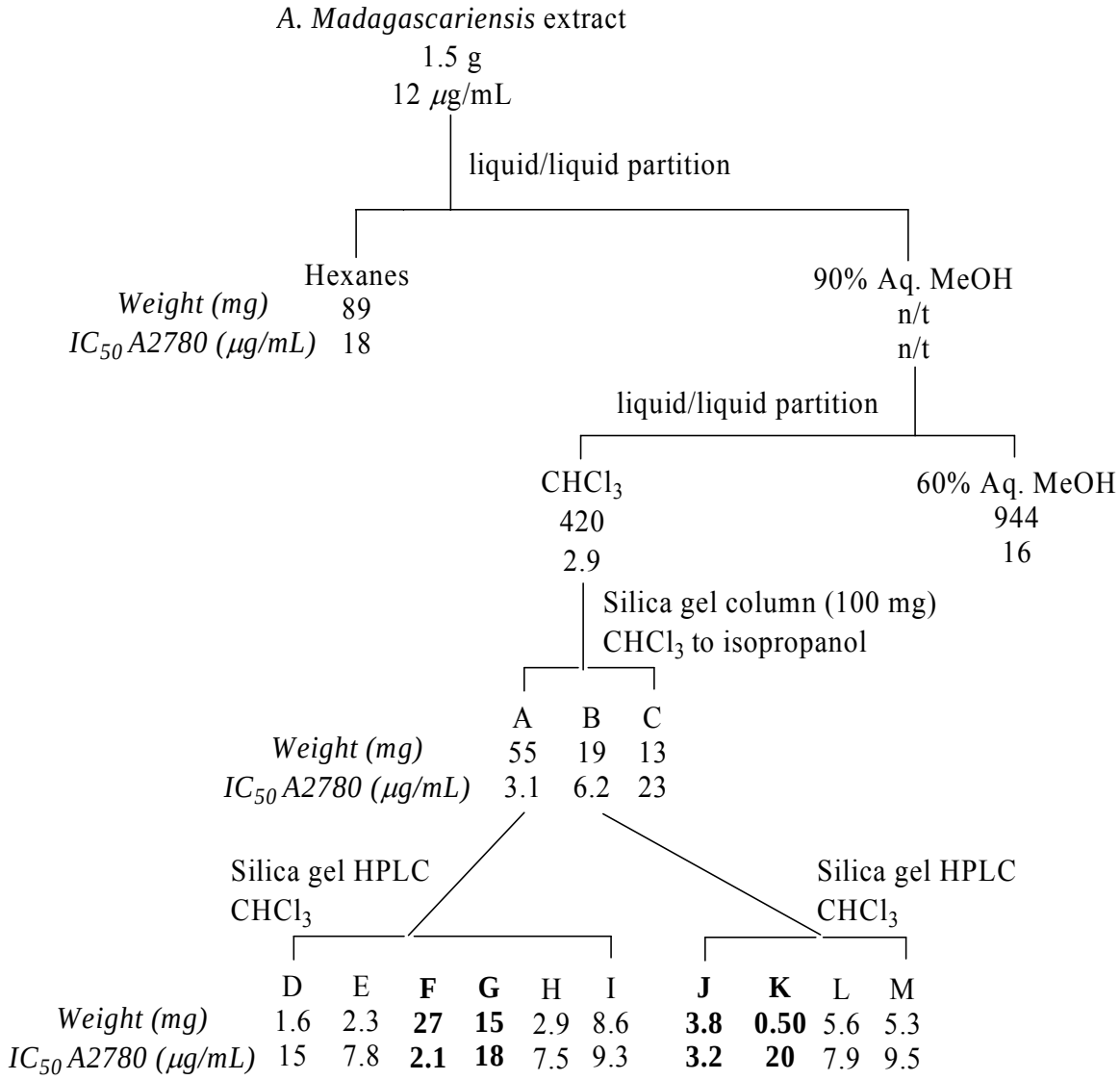

Scheme 3.1. *Isolation of compounds from A. madagascariensis.*

*3.2.2. Structure Elucidation of Artabotrene (**3.1**)*

Artabotrene (**3.1**) was obtained as a transparent oil. Positive-ion HRFABMS analysis gave a pseudomolecular ion at *m/z* 365.12430 ($[M+H]^+$), which suggested a molecular formula of $C_{18}H_{20}O_8$. ^1H and ^{13}C NMR data are presented in Table 3.1. The ^{13}C NMR spectrum of **3.1** in $CDCl_3$ displayed resonances for three ester carbonyls (δ_C 168.7, C-7';

170.3, 2-O<u>CO</u>CH_3; and 170.4, 3-O<u>CO</u>CH_3) as well as two acetyl methyls (δ_C 20.6, 2-OCO<u>CH_3</u>; and 20.9, 3-OCO<u>CH_3</u>), five sp^3-oxygenated carbons (δ_C 76.3, C-1; 74.7, C-2; 71.2, C-3; 73.8, C-4; and 65.1, C-7), and eight sp^2-carbons (δ_C 125.4, C-5; 131.6, C-6; 129.3, C-1'; 129.9, C-2', -6'; 128.6, C-3', -5'; and 133.7, C-4'). The ^{1}H NMR spectrum of **3.1** in $CDCl_3$ suggested the existence of a mono-substituted benzene ring, due to characteristic resonances in the aromatic region (δ_H 8.08, d, J = 8.0 Hz, H-2', -6'; 7.48, t, J = 8.0 Hz, H-3', -5'; and 7.61, t, J = 7.6 Hz, H-4'). This left two sp^2-carbons unaccounted for (C-5 and C-6), and analysis of the COSY spectrum identified them as being part of the six-membered ring *via* connectivity of H-6 (δ_H 5.83, ddd, J = 10.4, 2.0, 2.0 Hz) with H-5 (δ_H 5.62, ddd, J = 10.4, 2.8, 2.8 Hz), H-5 with H-4 (δ_H 4.53, m), H-4 with H-3 (δ_H 5.77, m), and H-3 with H-2 (δ_H 5.33, d, J = 8.0 Hz). The contour between H-4 and H-3 was weak, thus the proposed linkage was confirmed by the employment of 1D TOCSY. The HMBC correlation of H-2 to the carbonyl signal at δ_C 170.3 (Figure 3.2), proved the location of that particular acetoxy group. The placement of a hydroxyl moiety (δ_H 2.92, br s) at position 4 was also confirmed by a COSY spectrum. Another hydroxyl group was placed at the 1-position based on the molecular formula and the ^{13}C chemical shift of C-1. The location of the second acetoxy moiety at the 3-position was supported by the deshielded nature of H-3, in comparison with typical hydroxylated protons.

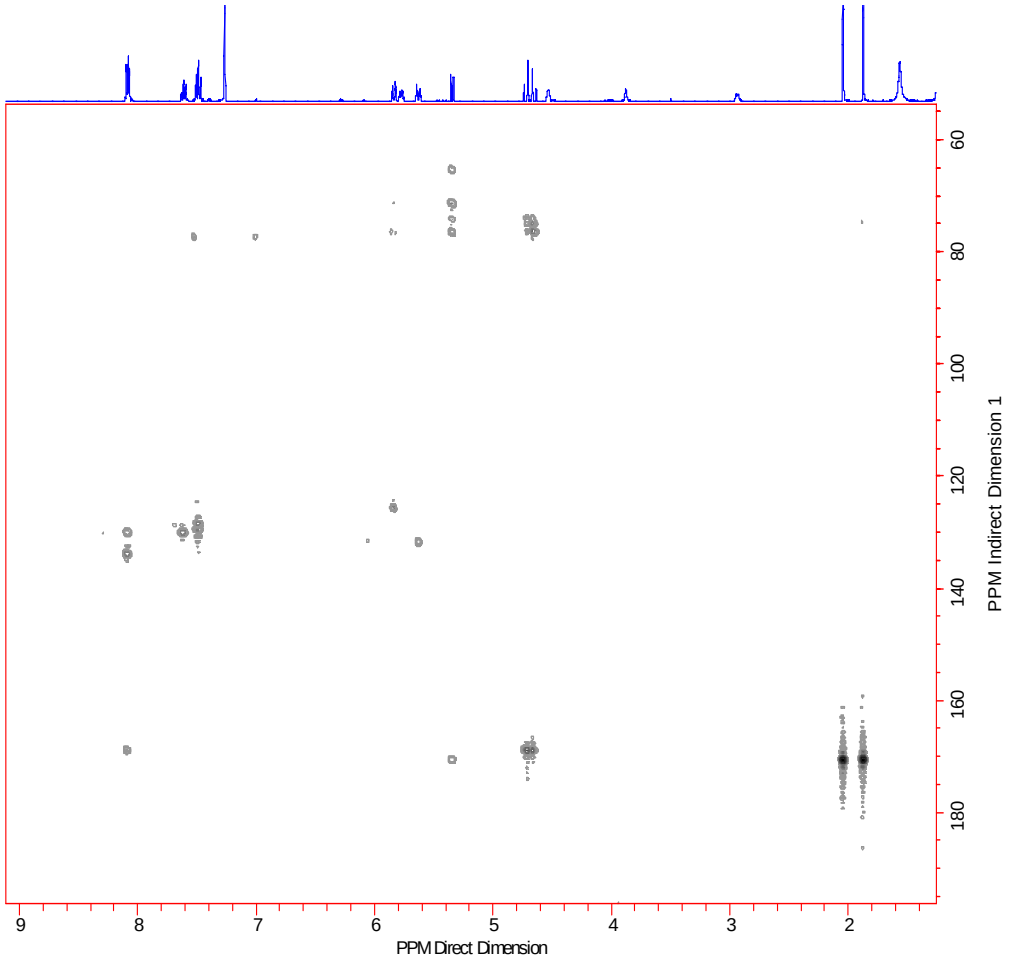

Figure 3.2. *HMBC spectrum of artabotrene (**3.1**).*

Key HMBC correlations of C-1 with protons H-2, -6, and -7 (δ_H 4.72, d, J = 12.8 Hz, H_α-7 and 4.65, d, J = 12.8 Hz, H_β-7), were observed. Finally, the flat structure was confirmed through HMBC correlations of H_2-7 and H-2′, -6′ with C-7′, thus placing the carbonyl directly adjacent to the aromatic ring. The relative configuration of **3.1** was determined by analysis of its ROESY spectrum (Figure 3.3). H-2 showed a through space correlation with H-4, representing axial-axial proton interactions, and the same type of interaction was observed between H-3 and the protons at H_2-7. This half-chair

conformation along with critical 2D correlations are shown in Figure 3.3. A compound with an identical flat structure was previously reported as a synthetic intermediate, though the configuration was slightly different.[12] The absolute configuration of **3.1** was determined by comparison of its CD spectrum with that of a known polyoxygenated cyclohexene derivative from *Uvaria rufa* with identical relative but known absolute configuration.[13] This analog, uvarirufol B, contained an OBz moiety at the 3-position as opposed to the acetoxy present in **3.1**. Artabotrol had a CD spectrum with a trend opposite to that of uvarirufol B. These differences indicated that the two compounds had the opposite absolute stereochemistry. In addition, the sign of optical rotation for **3.1** in $CHCl_3$ ($[\alpha]_D$ + 89.4°) was opposite to that of its counterpart uvarirufol B ($[\alpha]_D$ - 178°). Hence the absolute configuration of artabotrene (**3.1**) was determined to be (1*S*, 2*R*, 3*S*, 4*R*).

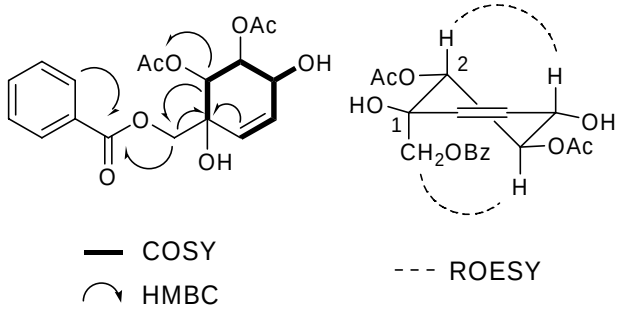

Figure 3.3. *Select 2D NMR correlations of artabotrene (**3.1**).*

Table 3.1. NMR Spectroscopic Data of Artabotrene (**3.1**) in $CDCl_3$[a]

	3.1	
position	^{13}C[b]	^{1}H[b,c] (*J*, Hz)
1	76.3	-
2	74.7	5.33 d (8.0)
3	71.2	5.77 m
4	73.8	4.53 m
5	125.4	5.62 ddd (10.4, 2.8, 2.8)
6	131.6	5.83 ddd (10.4, 2.0, 2.0)
7	65.1	4.72 d (12.8)
		4.65 d (12.8)
2-O<u>CO</u>CH_3	170.3	-
2-OCO<u>CH_3</u>	20.6	1.87 s
3-O<u>CO</u>CH_3	170.4	-
3-OCO<u>CH_3</u>	20.9	2.04 s
1'	129.3	-
2', 6'	129.9	8.08 d (8.0)
3', 5'	128.6	7.48 t (8.0)
4'	133.7	7.61 t (7.6)
7’	168.7	-
1-OH	-	3.87 br s
4-OH	-	2.92 br s

[a]Assignments based on COSY, HMBC, HSQC. [b]Chemical shifts (δ) in ppm. [c] br s: broad singlet; d: doublet; m: multiplet. *J* values in bracket.

3.2.3. Identification of Known Compounds from A. madagascariensis

The butenolides melodorinol (**3.2**) and acetylmelodorinol (**3.3**) were identified on the basis of their one- and two-dimensional NMR spectra (Figure 3.4), optical rotation data, and subsequent comparison to literature values.[2,14] The existence of benzoyl derivatives in Annonaceous plants is not uncommon, and a brief summary of biosynthetic origins of these compounds has been published.[14] However, there have been a few reports involving the isolation of such C-7 benzoyl derivatives,[2, 14, 17] and the total synthesis of these compounds by various methods has been reported.[15, 16]

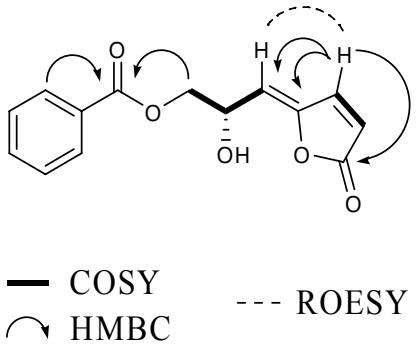

Figure 3.4. *Select 2D NMR correlations of melodorinol (**3.2**).*

The triterpene polycarpol (**3.4**) was originally isolated from the leaves and stem barks of *Polyalthia oliveri* (Annonaceae).[18] It has recently been reported to be an agonist of liver X receptors, thus increasing cellular cholesterol efflux, lowering LDL, and raising HDL levels.[19] Its flat structure was identified on the basis of one- and two dimensional NMR data, while analysis of its ROESY spectrum confirmed its configuration.

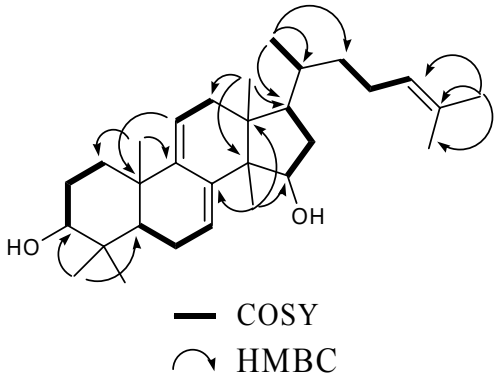

Figure 3.5. *Select 2D NMR correlations of polycarpol (**3.4**).*

3.2.4. Antiproliferative Evaluation of Compounds from A. madagascariensis.

All of the isolates were tested against the A2780 human ovarian cancer cell line,[20] and compounds **3.2** and **3.3** were tested against four additional cell lines (MDA-MB-435, breast cancer; HT-29, colon cancer; H522-T1, non-small cell cancer; U937, histiocytic lymphoma). The results are shown in Table 3.2. Of the four compounds, **3.2** and **3.3** displayed moderate antiproliferative activity, with the additional acetyl moiety of **3.3** apparently leading to the increase in activity. Overall, compounds **3.2** and **3.3** exhibited general antiproliferative activity toward tumor cells, and thus further exploration of their bioactive potential was stopped. It was postulated that the γ-(*Z*)-alkylidenebutenolide moiety was responsible for the general bioactivity of these compounds.[2]

Table 3.2. *Antiproliferative Data of Compounds **3.1-3.4***

compound	IC_{50} (μM)				
	A2780[a]	MDA-MB-435[b]	HT-29[b]	H522-T1[b]	U937[b]
3.1	55	-	-	-	-
3.2	12	8.6	5.8	7.3	6.2
3.3	6.9	6.8	2.6	2.4	5.6
3.4	41	-	-	-	-

[a]Concentration of each compound that inhibited 50% of the growth of the A2780 human ovarian cell line according to the procedure described,[21] with actinomycin D (IC_{50} 0.8-2.4 nM) as the positive control. Assay carried out by Ms. Peggy Brodie.

[b]Concentration of a compound which inhibited cell growth by 50% compared to untreated cell populations, with vinblastine as the positive control (average IC_{50} 0.27 nM (MDA-MB-435), 0.53 nM (HT-29), 1.38 nM (H522-T1) and 0.49 nM (U937). These assays were carried out at the Eisai Research Institute, Waltham, MA.

3.3 Experimental Section.

General Experimental Procedures.

IR and UV spectra were measured on MIDAC M-series FTIR and Shimadzu UV-1201 spectrophotometers, respectively. Optical rotations were recorded on a Perkin-

Elmer 241 polarimeter. CD analysis was performed on a Jasco J-720 spectropolarimeter, and data is expressed in terms of circular-dichroic absorption, $\Delta\varepsilon$ (cm^2 x $mmole^{-1}$). NMR spectra were obtained on JEOL Eclipse 500, Varion Inova 400, and Varion Unity 400 spectrometers. Mass spectra were obtained on a JEOL JMS-HX-110 instrument. Chemical shifts are given in δ (ppm), and coupling constants (*J*) are reported in Hz. HPLC was performed using either Shimadzu LC-8A pumps coupled with a Varian Dynamax preparative silica column (250 x 21.4 mm), or Shimadzu LC-10AT pumps coupled with a Varian Dynamax semi-preparative silica column (250 x 10 mm). Both HPLC systems employed a Shimadzu SPD-M10A diode array detector.

Plant Material.

Samples of leaves and fruits of *Artabotrys madagascariensis* Miq were collected by botanists from the Missouri Botanical Garden in December 2004. The plant was a well branched shrub with green aromatic fruit growing in a degraded forest, on calcareous rock on the Montagne des Français, Antsiranana province, Madagascar (12.23.27 S / 49.20.01. E, elevation 410 m). The herbarium voucher specimen for the sample is Stephan Rakotonandrasana et al. 884. Duplicate voucher specimens were deposited at herbaria of the Centre National d'Application des Recherches Pharmaceutiques, Madagascar (CNARP), the Parc Botanique et Zoologique de Tsimbazaza, Madagascar (TAN), the Missouri Botanical Garden, St. Louis, Missouri (MO), and the Muséum National d'Histoires Naturelles, Paris, France (P).

Antiproliferative Bioassays.

The A2780 ovarian cancer cell line antiproliferative assay was performed at Virginia Polytechnic Institute and State University as previously reported.[20]

Additional activity testing was performed at Eisai Research Institute, in Andover, MA. Antiproliferative effects of compounds **3.2** and **3.3** were evaluated in four cultured human cancer cell lines: MDA-MB-435 breast cancer cells, HT-29 colon cancer cells, H522-T1 non-small cell cancer cells, and U937 histiocytic lymphoma cells. The cells were placed into 96-well plates and grown in the absence or continuous presence of 0.3 – 10,000 nM compounds for 96 h. Cell growth was assessed using the CellTiter-Glo® Luminescent Cell Viability Assay (Promega) according to manufacturer's recommendations. Luminescence was read on a Victor^{2}V 1420 MultiLabel HTS Counter (Perkin-Elmer/Wallac). IC_{50} values were determined as the concentration of a compound which inhibits cell growth by 50% compared to untreated cell populations. Two separate replicate experiments were performed.

Extract Preparation

The leaves and fruit of A. madagascariensis were extracted with ethanol by scientists at CNARP, Antananarivo, Madagascar to yield extract MG 2898.

Bioassay-guided Fractionation of Compounds from *A. madagascariensis*.

Extract MG 2898 (1.5 g) was suspended in aqueous MeOH (MeOH-H_2O, 9:1, 350 mL) and extracted with hexanes (2 x 150 mL). The aqueous MeOH fraction was then

adjusted to 60 % aqueous MeOH, and extracted with $CHCl_3$ (2 x 150 mL). The $CHCl_3$ fraction displayed antiproliferative activity (420 mg, IC_{50} = 2.9 μg/mL), and 100 mg was further chromatographed over silica gel using a step gradient of $CHCl_3$-isopropanol to yield three fractions (A-C). Fraction A (54.8 mg, 3.1 μg/mL) was further chromatographed using an isocratic flow of 100 % $CHCl_3$ (10.0 mL/min) on a preparative silica HPLC column to furnish six fractions (D-I). Fraction F was identified as **3.3** (t_R 8.7 min, 27 mg). Fraction G was identified as **3.4** (t_R 12.0 min, 15 mg).

Fraction B (19.5 mg, 6.2 μg/mL) also displayed antiproliferative activity, therefore it was subjected to preparative silica HPLC using the previously described conditions to yield four fractions (J-M). Fraction J was identified as **3.2** (t_R 17.6 min, 3.8 mg). Fraction K was identified as the novel compound **3.1** (t_R 16.5 min, 0.5 mg). An additional 3.0 mg of **3.1** was later obtained through similar fractionation techniques. It should be noted that the activity of fraction B was due to the presence of the pair of butenolides (**3.3** and **3.4**), which proved to be quite abundant throughout the plant. The structure of the known compound **3.4** was identified by interpretation of one and two-dimensional NMR spectra.

Artabotrene (1*S*, 2*R*, 3*S*, 4*R*) (3.1): Transparent oil, $[\alpha]_D$ + 89.4° (c 0.10, $CHCl_3$); UV (CH_3OH) λ_{max} (log ε) 230 (3.92) nm, 272 (3.42) nm; IR ν_{max} 3454, 2956, 1748, 1722, 1369, 1272, 1241, 1227, 1114, 1044, 1026, 711 cm^{-1}; CD (MeOH) $[\theta]_{210}$ -69, $[\theta]_{240}$ 15.7, $[\theta]_{260}$ 21.4, $[\theta]_{287}$ 10.4; ^1H and ^{13}C NMR ($CDCl_3$), see Table 3.1; HRFABMS *m/z* 365.1243 $[M+1]^+$ (calcd for $C_{18}H_{21}O_8$, 365.1236).

Melodorinol (3.2): $[\alpha]_D$ + 35.9° (*c* 0.17, $CHCl_3$), ^{1}H-NMR (CD_3OD): δ_H 4.37 (2H, ddd, *J* = 6.0, 10.8, 16.8 Hz, H-8), 5.06 (1H, dt, *J* = 6.0, 8.4 Hz, H-7), 5.49 (1H, d, *J* = 8.4 Hz, H-6), 6.30 (1H, d, *J* = 5.6 Hz, H-3), 7.45 (2H, t, *J* = 8.0 Hz, H-13, 15), 7.59 (1H, t, *J* = 7.2 Hz, H-14), 7.67 (1H, d, *J* = 5.2 Hz, H-4), 8.03 (2H, d, *J* = 7.2 Hz, H-12, 16) ppm and ^{13}C-NMR (CD_3OD): δ_C 65.8 (C-7), 68.3 (C-8), 115.2 (C-6), 121.5 (C-3), 129.5 (C-13, 15), 130.6 (C-12, 16), 131.2 (C-11), 134.3 (C-14), 145.8 (C-4), 151.7 (C-5), 167.7 (C-10), 171.0 (C-2).

Acetylmelodorinol (3.3): $[\alpha]_D$ + 22.3° (*c* 0.21, $CHCl_3$), ^{1}H-NMR (CD_3OD): δ_H 2.07 (3H, s, H-17, 4.52 (2H, ddd, *J* = 6.4, 12.0, 29.6 Hz, H-8), 5.52 (1H, d, *J* = 8.0 Hz, H-6), 6.11 (1H, m, H-7), 6.34 (1H, d, *J* = 5.2 Hz, H-3), 7.46 (2H, t, *J* = 7.6 Hz, H-13, 15), 7.60 (1H, t, *J* = 7.2 Hz, H-14), 7.67 (1H, d, *J* = 5.2 Hz, H-4), 8.00 (2H, d, *J* = 7.2 Hz, H-12, 16) ppm and ^{13}C-NMR (CD_3OD): δ_C 20.7 (C-17), 65.7 (C-8), 68.5 (C-7), 109.7 (C-6), 122.1 (C-3), 129.6 (C-13, 15), 130.6 (C-12, 16), 130.9 (C-11), 134.5 (C-14), 145.5 (C-4), 152.7 (C-5), 167.4 (C-10), 170.5 (C-2), 171.6 (C-16).

Polycarpol (3.4): ^{1}H-NMR ($CDCl_3$): δ_H 0.60 (3H, s, H-18), 0.87 (3H, s, H-21), 0.87 (3H, s, H-28), 0.93 (3H, s, H-30), 0.97 (3H, s, H-19), 0.99 (3H, s, H-29), 1.03 (2H, m, H-22), 1.09 (1H, dd, *J* = 3.2, 9.6 Hz, H-5), 1.37 (1H, m, H-20), 1.44 (1H, dd, *J* = 3.2, 10.4 Hz, H_α-1), 1.59 (3H, s, H-27), 1.66 (1H, m, H-17), 1.68 (3H, s, H-26), 1.70-1.73 (2H, m, H-2), 1.73 (1H, m, H_α-16), 1.85 (1H, m, H_α-23), 1.94 (1H, m, H_β-16), 1.96 (1H, m, H_β-1), 1.97 (1H, m, H_β-23), 1.99 (1H, m, H_α-6), 2.02 (1H, m, H_α-12), 2.15 (1H, ddd, *J* = 3.6, 5.2, 13.6 Hz, H_β-6), 2.28 (1H, br d, *J* = 14.4, H_β-12), 3.24 (1H, dd, *J* = 3.6, 9.2, H-3),

4.26 (1H, dd, *J* = 4.4, 7.6, H-15), 5.08 (1H, br t, *J* = 6.0, H-24), 5.30 (1H, br d, *J* = 4.4, H-11), 5.84 (1H, br d, *J* = 5.6, H-11) ppm and ^{13}C-NMR ($CDCl_3$): δ_C 15.8 (C-21 or C-28), 15.9 (C-18), 17.1 (C-30), 17.6 (C-27), 18.4 (C-21 or C-28), 22.8 (C-19), 22.9 (C-6), 24.8 (C-23), 25.7 (C-26), 27.7 (C-2), 28.1 (C-29), 35.7 (C-20), 35.8 (C-1), 36.2 (C-22), 37.4 (C-10), 38.5 (C-4), 38.7 (C-12), 40.1 (C-16), 44.3 (C-13), 48.8 (C-17), 48.9 (C-5), 51.9 (C-14), 74.8 (C-15), 78.9 (C-3), 116.0 (C-11), 121.3 (C-7), 124.9 (C-24), 131.2 (C-25), 140.8 (C-8), 146.0 (C-9).

References

1. Murphy, B. T.; Cao, S.; Brodie, P.; Miller, J. S.; Ratovoson, F.; Andriantsiferana, R.; Rasamison, V. E.; TenDyke, K.; Suh, E. M.; Kingston, D. G. I. Antiproliferative compounds of *Artabotrys madagascariensis* from the Madagascar rainforest. *Nat. Prod. Res*., in press.
2. Tuchinda, P.; Udchachon, J.; Reutrakul, V.; Santisuk, T.; Taylor, W. C.; Farnsworth, N. R.; Pezzuto, J. M.; Kinghorn, A. D. Bioactive butenolides from *Melodorum fruticosm*. *Phytochemistry* **1991**, *30*, 2685-2689.
3. Mabberley, D. J. *The Plant Book*. 2nd ed. Cambridge University Press, Cambridge, **1997**.
4. Sagen, A-L.; Sahpaz, S.; Mavi, S.; Hostettmann, K. Isoquinoline alkaloids from *Atrabotrys brachypetalus*. *Biochem. Sys. Ecol.* **2003,** *31*, 1447.
5. Wu, Y. C.; Chen, C. H.; Yang, T. H.; Lu, S. T.; McPhail, D. R.; McPhail, A. T.; Lee, K. H. Antitumor agents. Part 101. Cytotoxic aporphines from *Artabotrys*

uncinatus and the structure and stereochemistry of artacinatine. *Phytochemistry* **1989**, *28*, 2191.

6. Wong, H-F.; Brown, G. D. β-Methoxy-γ-methylene-α,β-unsaturated-γ-butyrolactones from *Artabotrys hexapetalus*. *Phytochemistry* **2002**, *59*, 99.

7. Fleischer, T. C.; Waigh, R. D.; Waterman, P. G. Pogostol *O*-methyl ether and artabotrol: two novel sesquiterpenes from the stem bark of *Artabotrys stenopetalus*. *J. Nat. Prod*. **1997**, *60*, 1054.

8. Singh, A. P.; Sahai, M. Isolation of flavonol glycosides from the leaves of *Artabotrys odoratissimus*. *Planta Med*. **1996**, *62*, 192.

9. Liang, X-T.; Yu, D-Q. ; Wu, W-L. ; Deng, H-C. Structure of yingzhaosu A**.** *Huaxue Xuebao* **1979**, *37*, 215.

10. Liang, X-T.; Yu, D-Q. ; Pan, W-D. Structure of yingzhaosu B**.** *Huaxue Xuebao* **1979**, *37*, 231.

11. Zhang, L.; Zhou, W-S. ; Xu, X-X. A new sesquiterpene peroxide (yingzhaosu C) and sesquiterpenol (yingzhaosu D) from *Artabotrys unciatus* (L.) Meer. *J. Am. Chem. Soc., Chem. Commun.* **1988**, *8*, 523.

12. Kupchan, S. M.; Hemingway, R. J.; Smith, R. M. Tumor inhibitors. XLV. Crotepoxide, a novel cyclohexane diepoxide tumor inhibitor from *Croton macrostachys*. *J. Org. Chem.* **1969**, *34*, 3898-3903.

13. Zhang, L.; Yang, S-P.; Liao, S-G.; Wu, Y.; Yue, J-M. Polyoxygenated cyclohexene derivatives from *Uvaria rufa*. *Helv. Chim. Acta* **2006**, *89*, 1408.

14. Jung, J. H.; Pummangura, S.; Patarapanich, C.; Chaichantipyuth, C.; Fanwick, P. E.; Chang, C-J.; McLaughlin, J. L. New bioactive heptenes from *Melodorum fruticosm* (Annonaceae). *Tetrahedron* **1990**, *46*, 5043-5054.

15. Shen, C.; Chou, S.; Chou, C. Total synthesis of acetylmelodorinol. *Tetrahedron: Asymmetry* **1996**, *7*, 3141-3146.

16. Lu, X.; Chen, G.; Xia, L.; Guo, G. Total synthesis of both enantiomers of melodorinol. Redetermination of their absolute configuration. *Tetrahedron: Asymmetry*, **1997** *8*, 3067.

17. Jung, J. H.; Chang, C. J.; Smith, D. L.; McLaughlin, J. L.; Pummangura, S.; Chaichantipyuth, C.; Patarapanich, C. Additional bioactive heptenes from *Melodorum fruticosum*. *J. Nat. Prod.* **1991**, *54*, 500.

18. Hamonniere, M.; Leboeuf, M.; Cave, A. Alkaloids from Annonaceae. Part 15. Aporphine alkaloids and terpenoid compounds from *Polyalthia oliveri*. *Phytochemistry*, **1977** *16*, 1029-1034.

19. Jayasuriya, H.; Herath, K. B.; Ondeyka, J. G.; Guan, Z.; Borris, R. P.; Tiwari, S.; Jong, W.; Chavez, F.; Moss, J.; Stevenson, D. W.; Beck, H. T.; Slattery, M.; Zamora, N.; Schulman, M.; Ali, A.; Sharma, N.; MacNaul, K.; Hayes, N.; Menke, J. G.; Singh, S. B. Diterpenoid, steroid, and triterpenoid agonists of liver X receptors from diversified terrestrial plants and marine sources. *J. Nat. Prod*. **2005**, *68*, 1247-1252.

20. Cao S.; Brodie, P. J.; Miller J. S.; Randrianaivo, R.; Ratovoson, F.; Birkinshaw, C.; Andriantsiferana, R.; Rasamison, V. E.; Kingston D. G. I. Antiproliferative

xanthones of *Terminalia calcicola* from the Madagascar rain forest. *J. Nat. Prod*. **2007**, *70*, 679-681.

21. Louie K. G.; Behrens B. C.; Kinsella T. J.; Hamilton, T. C.; Grotzinger, K. R.; McKoy W. M.; Winker M. A.; Ozols, R. F. Radiation survival parameters of antineoplastic drug-sensitive and –resistant human ovarian cancer cell lines and their modification by buthionine sulfoximine. *Cancer Res.* **1985**, *45*, 2110.

IV. Antiproliferative Limonoids of a *Malleastrum* sp. from the Madagascar Rainforest [1]

4.1 Introduction

Bioassay-guided fractionation of an ethanol extract of a *Malleastrum* sp. afforded three new limonoids (**4.1 - 4.3**), designated malleastrones A-C, respectively. Structure elucidation of the isolates was carried out by analysis of one and two-dimensional NMR spectroscopy and X-ray diffraction data. The novel isolates **4.1 - 4.3** were tested for antiproliferative activity against the A2780 human ovarian cancer cell line, and exhibited IC_{50} values of 0.49, 0.63, and 18 μM, respectively. This chapter is an expanded version of a published paper on this plant species.[1]

4.1.1 Previous Investigations of Malleastrum sp.

Meliaceae, or the mahogany family, comprises approximately 550 species contained within 51 genera. Of the 51 genera, 22 are endemic to southern and eastern Africa and Madagascar.[2] Meliaceae is most widely known for its production of structurally unique, highly oxygenated, and biologically active limonoids. To our knowledge this is the first reported chemical investigation of the genus *Malleastrum*.

4.1.2 Chemical Investigation of Malleastrum sp.

In our continuing search for biologically active natural products from tropical rainforests as part of an International Cooperative Biodiversity Group (ICBG) program, we obtained an extract from *Malleastrum* sp. of the family Meliaceae. The taxonomy of the *Malleastrum* genus is complex, and it has not proved possible to identify this

collection to the species level. Bioassay-guided fractionation of an ethanol extract of *Malleastrum* sp. afforded three new limonoids (**4.1** - **4.3**), designated malleastrones A-C, respectively. Each contained a tetranortriterpenoid skeleton that has rarely been reported in literature.[3,4] Structure elucidation of **4.1** and **4.2** was carried out by analysis of one and two-dimensional NMR spectroscopy and X-ray diffraction data, while the structure of **4.3** was elucidated by analysis of g-COSY, g-HSQC, g-HMBC, and ROESY data, and comparison of ^{13}C chemical shifts with those of malleastrone A (**4.1**). The novel isolates were tested for antiproliferative activity against a variety of tumor cell lines, and exhibited IC_{50} values ranging from 0.19 – 0.63 μM.

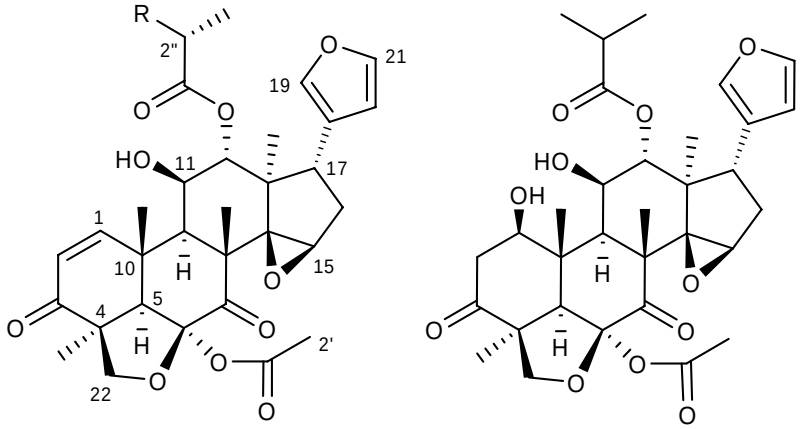

R

4.1 CH_3

4.2 CH_2CH_3

4.3

Figure 4.1. *Compounds of Malleastrum* sp.

4.1.3 Previous Investigations of Limonoids

Limonoids are a class of highly oxygenated and modified triterpenes called tetranortriterpenoids, and boast a diverse and imaginative structural repertoire.

Limonoids are best known for being responsible for the bitter taste of citrus fruits. The first limonoid to be isolated from a bitter citrus fruit was limonin (**4.4**), and the term "limonoids" is derived from this compound.[5] These molecules occur predominantly in plants of the order Rutales, and more specifically from the families Rutaceae and Meliaceae.[5] A wide range of biological activities for this compound class has been reported, including anti-microbial,[6] insecticidal,[7] anti-HIV,[8,9] anti-malarial,[10,11] and anti-cancer.[12,13]

In regard to the latter, obacunone (**4.5**) was found to significantly enhance the cytotoxicity against of two microtubule inhibitors, taxol and vinblastine, against drug-sensitive KB-3-1 and multidrug resistant KB-V1 cells.[12]

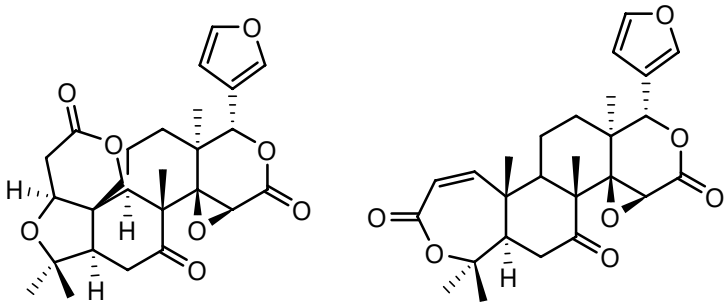

4.4. Limonin **4.5. Obacunone**

Figure 4.2. *Structures of bioactive limonoids.*

It has been reported that plants of the Meliaceae family are of frequent occurrence in southern and eastern Africa and Madagascar and that twenty-two out of fifty-one genera of Meliaceae can be found there.[14] Additionally, the chemistry of approximately forty-four species from only nineteen genera have been studied, leaving much potential

for further discovery of bioactive limonoids and other molecules from the Meliaceae family.[14]

4.2 Results and Discussion

4.2.1 Isolation of Compounds from Malleastrum sp.

Three new compounds were isolated from an extract of a *Malleastrum* sp. collected in Madagascar by employing bioassay-guided fractionation, as shown in Scheme 4.1. The crude plant extract was suspended between hexanes and 90% aqueous methanol. Dilution of the aqueous methanol fraction to 60% MeOH allowed further partitioning with dichloromethane. The dichloromethane fraction was found to be active, thus it was further separated over a flash silica column to afford three fractions, of which the chloroform fraction was active (fraction D). To further separate the rather large amount of material a more nonpolar step gradient was utilized on a flash silica column to afford eight fractions, of which fraction M contained both the majority of the weight and the activity. Finally, semi-preparative HPLC was utilized on a diol column with an isocratic flow of 68% hexanes / 32% DCM. This technique afforded two pure limonoids, fractions V (**4.1**, 1.8 mg) and W (**4.2**, 1.9 mg).

The aqueous methanol fraction (C) also displayed moderate antiproliferative activity, thus it was partitioned between butanol and water. The butanol fraction was selected for separation and was applied to a RP-C18 preparative HPLC column using a gradient from 50 – 100 % aqueous methanol. The most nonpolar fraction (U) displayed the greatest activity, thus it was separated via C8 semi-preparative HPLC to afford one new limonoid, X (**4.3**, 0.8 mg).

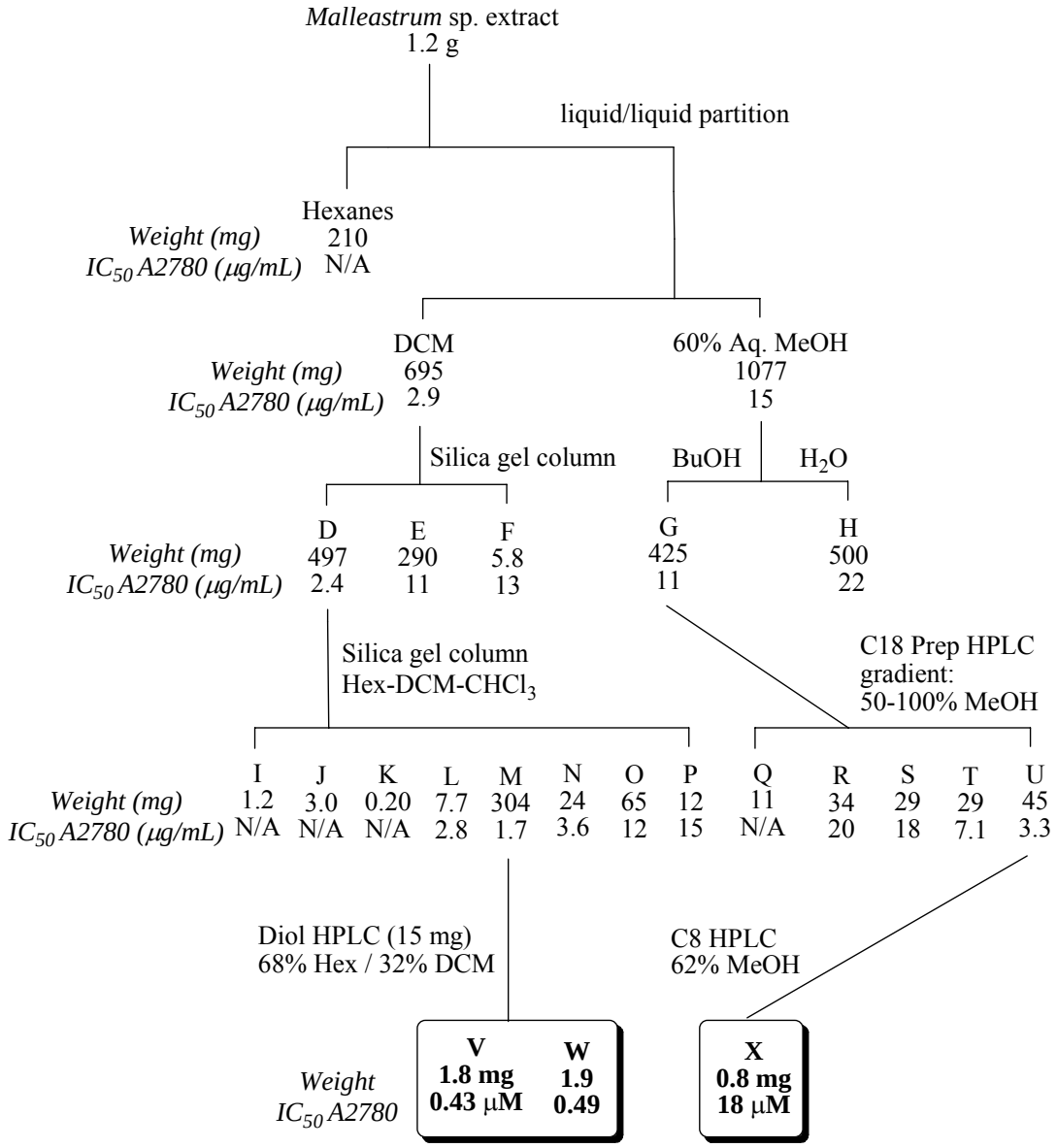

Scheme 4.1. *Separation of aqueous methanol fraction of Malleastrum sp.*

*4.2.2. Structure Elucidation of Malleastrone A (**4.1**)*

Compound **4.1** was obtained as a colorless oil. Positive-ion HRFABMS analysis gave a pseudomolecular ion at *m/z* 583.2518 ($[M+H]^+$), which suggested a molecular formula of $C_{32}H_{38}O_{10}$. The ^{13}C and g-HSQC NMR spectra of **4.1** in $CDCl_3$ afforded

evidence of two ester carbonyls (δ_C 179.7, C-1"; 170.7, C-1'), two ketone carbonyls (δ_C 201.3, C-3; 202.3, C-7), two sp^2-oxygenated carbons (δ_C 140.9, C-19; 142.0, C-21), and an additional four sp^2 carbons (δ_C 155.4, C-1; 128.4, C-2; 123.2, C-18; 112.5, C-20). There was also evidence of six sp^3-oxygenated carbons (δ_C 106.1, C-6; 75.6, C-11; 85.9, C-12; 74.6, C-14; 59.8, C-15; 77.8, C-22), one sp^3 methylene (δ_C 33.5, C-16), four sp^3 methines (δ_C 63.2, C-5; 43.0, C-9; 38.7, C-17; 33.9, C-2"), four quaternary carbons (δ_C 51.8, C-4; 49.1, C-8; 38.4, C-10; 46.3, C-13), and seven methyl groups (δ_C 28.0, C-23; 26.8, C-24; 25.6, C-25; 16.1, C-26; 21.0, C-2'; 18.1, C-3"; 19.1, C-4"). Select ^{1}H NMR resonances of **4.1** in $CDCl_3$ exhibited the characteristic pattern of a monosubstituted furan moiety (δ_H 7.16, br s, H-19; 6.17, br d, J = 1.0 Hz, H-20; 7.34, br t, J = 1.5 Hz, H-21), in addition to four sp^3-oxygenated hydrogens (δ_H 4.27, t, J = 3.0 Hz, H-11; 5.01, d, J = 3.5 Hz, H-12; 3.84, s, H-15; 4.34, d, J = 9.5 Hz, and 4.15, d, J = 9.5 Hz, H_2-22), and two unsaturated methines (δ_H 7.51, d, J = 10 Hz, H-1; 6.03, d, J = 10 Hz, H-2). ^{1}H and ^{13}C NMR data can be found in Table 4.1.

The combination of g-COSY and g-HMBC spectra were critical in both assembling and linking together rings A-E (Figure 4.3). Ring A was assembled via a COSY correlation from H-1 to H-2, and subsequent HMBC correlations of H-1, H-2, and H_3-23 (δ_H 1.50, s) to the carbonyl (C-3). The linkage of ring A to B was evidenced by HMBC correlations from H_3-24 (δ_H 1.62, s) to C-1, C-10, and C-9, in addition to a correlation of H_3-25 (δ_H 1.73, s) to C-9 and a carbonyl at C-7. Also, the H-5 methine (δ_H 2.91, s) displayed long range correlations with C-1 and a signal typical for a di-oxygenated quaternary carbon (δ_C 106.1, C-6). The H_2-22 oxymethylene was found to be

cyclized between rings A and B via HMBC correlations to C-3, C-4, C-5 and C-6. Fusion of ring B to the highly oxygenated C ring was determined primarily on the basis of COSY correlations from H-9 (δ_H 3.38, d, J = 3.5 Hz) to H-11, and H-11 to H-12, but was further supported by HMBC correlations from H_3-25 and H_3-26 (δ_H 1.33, s) to the quaternary epoxide carbon C-14. H_3-26 also exhibited long range correlations with C-12, C-13, and C-17. The aforementioned data along with COSY connectivity from H-17 (δ_H 3.00, dd, J = 11, 6.0 Hz) to a methylene at position 16 (δ_H 2.12, dd, J = 13, 6.5 Hz, and 1.83, dd, J = 13, 11 Hz), and H_2-16 to an oxymethine (δ_H 3.84, s, H-15), thus suggested the fusion of ring C with a five-membered ring. The C ring epoxide moiety was partly deduced based on a characteristic ^{13}C signal for a shielded, cyclic epoxide carbon (δ_C 59.8, C-15). A long range correlation from H-17 to C-18 and C-19 placed the monosubstituted furan moiety on C-17. The hydroxyl substituent was assigned to C-11 based on the chemical shit of H-11 (δ_H 4.27) and C-11 (δ_C 75.6).

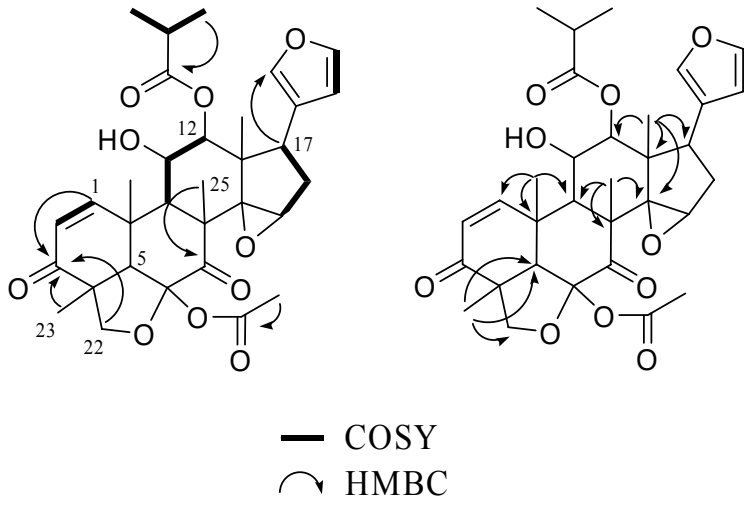

Figure 4.3. Select 2D NMR correlations of malleastrone A (**4.1**).

Despite repeated efforts the relative positions of the remaining isobutyroxy and acetoxy substituents could not be assigned by NMR techniques due to a weak 2-D resonance of H-12 in conjunction with the absence of a hydrogen atom at C-6. Compound **4.1** was thus crystallized from a mixture of $CHCl_3$ and EtOH at room temperature and subjected to X-ray crystallography by Dr. Carla Slebodnick. The X-ray diffraction pattern (Figure 4.4) placed the isobutyroxy moiety at C-12 and the acetoxy substituent at C-6, completing the flat structure of **4.1**. The relative configuration of **4.1** was also established by its crystal structure, although the crystal quality did not allow assignment of absolute configuration.

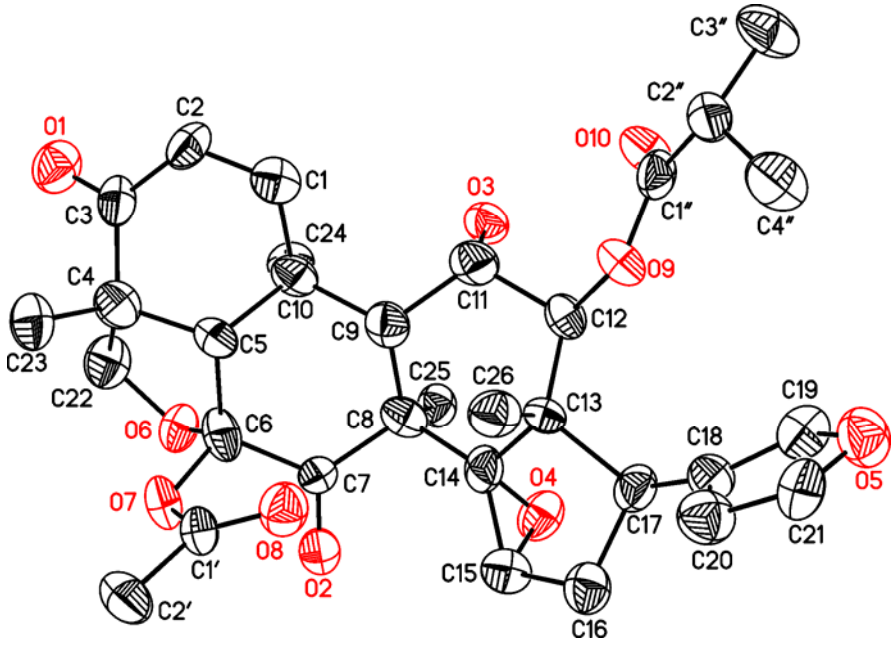

Figure 4.4. *Crystal structure of malleastrone A (**4.1**).*

Table 4.1. NMR Spectral Data of Limonoids **4.1-4.3** in $CDCl_3$ [a,b]

	4.1		**4.2**		**4.3**	
Pos	^{13}C	$^{1}H^{c}$ (*J*, Hz)	^{13}C	$^{1}H^{c}$ (*J*, Hz)	^{13}C	$^{1}H^{c}$ (*J*, Hz)
1	155.4	7.51 d (10)	155.3	7.50 d (10)	71.9	4.35 d (8.4)
2	128.4	6.03 d (10)	128.4	6.03 d (10)	46.4	3.04 dd (17, 8.4)
						2.55 d (17)
3	201.3		201.3		212.4	
4	51.8		51.8		52.8	
5	63.2	2.91 s	63.2	2.91 s	56.1	3.68 s
6	106.1		106.1		109.4	
7	202.3		202.3		199.6	
8	49.1		49.1		49.5	
9	43.0	3.38 d (3.5)	43.0	3.38 d (4.0)	41.0	3.26 s
10	38.4		38.4		40.4	
11	75.6	4.27 t (3.0)	75.6	4.27 t (3.0)	75.2	4.07 br s
12	85.9	5.01 d (3.5)	85.8	5.01 d (3.5)	85.3	4.90 br s
13	46.3		46.3		45.4	
14	74.6		74.6		70.9	
15	59.8	3.84 s	59.8	3.84 s	57.3	4.02 s
16	33.5	2.12 dd (13, 6.5)	33.6	2.12 dd (13, 6.5)	32.3	2.21 dd (14, 6.5)
		1.83 dd (13, 11)		1.83 dd (13, 11)		1.94 dd (14, 11)
17	38.7	3.00 dd (11, 6.0)	38.7	3.00 dd (11, 6.0)	41.2	2.89 dd (11, 6.8)
18	123.2		123.2		122.7	
19	140.9	7.16 br s	140.9	7.16 br s	140.4	7.12 d (1.0)
20	112.5	6.17 br d (1.0)	112.6	6.18 br s	111.9	6.12 br s
21	142.0	7.34 br t (1.5)	142.0	7.34 br t (1.6)	142.3	7.31 d (1.6)
22	77.8	4.34 d (9.5)	77.8	4.34 d (9.5)	78.9	4.48 d (9.0)
		4.15 d (9.5)		4.15 d (9.5)		4.08 d (9.0)
23	28.0	1.50 s	28.0	1.50 s	26.7	1.49 s
24	26.8	1.62 s	26.8	1.62 s	17.3	1.29 s
25	25.6	1.73 s	25.6	1.73 s	23.0	1.51 s
26	16.1	1.33 s	16.1	1.33 s	14.8	1.12 s
1'	170.7		170.7		170.8	
2'	21.0	2.10 s	21.0	2.10 s	21.4	2.13 s
1"	179.7		179.4		178.2	
2"	33.9	2.44 m	40.9	2.24 m	34.1	2.43 m
3"	18.1	1.07 d (6.5)	25.8	1.60 m	18.4	1.03 d (7.0)[d]
				1.36 m		
4"	19.1	1.06 d (7.5)	11.8	0.90 t (7.0)	18.9	1.04 d (7.0)[d]
5"			16.9	1.03 d (7.5)		
11-OH		4.09 br s		4.14 s		3.49 s
1-OH						3.11 br s

[a] Assignments based on COSY, HMBC, HSQC. [b] Chemical shifts (δ) in ppm. [c] br s: broad singlet; d: doublet; m: multiplet. [d] Values are interchangeable. [e] Signal overlapped with H-6'.

*4.2.3. Structure Elucidation of Malleastrone B (**4.2**)*

Compound **4.2** was obtained as a colorless oil. Positive-ion HRFABMS analysis gave a pseudomolecular ion at *m/z* 597.2781 ($[M+H]^+$), which suggested a molecular formula of $C_{33}H_{40}O_{10}$. Compound **4.2** exhibited nearly identical ^1H and ^{13}C NMR resonances to those of **4.1**, and the g-COSY and g-HMBC spectra further confirmed that both compounds shared an identical basic skeleton. The distinction between the two sets of spectra, however, is demonstrated by the presence of an additional methylene carbon signal at δ_C 25.8 (C-3"), consistent with the additional fourteen mass units found by mass spectrometry. As opposed to consecutive doublets in the upfield region of the ^1H NMR spectrum of **4.1** (δ_H 1.07, d, J = 6.5 Hz, H_3-3"; 1.06, d, J = 7.5 Hz, H_3-4"), **4.2** displayed adjacent doublet (δ_H 1.03, d, J = 7.5 Hz, H_3-5") and triplet signals (δ_H 0.90, t, J = 7.0 Hz, H_3-4") suggesting a modification to the C-12 substituent. The COSY spectrum of **4.2** afforded connectivity between H-2" (δ_H 2.24, m) and H_3-5", and H_2-3" and H_3-4", though no contour was present to represent H-2" and H_2-3". Thus, to finalize the flat structure of **4.2** and to avoid overlapping proton resonances, 1-D TOCSY was employed with enhancement of the methyl triplet (H_3-4") (Figure 4.5). Five resonances were observed, and two of them were assigned as non-equivalent methylene hydrogens (δ_H 1.60 m, H_a-3"; 1.36, m, H_b-3").

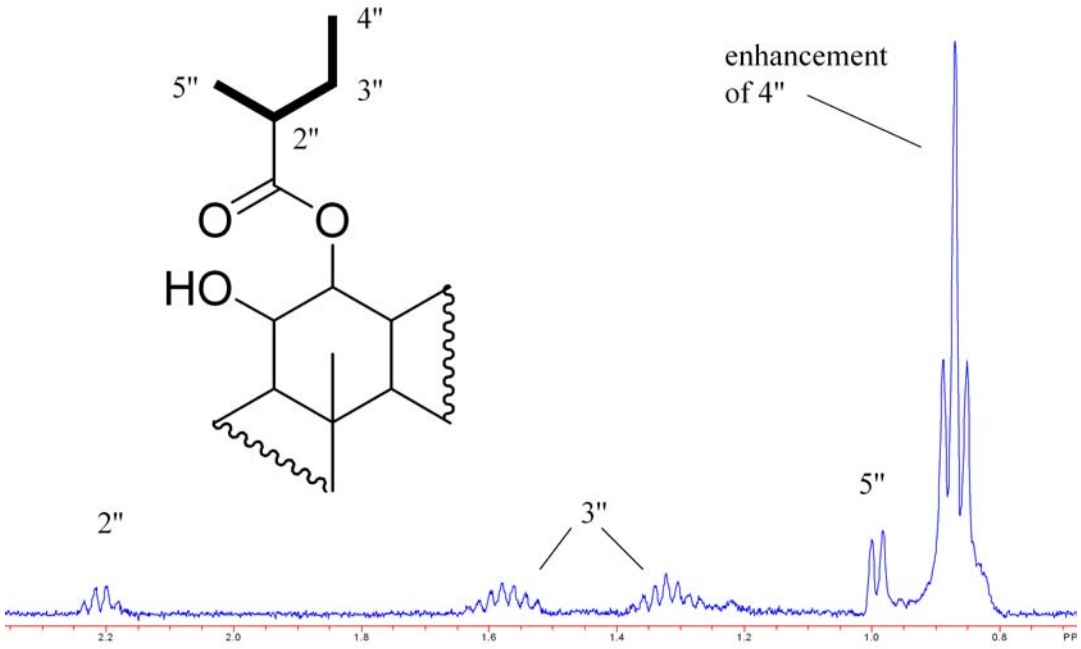

Figure 4.5. *1D TOCSY spectrum of malleastrone B (**4.2**).*

The relative configuration of **4.2** was determined upon analysis of its ROESY spectrum (Figure 4.6) and by comparison of ^{1}H and ^{13}C NMR chemical shifts to that of **4.1,** though the configuration at C-2" was unable to be determined. For this reason, several attempts to crystallize **4.2** were made until finally a slow and controlled evaporation of $CHCl_3$ / ethanol proved to be successful. The resulting crystals were of good quality, and analysis of their X-ray diffraction data (obtained by Dr. Carla Slebodnick) confirmed the previously assigned relative configuration of **4.2**, identified the configuration at C-2", and allowed for the determination of the absolute configuration of malleastrone B due to sufficient crystal quality (4*S*, 5*R*, 6*R*, 8*R*, 9*R*, 10*R*, 11*R*, 12*R*, 13*R*, 14*R*, 15*R*, 17*S*, 2"*S*). Since compound **4.1** has an identical relative configuration

and a nearly superimposable CD spectrum with that of **4.2**, its absolute configuration could also be assigned as (4*S*, 5*R*, 6*R*, 8*R*, 9*R*, 10*R*, 11*R*, 12*R*, 13*R*, 14*R*, 15*R*, 17*S*).[26]

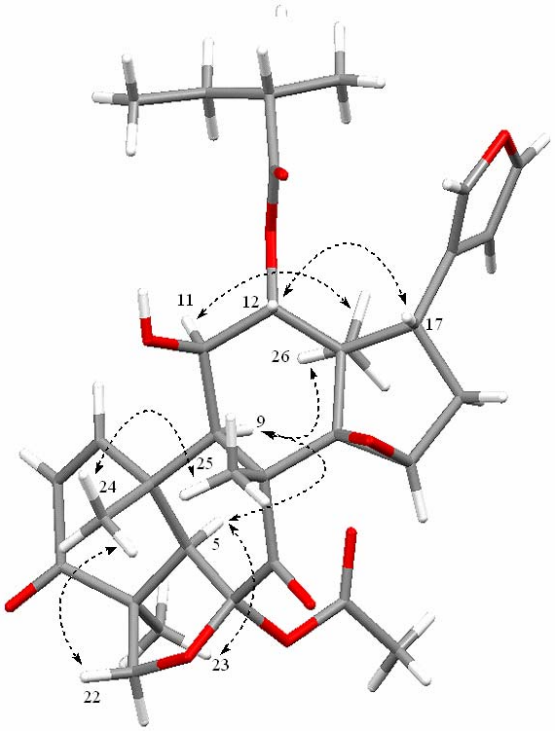

Figure 4.6. *Crystal structure and select ROESY correlations of malleastrone B (**4.2**).*

*4.2.4. Structure Elucidation of Malleastrone C (**4.3**)*

Compound **4.3** was obtained as light-green oil. Positive-ion HRFABMS analysis gave a pseudomolecular ion at *m/z* 583.2925, assigned as $[M\text{-}H_2O+H]^+$. To confirm this assignment, low-resolution positive-ion ESIMS under direct infusion afforded a pseudomolecular ion $[M+H]^+$ of *m/z* 601.2, which confirmed the molecular formula of $C_{32}H_{40}O_{11}$. The molecular ion peak proved to be unstable even under a low collision energy condition of 10 volts. The dominant ion was observed at *m/z* 541.2 $[M\text{-}C_2H_3O_2]$, namely loss of the acetoxy moiety at position 6. Compound **4.3** shared similar ^1H and

^{13}C spectral patterns to those of **4.1**, although additional signals and noticeable differences in chemical shift suggested the presence of slightly different functionalities. The molecular weight of **4.3** was eighteen mass units greater than that of **4.1**, indicating the addition of a molecule water. The absence of two olefinic hydrogen resonances in the ^{1}H NMR spectrum in addition to a downfield shift of the C-3 carbonyl (δ_C 212.4) signal signified a change to the A-ring. Two α-methylene hydrogens (δ_H 3.04, dd, J = 17.4, 8.4 Hz, H_a-2 and 2.55, d, J = 17 Hz, H_b-2) showed a COSY correlation to one sp^3-oxygenated methine (δ_H 4.35, d, J = 8.4 Hz, H-1), thus a hydroxyl moiety was placed at the 1-position.

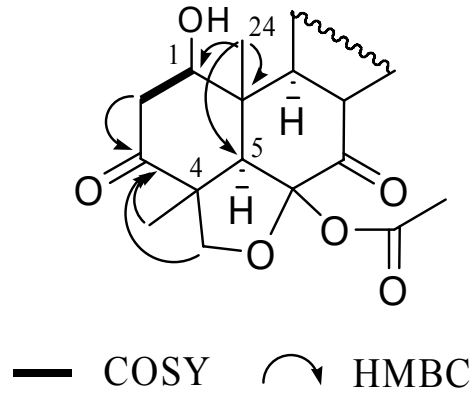

Figure 4.7. *Select A-ring 2D NMR correlations of malleastrone C (**4.3**).*

J-based analysis of the ^{1}H NMR signal of H-1 determined the 1-OH (δ_H 3.11, br s) to be equatorial. Further analysis of ROESY and CD spectra confirmed the relative and absolute configuration of the remainder of the molecule to be (1*R*, 4*S*, 5*R*, 6*R*, 8*R*, 9*R*, 10*R*, 11*R*, 12*R*, 13*R*, 14*R*, 15*R*, 17*S*), similar to that of **4.1** and **4.2**.

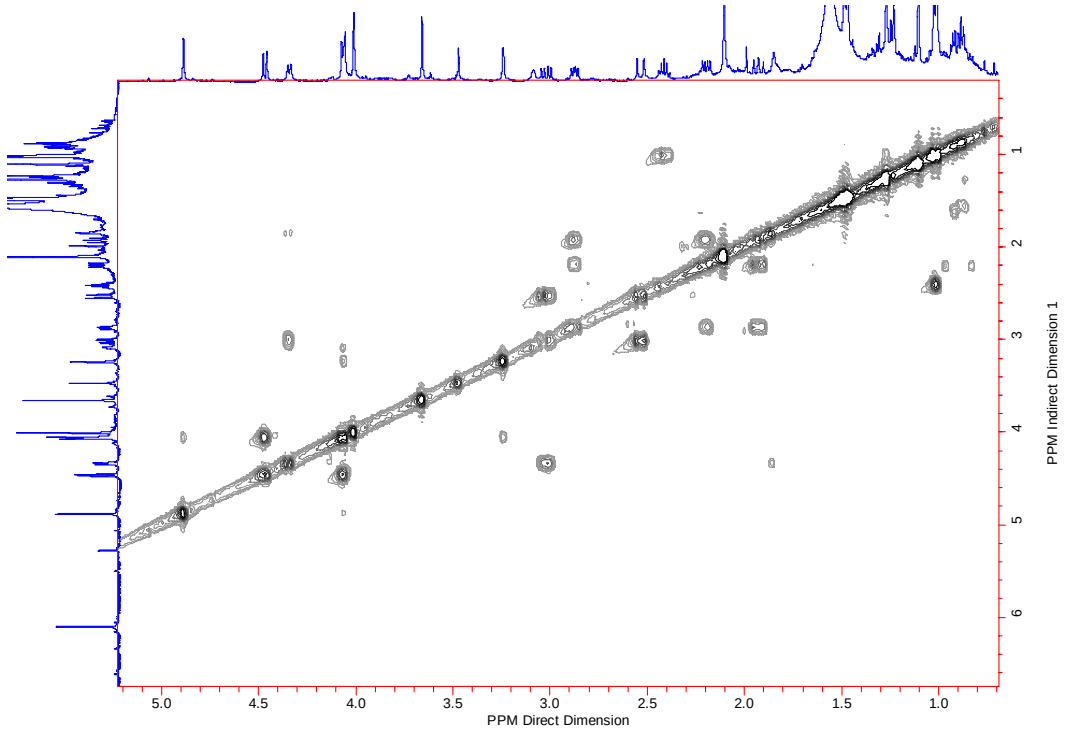

Figure 4.8. *COSY spectrum of malleastrone C (**4.3**).*

4.2.5. Evaluation of the Antiproliferative Activities of Compounds from Malleastrum sp.

All of the isolates were tested against the A2780 human ovarian cancer cell line as previously reported[15] and compounds **4.1** and **4.2** were tested against four additional cell lines. The results are shown in Table 4.2. Of the three compounds, **4.1** and **4.2** displayed considerable antiproliferative activity, while **4.3** was comparatively inactive (18 μM) against the A2780 cell line. It is apparent that saturation at the 1-position of this particular limonoid skeleton results in a complete loss of its antiproliferative properties. Overall, **4.1** and **4.2** appeared to exhibit general antiproliferative activity toward tumor cells, and so no further exploration of their bioactive potential was carried out.

Table 4.2. Antiproliferative Data of Compounds **4.1-4.3**

compound	IC_{50} (μM)				
	A2780[a]	MDA-MB-435[b]	HT-29[b]	H522-T1[b]	U937[b]
4.1	0.49	0.41	0.24	0.24	0.20
4.2	0.63	0.34	0.22	0.23	0.19
4.3	18	-	-	-	-

[a]Concentration of each compound that inhibited 50% of the growth of the A2780 human ovarian cell line according to the procedure described,[15] with paclitaxel (IC_{50} 23.4 nM) as the positive control. Assay was carried out by Ms. Peggy Brodie.
[b]Concentration of a compound which inhibited cell growth by 50% compared to untreated cell populations, with vinblastine as the positive control (average IC_{50} 0.27 nM (MDA-MB-435), 0.53 nM (HT-29), 1.38 nM (H522-T1) and 0.49 nM (U937). Assays were carried out by Eisai Research Institute, Waltham, MA.

4.2.6. Biosynthetic History of Limonoids.

Regarding isolates **4.1 - 4.3**, the particular hexacyclic tetranortriterpenoid skeleton is of rare occurrence in nature.[3,4] Generally speaking the biosynthetic origin of limonoids is traced to the triterpene euphane, whose C_8 side chain undergoes cyclization and loss of four carbons to yield the C-17 substituted furan moiety.[16]

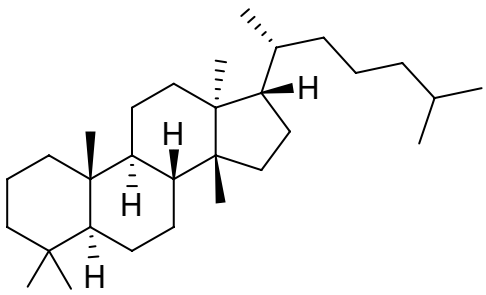

Figure 4.9. *Structure of euphane.*

Aside from the latter, reports of further biosynthetic modifications to the limonoid skeleton that describe mechanistic details have been limited. It is widely accepted and generally stated that after initial formation of the tetranortriterpenoid skeleton limonoids

undergo a series of oxidations and skeletal rearrangements via ring cleavage reactions.[16-19] In the case of the *Malleastrum* limonoids, esterification, D-ring epoxidation, and cyclization to yield an A/B-ring substituted tetrahydrofuran moiety are some of the modifications required to afford structures **4.1 - 4.3**. Thus, much work remains in order to divulge the specific biosynthetic mechanisms of such highly oxidized and bioactive chemical species.

4.3 Experimental Section.

General Experimental Procedures. IR and UV spectra were measured on MIDAC M-series FTIR and Shimadzu UV-1201 spectrophotometers, respectively. Melting point was obtained on a Buchi MP B-540 apparatus. NMR spectra were obtained on JEOL Eclipse 500, Varion Inova 400, and Varion Unity 400 spectrometers. Mass spectra were obtained on a JEOL JMS-HX-110 instrument and a Finnigan LTQ LC/MS. CD analysis was performed on a JASCO J-720 spectropolarimeter. Chemical shifts are given in δ (ppm), and coupling constants (*J*) are reported in Hz. HPLC was performed using Shimadzu LC-10AT pumps coupled with Varian Dynamax semi-preparative diol and C-8 columns (250 × 10 mm). The HPLC system employed a Shimadzu SPD-M10A diode array detector.

Plant Material. The sample of *Malleastrum* sp. (Meliaceae) was collected by botanists from the Missouri Botanical Garden in mid elevation humid forest in the Zahamena region of Madagascar, in the province of Toamasina, 250 m from the hamlet of Antenina, 4 km from Ankosy (17°32’32”S, 48°43’20” E, 1250 m elevation) under the vernacular

name Fanazava beravina, in December 2002. Duplicates of the voucher specimen (Randrianjanaka 766) were deposited at the Missouri Botanical Garden, the Muséum National d'Histoire Naturelle, Paris, the Département des Recherches Forestières et Pisicoles, Madagascar, and the Centre National d'Application des Recherches Pharmaceutique, Madagascar. The tree had a height of 7 m and trunk diameter at breast height of 8 cm.

Antiproliferative Bioassays. The A2780 ovarian cancer cell line antiproliferative assay was performed by Ms. Peggy Brodie at Virginia Polytechnic Institute and State University as previously reported.[15]

Antiproliferative effects of compounds **4.1** and **4.2** were evaluated by scientists at the Eisai Research Institute in four cultured human cancer cell lines: MDA-MB-435 breast cancer cells, HT-29 colon cancer cells, H522-T1 non-small cell cancer cells, and U937 histiocytic lymphoma cells. The cells were placed into 96-well plates and grown in the absence or continuous presence of 0.3 – 10000 nM compounds for 96 h. Cell growth was assessed using the CellTiter-Glo® Luminescent Cell Viability Assay (Promega) according to manufacturer's recommendations. Luminescence was read on a Victor^{2}V 1420 MultiLabel HTS Counter (Perkin-Elmer/Wallac). IC_{50} values were determined as the concentration of a compound which inhibits cell growth by 50% compared to untreated cell populations. Two separate replicate experiments were performed.

Bioassay Guided Fractionation of Compounds from *Malleastrum* sp. The dried plant sample described above (422 g) was extracted by scientists at CNARP, Antananarivo,

Madagascar with EtOH to give 3.57 g of extract designated MG 1695. Extract MG 1695 (1.2 g) was suspended in aqueous MeOH (MeOH-H_2O, 9:1, 500 mL) and extracted with hexanes (2 × 200 mL; > 20 μg/mL). The aqueous layer was then diluted to 40% water and extracted with DCM (2 × 200 mL). The DCM and aqueous MeOH fractions displayed antiproliferative activity (IC_{50} = 2.9 and 15 μg/mL, respectively). The DCM fraction was further chromatographed over a flash silica gel column to yield three fractions (D-F). Fraction D (497 mg, IC_{50} = 2.4 μg/mL) was chromatographed over a flash silica column to yield eight fractions (I-P). Malleastrone A (**4.1**, t_R 25 min, 1.9 mg, IC_{50} = 0.49 μM, A2780) and B (**4.2**, t_R 21.5 min, 1.8 mg, IC_{50} = 0.63 μM, A2780) were isolated from fraction M (304 mg, IC_{50} = 1.7 μg/mL) via semi-preparative diol HPLC using an isocratic flow of hexanes-DCM (68:32). Compound **4.3** was extracted out of the aqueous MeOH fraction, which was partitioned between H_2O and BuOH. The BuOH fraction (425 mg, IC_{50} = 11 μg/mL) was subjected to a flash C18 column and subsequent preparative C18 HPLC over 25 minutes with a gradient of 50-100 % MeOH to yield five fractions (Q-U). Fraction U (t_R 25-35 min, 45 mg, IC_{50} = 3.3 μg/mL), or the MeOH flush, was subjected to semi-preparative C8 HPLC employing an isocratic flow of MeOH-H_2O (62:38) to afford malleastrone C (**4.3**, t_R 23.5 min, 0.8 mg, IC_{50} = 18 μM, A2780).

X-ray Diffraction Studies.[20] Colorless needles of **1** were crystallized from $CHCl_3$/EtOH at room temperature. The chosen crystal was cut (0.016 × 0.067 × 0.194 mm^3) and mounted on the goniometer of an Oxford Diffraction Gemini diffractometer equipped with a Sapphire 3™ CCD detector. The data collection routine, unit cell refinement, and

data processing were carried out with the program CrysAlisPro.[21] The Laue symmetry and systematic absences were consistent with the orthorhombic space group $P2_12_12_1$. The structure was solved by direct methods and refined using SHELXTL NT.[10] The asymmetric unit of the structure comprises one crystallographically independent molecule. The final refinement model involved anisotropic displacement parameters for non-hydrogen atoms and a riding model for all hydrogen atoms. Due to insufficient crystal quality, the absolute configuration could not be determined from the Friedel pairs; the Friedel pairs were therefore merged for the final refinement. SHELXTL NT was used for molecular graphics generation.[22]

A colorless paralellepiped crystal of **2** (0.053 mm × 0.087 mm × 0.121 mm) was crystallized from chloroform/ethanol at room temperature. The crystal was centered on the goniometer of an Oxford Diffraction Nova Diffractometer operating with Cu radiation. The data collection routine, unit cell refinement, and data processing were carried out with the program CrysAlis.[23] The Laue symmetry and systematic absences were consistent with the monoclinic space groups $P2_1$ and $P2_1/m$. As **2** was known to be enantiomerically pure, the chiral space group $P2_1$ was chosen. The structure was solved by direct methods and refined using SHELXTL NT.[22] The asymmetric unit of the structure comprises one crystallographically independent molecule. The final refinement model involved anisotropic displacement parameters for non-hydrogen atoms and a riding model for all hydrogen atoms. The absolute configuration was established from anomalous dispersion effects with the Flack parameter refining to 0.0(2). Using the Bijvoet pair method,[24, 25] the correlation for the correct enantiomer, P2(true), was 1.000

and the incorrect enantiomer, P3(false), was $0.2x10^{-24}$. SHELXTL NT was used for molecular graphics generation.[22]

Malleastrone A (4.1): colorless needles; mp 252-254 °C; UV ($CHCl_3$) λ_{max} (log ε) 243 (3.46) nm; IR ν_{max} 3473, 2918, 2850, 1721, 1685, 1458, 1375, 1259, 1162, 1004 cm^{-1}; CD (MeOH, *c* 0.0180) $[\theta]_{233}$ 53.7, $[\theta]_{337}$ -11.1; ^1H and ^{13}C NMR, see Table 4.1; HRFABMS *m/z* 583.2518 $[M+1]^+$ (calcd for $C_{32}H_{39}O_{10}$, 583.2543).

Malleastrone B (4.2): colorless needles; mp 239-241 °C; UV ($CHCl_3$) λ_{max} (log ε) 246 (3.47) nm; IR ν_{max} 3462, 2934, 1722, 1687, 1457, 1375, 1260, 1159, 1006 cm^{-1}; CD (MeOH, *c* 0.0012) $[\theta]_{235}$ 16.7, $[\theta]_{335}$ -1.65; ^1H and ^{13}C NMR, see Table 4.1; HRFABMS *m/z* 597.2781 $[M+1]^+$ (calcd for $C_{33}H_{41}O_{10}$, 597.2700).

Malleastrone C (4.3): light-green oil; UV ($CHCl_3$) λ_{max} (log ε) 245 (3.52), 275 (3.20) nm; IR ν_{max} 3423, 2919, 2850, 1719 (br), 1456, 1377, 1256 cm^{-1}; CD (MeOH, *c* 0.0090) $[\theta]_{249}$ 3.02, $[\theta]_{275}$ 5.05, $[\theta]_{319}$ -1.04; ^1H and ^{13}C NMR, see Table 4.1; HRFABMS *m/z* 583.2925 $[M-H_2O+1]^+$ (calcd for $C_{32}H_{39}O_{10}$, 583.2543) and ESIMS *m/z* 601.2 ($C_{32}H_{40}O_{11}$).

References

1. Murphy, B. T.; Slebodnick, C.; Brodie, P.; Miller, J. S.; Rasamison, V. E.; Tendyke, K.; Suh, E. M.; Kingston, D. G. I. Antiproliferative limonoids of a *Malleastrum* sp. from the Madagascar rainforest. **2007**, *J. Nat.Prod*. In press.

2. Mulholland, D. A.; Parel, B.; Coombes, P. H. The chemistry of the Meliaceae and Ptaeroxylaceae of southern and eastern Africa and Madagascar. *Curr. Org. Chem.* **2000**, *4*, 1011-1054.

3. Siddiqui, S.; Ghiasuddin; Siddiqui, B. S.; Faizi, S. Tetranortriterpenoids and steroidal glycosides from the seeds of *Azadirachta indica* A. Juss. *Pak. Sci. J. Ind. Res.* **1989**, *32*, 435-438.

4. Rajab, M. S.; Bentley, M. D.; Fort, R. C. Biomimetic formation of a nimbin class limonoid. *J. Nat. Prod.* **1988**, *51*, 1291-1293.

5. Saraf, S.; Roy, A. *Biol. Pharm. Bull.* Limonoids: overview of significant bioactive triterpenes distributed in plants kingdom. **2006**, *29*, 191-201.

6. Germano, M. P.; D'Angelo, V.; Sanogo, R.; Catania, S.; Alma, R.; De Pasquale, R.; Bisignano, G. Hepatoprotective and antibacterial effects of extracts from *Trichilia emetica* Vahl. (Meliaceae). *J. Ethnopharmacol.* **2005**, *96*, 227-232.

7. Siddiqui, B. S.; Afshan, F.; Gulzar, T.; Sultana, R.; Naqvi, S. N.; Tariq, R. M. Tetracyclic triterpenoids from the leaves of *Azadirachta indica* and their insecticidal activities. *Chem. Pharm. Bull.* **2003**, *51*, 415-417.

8. Battinelli, L.; Mengoni, F.; Lichtner, M.; Mazzanti, G.; Saija, A.; Mastroianni, C. M.; Vullo, V**.** Effect of limonin and nomilin on HIV-1 replication on infected human mononuclear cells. *Planta Med.* **2003**, *69*, 910-913.

9. Sunthitikawinsakul, A.; Kongkathip, N.; Kongkathip, B.; Phonnakhu, S.; Daly, J. W.; Spande, T. F.; Nimit, Y.; Napaswat, C.; Kasisit, J.; Yoosook, C. Anti-HIV-1 limonoid: first isolation from *Clausena excavate*. *Phytother. Res.* **2003**, *17*, 1101-1103.

10. Saxena, S.; Pant, N.; Jain, D. C.; Bhakuni, R. S. Antimalarial agents from plant sources. *Curr. Sci.* **2003**, *85*, 1314-1329.

11. Bickii, J.; Njifutie, N.; Ayafor Foyere, J.; Basko, L. K.; Ringwald, P. In vitro antimalarial activity of limonoids from *Khaya grandifoliola* C.D.C. (Meliaceae). *J. Ethnopharmacol.* **2000**, *69*, 27-33.

12. Jung, H. J.; Sok, D. E.; Kim, Y. H.; Min, B. S.; Lee, J. P.; Bae, K.-H. Potentiating effect of obacunone from *Dictamnus dasycarpus* on cytotoxicity of microtubule inhibitors, vincristine, vinblastine, and taxol. *Planta Med.* **2000**, *66*, 74-76.

13. Manners, G. D.; Jacob, R. A.; Breksa, A. P.; Hasegawa, S.; Schoch, T. K. Bioavailability of citrus limonoids in humans. *J. Agric. Food Chem.* **2003**, *51*, 4156-4161.

14. Mullholland, D. A.; Parel, B.; Poombes, P. H. The chemistry of the Meliaceae and Ptaeroxylaceae of southern and eastern Africa and Madagascar**.** *Curr. Org. Chem.* **2000**, *4*, 1011-1054.

15. Cao S.; Brodie, P. J.; Miller J. S.; Randrianaivo, R.; Ratovoson, F.; Birkinshaw, C.; Andriantsiferana, R.; Rasamison, V. E.; Kingston D. G. I. Guttiferones K and L, antiproliferative compounds of *Rheedia calcicola* from the Madagascar rain forest. *J. Nat. Prod*. **2007**, *70*, 686-688.

16. Dewick, P. M. *Medicinal Natural Products; A Biosynthetic Approach.* John Wiley & Sons: West Sussex, England, 1981; p 255.

17. Champagne, D. E.; Koul, O.;. B.; Scudder, G. G. E.; Towers, G. H. N. Biological activity of limonoids from the Rutales. *Phytochemistry* **1992**, *31*, 377-394.

18. Ley, S. V.; Denholm, A. A.; Wood, A. The chemistry of azadirachtin. *Nat. Prod. Rep.* **1993**, *10*, 109-157.

19. Roy, A.; Saraf, S. Limonoids: overview of significant bioactive triterpenes distributed in plants kingdom. *Biol. Pharm. Bull.* **2006**, *29*, 191-201.

20. The section was prepared by Carla Slebodnick.

21. CrysAlisPro v1.171, Oxford Diffraction: Wroclaw, Poland, **2006**.

22. Sheldrick, G. M. SHELXTL NT ver. 6.12; Bruker Analytical X-ray Systems, Inc.: Madison, WI, **2001**.

23. CrysAlis v1.171, Oxford Diffraction: Wroclaw, Poland, **2004**.

24. Spek, A. L. *J. Appl. Cryst.* **2003,** *36,* 7-13.

25. Hooft, R. W. W., Straver, L. H., Spek, A. L. Optimal use of measured data to determine the absolute configuration of parmaceutically interesting molecules, *Abstract of Papers*, Annual Meeting of the American Crystallographic Association: Salt Lake City Utah; **2007**, Abstract 10.07.02.

26. The ChemDraw program assigned the configuration at C-17 as *R*, but a careful application of the Cahn-Ingold-Prelog priority rules (Smith, M. B.; March, J. *March's Advanced Organic Chemistry, 5th Edition.* John Wiley and Sons, Inc. New York, 2001; pp. 139-141) indicates that the configuration is *S.*

V. Antiproliferative Bistramides from the Ascidian *Tridemnum* sp. from Madagascar.[1]

5.1 Introduction

Bioassay-guided fractionation of a marine extract from a *Tridemnum* sp. (Didemnidae) afforded two known bistramides, compounds that have been reported to exhibit antiproliferative activity in the nanomolar range against a number of tumor cell lines *in vitro*. In addition, screening of ^{1}H NMR spectra of a number of HPLC fractions showed the presence of several potentially new bistramide derivatives in this extract, though small sample weights prevented attempts at structure elucidation. This chapter explores the metabolite-producing pattern of *Tridemnum* sp., and probes its therapeutic potential. The current chapter is an expanded version of a conference paper and an oral presentation given on this topic.[1]

5.1.1 Previous Investigations of Tridemnum species

Tridemnum is an ascidian of the family Didemnidae. This marine invertebrate has been the source of a number of potent bioactive compounds whose structural repertoire is a classic example of the metabolic diversity to be expected from such aquatic organisms. Of the classes of compound derived from this genus, the most frequently reported in literature and subsequently the most bioactive are the didemnins.

Didemnins are a class of cyclic depsipeptides with a short amino acid side chain, as previously discussed in regard to the antineoplastic agent Aplidin®.[2] Rinehart *et al.*

reported the first occurrence of these amino acid macrocycles from *Tridemnum solidum*,[3] and several more studies reporting didemnin analogs were to follow.[4-8]

One of the original isolates was didemnin B, a compound with potent antiviral and antitumor activity that focused attention on the study of marine metabolites as sources for potential drugs. Didemnin B inhibited several DNA and RNA viral diseases,[3b] including Dengue[9] and Rift Valley fevers,[10] the latter of which did not have an existing therapy. It was also the first marine-derived compound to enter Phase I and Phase II clinical trials by the National Cancer Institute as a potential antitumor agent.[11-13] It exerts its activity by inhibiting protein and DNA synthesis,[14] though host toxicity and a short bioactive lifespan necessitated its withdrawal from Phase II clinical trials in the mid 1990's.

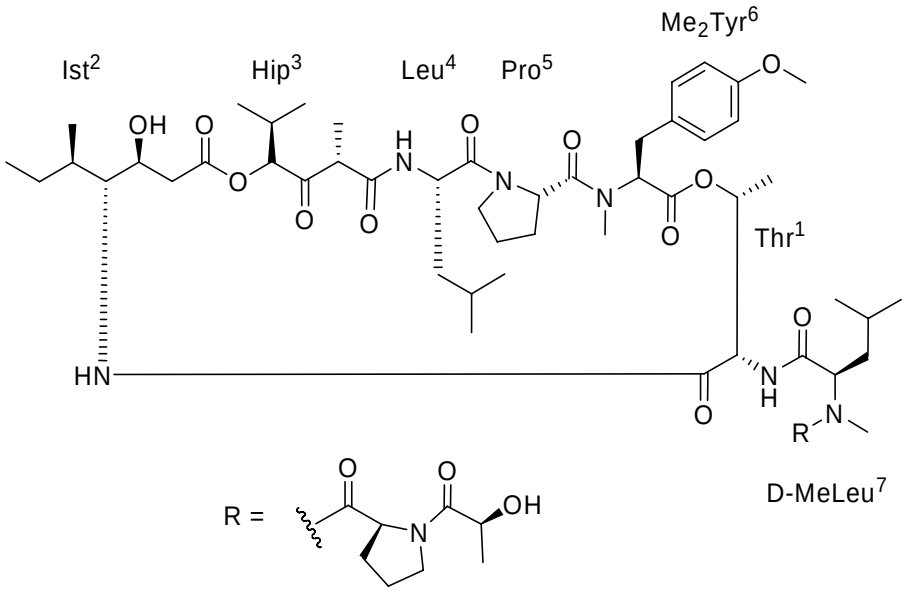

Figure 5.1. *Structure of didemnin B*

As much as this was a disappointment, the didemnin B experience initiated many marine natural products studies and allowed for the facile clinical development of other

marine compounds, such as the didemnin B analog Aplidine.[2] To date, a plethora of compounds with bioactivity in the nanomolar range are being discovered from sources in the ocean, including a structural class known as the bistramides.

5.1.2 Previous Investigations of Bistramides

Bistramides are a class of polyethers with methylated tetrahydropyran and spiroketal subunits. The first of its kind, bistramide A, was discovered in 1988 by Gouiffes et al. from the ascidian *Lissoclinum bistratum.*[15] Since that study there has been only one report of the isolation of additional bistramides (analogs B-D and K).[16] Interestingly, of the 31 studies to date that focus on these bistramides, only two are reports of isolation, while three examine structural elucidation techniques,[17-19] ten pertain to their synthesis,[20-28] and the remaining 16 investigate their mechanistic and bioactive properties.[29-44] Two patents have also been filed on behalf of the bistramides in regard to their bioactive properties and potential pharmaceutical preparation.[45-46]

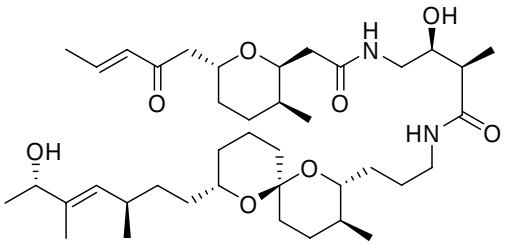

5.1. Bistramide A

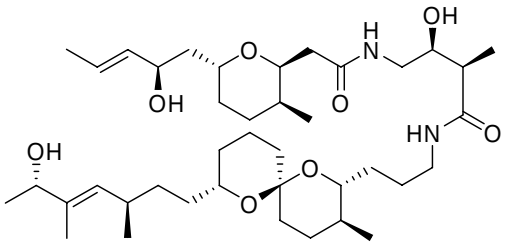

5.2. Bistramide D

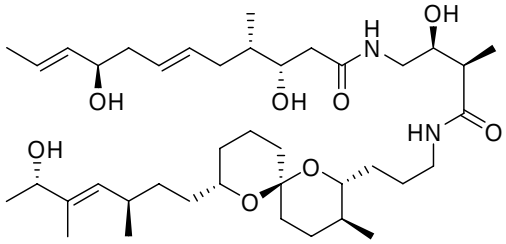

5.3. Bistramide K

Figure 5.2. *Structures of bistramides A, D, and K.*

5.1.3 Bioactive Properties of Bistramides

The bistramides have been shown to display diverse bioactive behavior including immunomodulating[35] and weak antimalarial activity,[33] but their most important trait is their antitumor properties. Bistramide A was originally determined to be a potent cytotoxic agent, displaying IC_{50} values of 45, 20, and 22 nM against the KB, P388, and normal endothelial cells, respectively.[3] It later caused *in vitro* arrest of a non-small cell bronco-pulmonary carcinoma cell line (NSCLC-N6), and induced terminal differentiation in the G_1 phase of the cell cycle.[41] A follow-up study reported similar NSCLC-N6 *in vivo* activity for bistramides D and K, but with less toxicity.[40,16] Soon thereafter, Liscia et al. monitored the expression of a number of different genes in NSCLC-N6 and found that bistramide D increased the expression of the p53 gene, thus emphasizing the role of

bistramides in cell proliferation and differentiation.[34] These findings eventually led to the major breakthrough that allowed the determination of how the bistramides exert their potent antiproliferative activities.

Statsuk et al. reported in *Nature, Chemical Biology* that actin, a protein essential for cellular motility and division, was the primary cellular receptor of bistramide A.[31] Much like tubulin, actin is a chief component of the cytoskeleton and plays a critical role in various cellular processes.[47] In a series of cell-based and *in vitro* studies in conjunction with affinity-based protein isolation, it was determined that bistramide A aggravates the actin cytoskeleton by depolymerizing filamentous F-actin and binding to monomeric G-actin. An actin-bistramide A complex was later crystallized, allowing for detailed analysis of the binding interactions of the marine metabolite with its monomeric G-actin counterpart (Figure 5.3).[30] Using multiple hydrogen-bonding and hydrophobic interactions with nearby residues, bistramide A was found to occupy a "deep cleft" between subdomains 1 and 3. Though the precise mechanistic details for depolymerization of F-actin have yet to be elucidated, it is thought that the marine metabolite caps F-actin at its barbed end.[30]

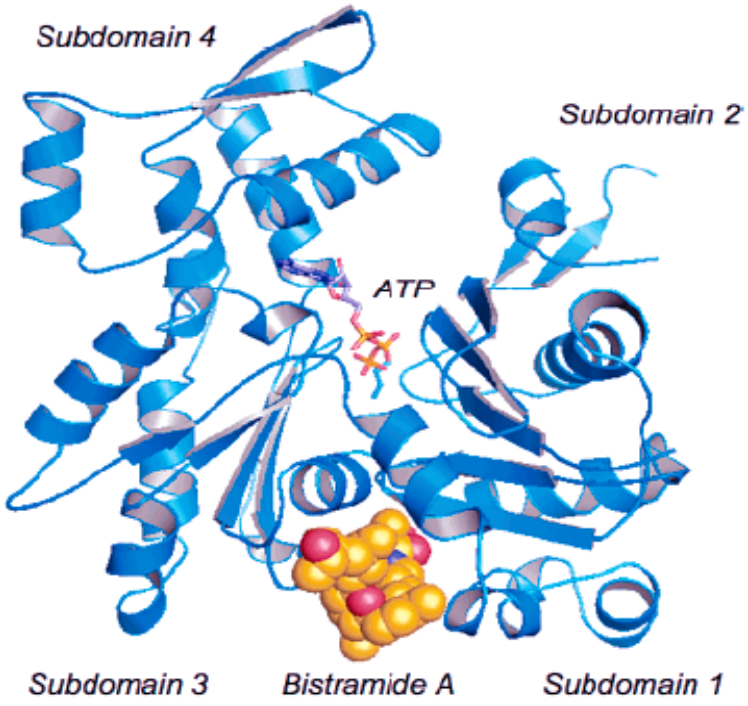

*Reprinted with permission from Rizvi et al. Copyright 2006 American Chemical Society. Approved by C. Arleen Courtney, ACS Copyright office, *J. Am. Chem Soc*. **2006**, *128*, 3882-3883, Figure 1B.

Figure 5.3. *Crystal structure of bistramide A-actin complex.*[30]

The inhibition of actin polymerization by such a unique class of natural products emphasizes the need to further explore the bistramides as potential leads for a new class of anticancer agent. From a pharmaceutical standpoint, the issue of sufficient supply of these compounds must be addressed. Though there have been many total synthetic studies, from a biochemical standpoint it is still unclear as to whether these metabolites are products derived from the ascidian itself or if they result from a symbiotic relationship with particular marine algae. Comparative studies of the biological and chemical environment to which two different organisms produce such bistramides may shed light on the true metabolic origin of such structurally unique compounds, and may potentially provide researchers with the ammunition necessary for their facile production.

To date the only natural source of bistramides has been from *L. bistratum*, and herein is the first report of these potential antitumor therapies from any other source.

5.1.4 Chemical Investigation of a Tridemnum sp.

In our continuing search for biologically active natural products from Madagascar as part of an International Cooperative Biodiversity Group (ICBG) program, we obtained an extract from a *Tridemnum* sp. of the family Didemnidae. The ethanol extract of *Tridemnum* sp. was found to be active in the A2780 human ovarian cancer cell assay, with an IC_{50} value of 2.0 μg/mL. Bioassay-guided fractionation of this extract led to the isolation of two known bistramides. In addition, analysis of NMR spectra of several other HPLC fractions displays the ability of this genus to produce a number of unique polyketide derivatives that would undoubtedly expand upon the structural repertoire of the bistramide class. The bioactivity and structure elucidation of the known compounds will be reported, as will the broader theme of potential therapeutic value of the genus *Tridemnum*.

5.2 Results and Discussion

5.2.1 Isolation of Compounds from a Tridemnum sp.

Two known compounds were isolated from a *Tridemnum* sp. by employing bioassay-guided fractionation, as shown in Schemes 5.1 and 5.2. For initial fractionation (Scheme 5.1), the crude extract was suspended between hexanes and 90% aqueous methanol. Dilution of the aqueous methanol fraction to 60% MeOH allowed further partitioning with dichloromethane. The dichloromethane fraction was found to be active,

thus it was further separated over a reversed phase flash C18 column to afford six fractions, of which fraction G displayed the greatest activity. Finally, semi-preparative reversed phase C18 HPLC was used to separate fraction G with an isocratic flow of 73% aqueous methanol. This technique afforded one pure bistramide, fraction 27 (**5.1**, 1.1 mg), although many of the adjacent fractions displayed similar ^{1}H NMR profiles.

In order to isolate a greater quantity of these bistramides for the purpose of structure elucidation and further bioactivity testing, an additional mass of crude marine extract was obtained and an identical liquid-liquid partitioning procedure was employed (Scheme 5.2). The active dichloromethane fraction was separated over a reversed phase flash C18 column to afford four fractions, of which fraction U displayed the greatest activity. Semi-preparative reversed phase C18 HPLC was used to separate U with an isocratic flow of 73% aqueous methanol. This technique afforded bistramide D, as fraction 67 (**5.2**, 0.8 mg).

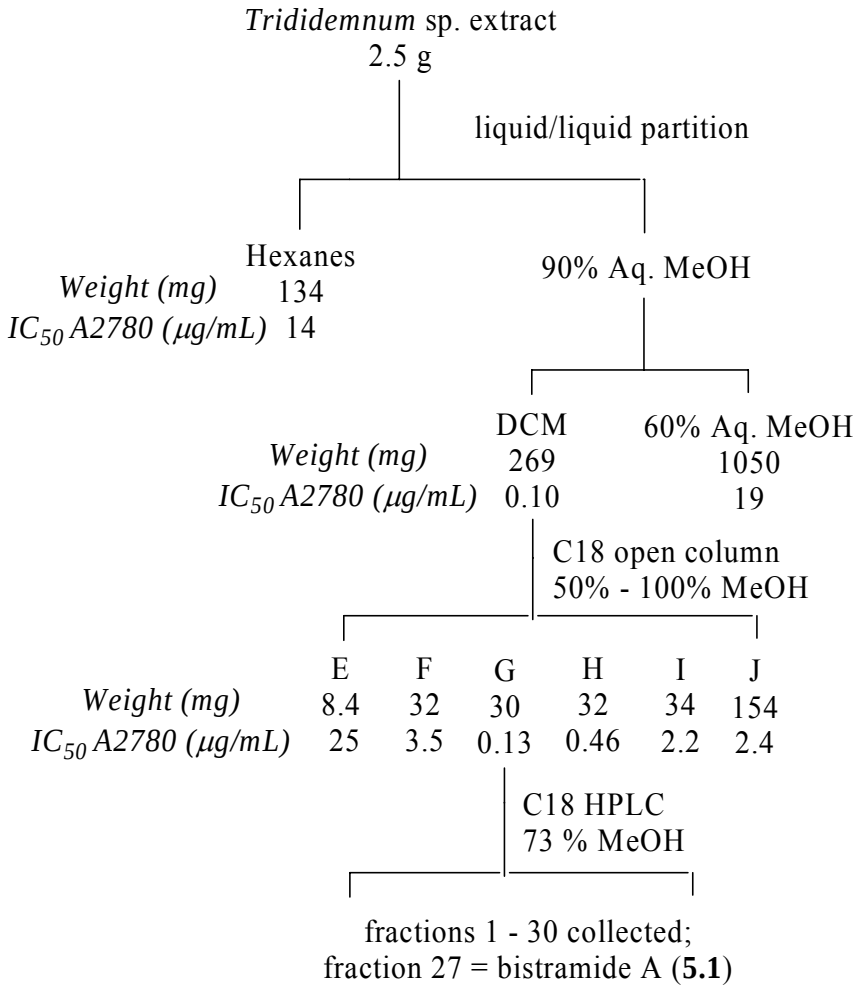

Scheme 5.1. *Separation of the DCM fraction of a Tridemnum sp.*

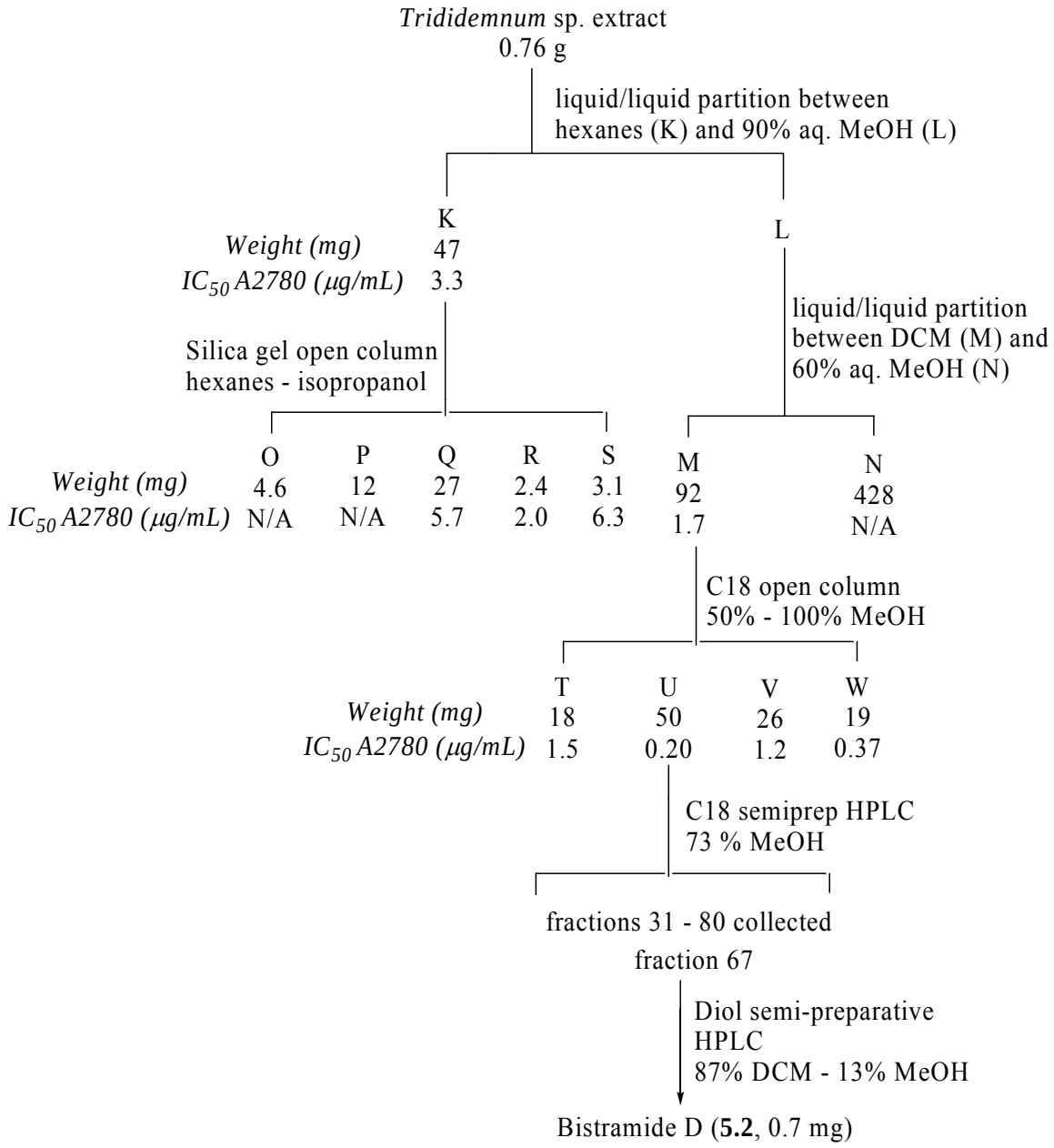

Scheme 5.2. *Second separation of the DCM fraction of a Tridemnum sp.*

Table 5.1. ^{13}C NMR Spectral Data of Bistramide A (**5.1**) in $CDCl_3$ [a,b]

	5.1	**Bistramide A**[16]	$\Delta\delta_C$
Pos.	^{13}C (ppm)		(ppm)
1	18.4	18.4	-
2	144.5	144.5	-
3	132.1	132.1	-
4	198.9	198.9	-
5	45.2	45.2	-
6	64.8	64.8	-
7	30.8	30.8	-
8	26.5	26.5	-
9	33.3	33.3	-
10	17.1	17.1	-
11	74.8	74.8	-
12	32.3	32.3	-
13	173.5	173.4	0.1
14	44.7	44.9	0.2
15	73.8	73.8	-
16	43.3	43.4	0.1
17	15.6	15.6	
18	175.2	175.1	0.1
19	39.5	39.5	-
20	25.9	25.9	-
21	30.4	30.4	-
22	74.3	74.3	-
23	34.9	34.9	-
24	18.0	17.9	0.1
25	27.9	27.9	-
26	36.1	36.1	-
27	95.5	95.4	0.1
28	35.5	35.5	-
29	19.2	19.2	-
30	31.3	31.3	-
31	69.1	69.1	-
32	34.1	34.1	-
33	33.5	33.5	-
34	31.9	31.9	-
35	21.0	21.0	-
36	131.4	131.3	0.1
37	137.2	137.1	0.1
38	11.8	11.8	-
39	73.3	73.3	-
40	21.7	21.8	0.1

*5.2.2. Structure Confirmation of Bistramide A (**5.1**)*

Initial screening of the active parent fraction of bistramide A (fraction G) by LCMS afforded a complex mixture of peaks. The purpose of this screening was to use molecular weight to identify the structural class of the active components in this fraction. Therefore, a thorough literature search led to the composition of a mini-library of compounds that had previously been isolated from the family Didemnidae, or the genus *Tridemnum*; the molecular weights obtained from some of the major peaks in the LCMS chromatogram closely resembled the range of molecular weights for the class of secondary marine metabolites known as the bistramides.

Bistramide A was identified primarily by comparison of its MS, ^{1}H and ^{13}C NMR data in $CDCl_3$ with those in the literature.[16] A molecular ion of *m/z* 705.5 $[M+H]^+$ suggested a formula of $C_{40}H_{68}N_2O_8$, identical to that observed for bistramide A. A comparison of ^{13}C data is shown in Table 5.1. Of the 40 carbons in the skeleton, eight deviate from literature values by only 0.1 ppm, while one carbon deviates by 0.2 ppm. The remaining resonances display identical chemical shift values to their corresponding literature carbons, indicating a high probability that **5.1** is indeed bistramide A. Select HMBC and COSY correlations positioned each spin system in the vicinity of its corresponding functional groups, and thus further solidified the proposed structural assignment.

*5.2.3. Structure Elucidation of Bistramide D (**5.2**)*

The structure elucidation process of bistramide D was more difficult than that of bistramide A. Since a relatively small amount was isolated (0.7 mg), NMR data had to

be acquired in a Shigimi NMR tube. This made the task of acquiring NMR data in $CDCl_3$, the solvent used in the literature, a difficult process predominantly due to difficulties involved with sample shimming in the Shigemi tube. The use of CD_3OD avoided these problems and allowed facile shimming that improved the quality of the NMR spectra, especially giving improved signal resolution in the ^1H NMR spectrum. Unfortunately, the advantage of comparing exact chemical shift values with those in literature was lost.

A molecular ion of *m/z* 707.6 ($[M+H]^+$) suggested a molecular formula of $C_{40}H_{70}N_2O_8$, which is two mass units greater than **5.1**. The ^1H NMR spectrum of **5.2** displayed a similar overall pattern to that of **5.1**, suggesting the structural similarity of the two compounds. The major difference was the loss of a ketone carbonyl resonance and the addition of a hydroxylated methine resonance in the ^{13}C NMR spectrum. Furthermore, there was a dramatic shielding effect on C-2 as a result of the loss of a conjugated system (127.0 and 144.5 ppm for **5.2** and **5.1**, respectively). These data suggested the possible reduction of the C-4 carbonyl group to a hydroxyl group; this would account for the additional two mass units in the mass spectrum. HMBC spectroscopy and a series of 1D TOCSY experiments proved this to be the case. Connectivity from H_3-1 to H_2-12 was established through the employment of COSY and 1D TOCSY, which also served to confirm the spin system between H_2-14 and H_3-17. HMBC correlations of H_2-14 and H_2-12 to C-13, H_3-17 to C-15, C-16, and C-18, and H_2-19 to C-18, helped locate the multifunctional unit in the center of the molecule (Figure 5.4).

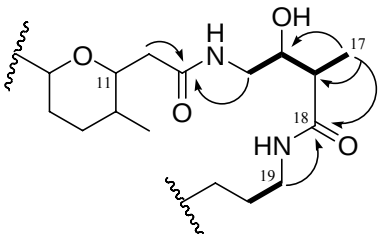

Figure 5.4. *Select 2D NMR correlations of C12-C19 of* ***5.2***

COSY and 1D TOCSY experiments also exposed the spin system from H-34 to H_3-40. HMBC correlations supported the fragment shown in Figure 5.5, namely from H_3-40 to C-37, and H-39, H_3-38 and H_3-35 to C-36.

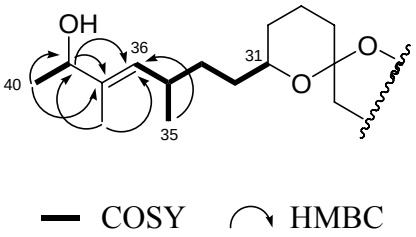

Figure 5.5. *Select 2D NMR correlations of C31-C40 of* ***5.2***

Severe overlapping in the 1.2 to 1.7 ppm region of the ^{1}H NMR spectrum prevented assignment of methylene resonances involved in the spiroketal moiety, and this task was further hindered by the lack of comparable literature data. As a direct result definitive assignment of certain methylene resonances in the ^{13}C spectrum was not possible. However, existence of a spiroketal system in the fragment of the molecule yet to be discussed (C-22 to C-31) was strongly supported by a ^{13}C resonance at 96.8, typical of the resonance for the deshielded ketal carbon at position 27. Moreover, based on the

molecular formula the degrees of unsaturation support the bicyclic structure, as opposed to an acyclic derivative as found in bistramide K.

Unfortunately, bistramide D decomposed in the NMR tube when an attempt was made to acquire 2D spectra in $CDCl_3$ for comparison with literature NMR data. This prevented stereochemical studies on the molecule, and consequently prohibited any further spectroscopic or biochemical analysis. Regardless, a comparison of the ^{13}C data of **5.2** with those of bistramide A is shown in Table 5.2. Despite differing solvents, chemical shift similarities between the two metabolites provide strong evidence for the proposed structure of **5.2**.

Table 5.2. ^{13}C NMR Spectral Data of **5.2** in CD_3OD and bistramide A in $CDCl_3$ [a,b]

	5.2	**Bistramide A**[16]	$\Delta\delta_C$
Pos.	^{13}C (ppm)		(ppm)
1	17.9	18.4	0.5
2	127.0	144.5	17.5
3	135.2	132.1	3.1
4	71.7	198.9	127.2
5	44.0	45.2	1.2
6	69.4	64.8	4.6
7	29.1	30.8	1.7
8	27.6	26.5	1.1
9	N/A	33.3	N/A
10	17.1	17.1	-
11	75.6	74.8	0.8
12	34.4	32.3	2.1
13	174.6	173.4	1.2
14	44.6	44.9	0.3
15	73.3	73.8	0.5
16	45.5	43.4	0.1
17	15.3	15.6	0.3
18	177.5	175.1	2.4
19	40.6	39.5	1.1
20	N/A	25.9	N/A
21	N/A	30.4	N/A
22	75.8	74.3	1.5
23	N/A	34.9	N/A
24	18.4	17.9	0.5
25	N/A	27.9	N/A
26	N/A	36.1	N/A
27	96.8	95.4	1.4
28	N/A	35.5	N/A
29	N/A	19.2	N/A
30	N/A	31.3	N/A
31	70.3	69.1	1.2
32	N/A	34.1	N/A
33	34.9	33.5	1.4
34	N/A	31.9	N/A
35	21.5	21.0	0.5
36	132.2	131.3	0.9
37	138.6	137.1	1.5
38	11.9	11.8	0.1
39	74.1	73.3	0.8
40	22.2	21.8	0.4

*5.2.4. Antiproliferative Activity of (**5.1**)*

Bistramide A (**5.1**) exhibited an IC_{50} value of 0.26 μM against the A2780 human ovarian cancer cell line. Compared with IC_{50} values against other cell lines reported in literature (45, 20, and 22 nM against the KB, P388, and normal endothelial cells, respectively),[3] the value against the A2780 cell line is about ten fold less active. This suggests that bistramide A may show some selectivity toward tumor cells, rather than exhibiting general cytotoxicity. It is probable however, that bistramide A is not the most active compound from its parent fraction. The NMR spectra of the HPLC fractions flanking the fraction containing bistramide A had resonances that were similar to those of bistramide A but were not assignable to any known bistramide. Lack of sample prevented the isolation and structure elucidation of these compounds. Further isolation of these derivatives will only be possible if more crude marine extract was to become available.

5.2.5. Biosynthetic Studies and the Future of the Tridemnum Genus

The work described above took several months to complete, and although it did not yield any new compounds it did serve to illustrate the rich chemical diversity of this species of *Tridemnum*. The analysis has detected a minimum of 10-15 bistramide or bistramide-derived secondary metabolites from one fraction alone (fraction U). Taking into account that only five known naturally occurring bistramides have been isolated over the past 20 years, this represents a large increase in the members of this structural class. Given the nanomolar potency against certain cell lines and their unique mechanism of

action against cancer, further isolation of novel bistramide derivatives will increase the chances of discovering analogs that exhibit similar activity with less toxicity.

The current work has proven this species to be a prolific supplier of diverse, yet small quantities of these structurally unique bistramides, and furthermore suggests that the *Tridemnum* sp. is a potential source of a diverse range of potently bioactive molecules. From the cyclic depsipeptide didemnins that inhibit protein biosynthesis, to the polyketide derived bistramides that bind to actin, the prolific metabolite-producing pattern of this ascidian certainly warrants further investigation.

Another example of a genus prone to producing bioactive metabolites is that of the marine actinomycete *Salinispora*. The several species identified to date have produced the ornithine decarboxylase inhibitors saliniketal A and B (bicyclic polyketides),[48] the potent DNA damaging agent and highly cytotoxic lomaiviticin A (a diazobenzofluorene glycoside),[49] and the proteasome inhibitor salinosporamide A with a β-lactone-γ-lactam ring system, currently in clinical trials,[50] among others. Should *Tridemnum* follow the metabolite-producing pattern exhibited by *Salinispora*, it is strongly urged that more focus be placed on taxonomic classification, structural characterization and subsequent biomedical application of this genus, as it may serve as a significant source of diverse chemotherapeutic agents.

Another important question must be raised, however, and that is of the true biosynthetic origin of these actin-binding bistramides. Unlike traditional phytochemical systems, it is often the case that marine invertebrates rely directly on symbiotic microorganisms for survival. These microorganisms may contribute to the diet or may even serve as primary or secondary chemical defenses of the host organism.[51]

Consequently, the task of pinpointing the true producer of a secondary metabolite becomes quite difficult. The current frontier of biosynthetic investigations of naturally occurring marine metabolites involves selective DNA sequencing and genome mapping of natural product producing genes, and this technique has been demonstrated on a few occasions.[52-54]

In the case of this *Tridemnum* sp. a survey of the literature reveals significant evidence that may provide a glimpse into some of its intricate biosynthetic machinery. As stated earlier, the bistramides were originally isolated from the ascidian *Lissoclinum bistratum*.[15,16] It has been reported that other species of *Lissoclinum*, as well as a few species of *Tridemnum*, contain an obligate symbiont of bacterial nature, namely *Prochloron* spp.[55] *Prochloron* spp. act as important nutrient sources for their host ascidians (particularly of the family Didemnidae) via photosynthesis and nitrogen fixation.[56] These bacteria have been implicated in the production of cyclic peptides,[57,58] a class of compounds found in both *Lissoclinum* (bistratamides) and *Tridemnum* (didemnins). Since *Prochloron* spp. exist in both of these genera, it is reasonable to hypothesize that bistramides are of a bacterial origin, and not a product of two separate ascidians. Furthermore, a recent study by Frank et al. gives further weight to the bacterial origin hypothesis.[59] Employing gene sequencing, genetic engineering of specific polyketide pathways, and site-directed mutagenic techniques, a biosynthetic pathway was proposed for spirangien, a cytotoxic metabolite from the myxobacterium *Sorangium cellulosum*. This metabolite is significant to the current study because it contains the unique bicyclic spiroketal ring system found in the bistramides (C22 - C31, Figure 5.6).

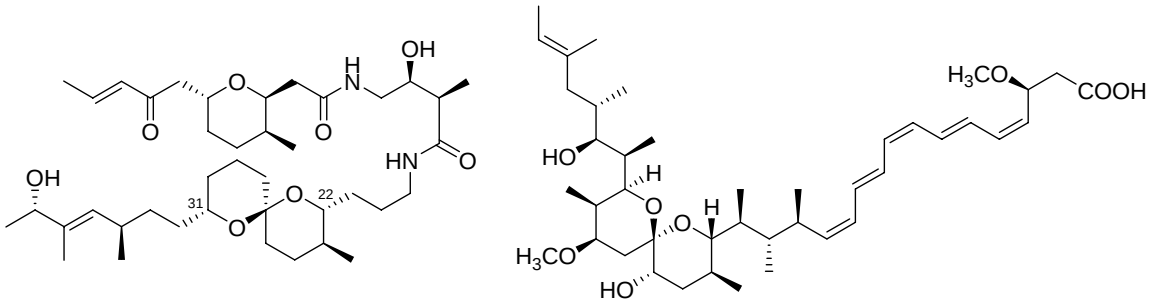

5.1. Bistramide A **5.4**. Spirangian A

Figure 5.6. *Spiroketal-containing marine metabolites*

The bacterium was shown to contain enzymes capable of catalyzing the formation of the spiroketal moiety. Similar spiroketal ring systems were found in the polyketide monensin from *Streptomyces cinnamonensis*, and were proposed to derive from a set of bacterial enzymes termed MonB.[60] Although slightly different biosynthetic mechanisms were proposed for each of the aforementioned spiroketal functionalities, it is evident that all of the metabolites were isolated from bacteria, thus strengthening the current proposition that *Prochloron* spp. are at least partly responsible for the production of bistramides in *Lissoclinum bistratum* and *Tridemnum* sp.

5.3 Experimental Section.

General Experimental Procedures. NMR spectra were obtained on JEOL Eclipse 500 and Varion Inova 400 spectrometers. Mass spectra were obtained on a JEOL JMS-HX-110 instrument and a Finnigan LTQ LC/MS. CD analysis was performed on a JASCO J-720 spectropolarimeter. Chemical shifts are given in δ (ppm), and coupling constants (*J*) are reported in Hz. HPLC was performed using Shimadzu LC-10AT pumps coupled with analytical and semi-preparative Phenomenex Luna C18 columns (250 × 4.6 and 250 × 10

mm, respectively) and a semi-preparative Varian Lichrosorb diol phase column (250 × 10 mm). The HPLC system employed a Shimadzu SPD-M10A diode array detector and a Shimadzu FRC-10A fraction collector.

Antiproliferative Bioassays. The A2780 ovarian cancer cell line antiproliferative assay was performed at Virginia Polytechnic Institute and State University by Ms. Peggy Brodie as previously reported.[61]

Bioassay Guided Fractionation of Compounds from *Tridemnum* sp. The dried marine sample was extracted with EtOH to give 3.3 g of extract designated NB 0405_31. Extract NB 0405_31 (2.5 g; 2.0 μg/mL) was suspended in aqueous MeOH (MeOH-H_2O, 9:1, 1,000 mL) and extracted with hexanes (2 × 500 mL; 14 μg/mL). The aqueous layer was then diluted to 40% water and extracted with DCM (2 × 500 mL). The DCM fraction displayed antiproliferative activity (IC_{50} = 0.10 μg/mL), thus it was further chromatographed over a reversed phase C18 column to yield six fractions (E-J). Fraction G (30.3 mg, IC_{50} = 0.13 μg/mL) was determined to be the most active.

Fraction G was found to be extremely complex, and a direct HPLC separation method required an abnormally long run time. After much trial and error, a method was developed that gave excellent separation of most fractional components, but the last compound to elute was at t_R 155 minutes. Before proceeding with such a long separation process it was necessary to determine whether the later eluting species exhibited activity; if these species were found to be inactive, it would be possible to reduce the run time by simply recovering all of the inactive and highly retained components with a methanol

flush. To locate the source(s) of activity, a unique small-scale microplate collection method was used. The newly developed semi-preparative HPLC conditions (column: 250 × 10.0 mm, flow rate: 2.0 mL/min) were adjusted to be compatible on an analytical scale (column: 250 × 4.60 mm, flow rate: 1.0 mL/min). Fraction G (0.5 mg) was injected into the analytical column and 1 mL of eluent was collected in each of 70 wells of the microplate, each well corresponding to one specific minute of the run. The sample was then concentrated at the bottom of the wells by evaporation on a Genevac evaporator and the plate was submitted directly for bioassay against the A2780 cell line. Since the exact weight of sample in each well was unknown, it was assumed that the HPLC separation resulted in an equal distribution of sample throughout the wells. This allowed for approximation of the sample weight in each well and therefore an approximate concentration of sample that was applied to the single-dose A2780 assay (in the "single-dose" method one concentration of a given sample is tested, rather than a series of concentrations of a given sample). This served to give a preliminary indication of where the activity might be located.

Unfortunately, the assay results showed that the activity was distributed through several wells toward the middle and end of the run, eliminating the possibility of shortening the method. Consequently, semi-preparative reversed phase C18 HPLC with an isocratic flow of 73% aqueous methanol was used to separate fraction G (Figure 5.7). This technique afforded one pure compound, bistramide A (**5.1**, fraction 27, t_R 135 min, 1.1 mg, IC_{50} = 0.27 μM). It should be noted that other pure compounds were collected, but the very small quantities obtained prevented their structure elucidation. Fraction H was also active (32.5 mg, IC_{50} = 0.46 μg/mL), and its HPLC profile was nearly identical

chromatogram to that of fraction G, with the exception of a few more strongly retained species.

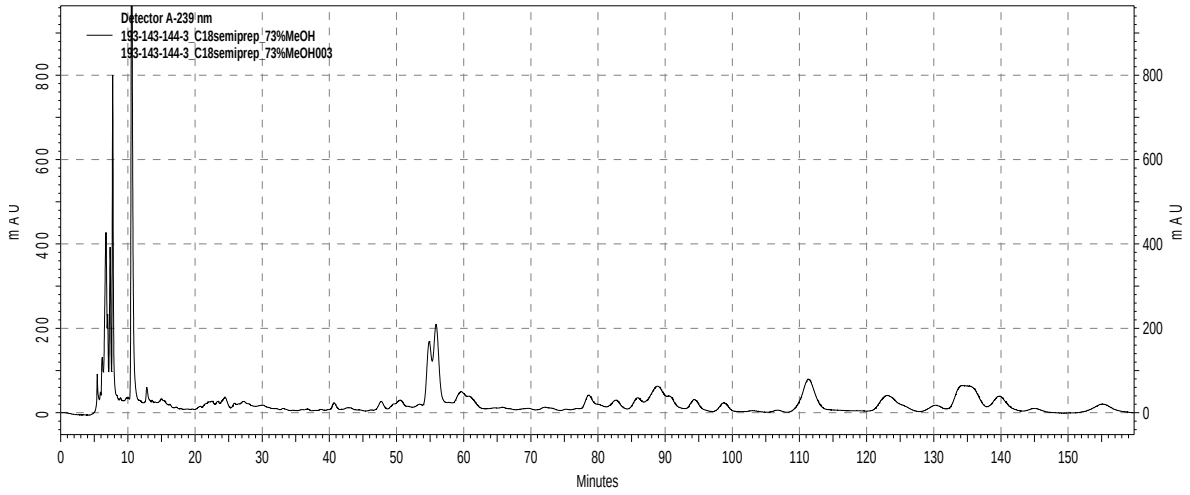

Figure 5.7. *Semi-preparative HPLC chromatogram of fraction G @ 239 nm*

The separation of fraction G yielded many potentially active fractions, which ranged in weight from 0.20 mg to 0.90 mg. This limited weight prevented further bioassay testing, because if each sample was tested it would not be able to be recovered for structure elucidation. This necessitated the use of more unconventional methods for which to guide the fractionation process. A quick screening of the ^{1}H NMR spectra of these HPLC fractions revealed that many had characteristic resonances of a bistramide-type skeleton. Since bistramides are known bioactive agents, there was a high probability that this was the cause of the bioactivity exhibited by the sample. Due to their structural complexity and insufficient sample weight for analysis by NMR spectroscopy, a re-extraction of NB 0405_31 was undertaken in the hope of re-isolating some of these bistramides.

Extract NB 0405_31 (0.76 g) was suspended in aqueous MeOH (MeOH-H_2O, 9:1, 500 mL) and extracted with hexanes (2 × 250 mL; 3.3 μg/mL). The aqueous layer was then diluted to 40% water and extracted with DCM (2 × 250 mL). The DCM fraction displayed antiproliferative activity (IC_{50} = 1.7 μg/mL) and was further chromatographed over a reversed phase C18 column to yield four fractions (T-W). Fraction U (49.6 mg, IC_{50} = 0.20 μg/mL) was the most active. Semi-preparative reversed phase C18 HPLC using 73% aqueous MeOH resulted in the collection of fractions 31-80 (Figure 5.8). Based on sample weight and its ^{1}H NMR spectrum, fraction 67 was purified on a semi-preparative diol phase HPLC column using an isocratic flow of 87% DCM and 13% MeOH to afford bistramide D (**5.2**, t_R 7.0 min, 0.7 mg, IC_{50} = not tested). Fractions V and W were also moderately active (26.2 mg, IC_{50} = 1.2 μg/mL and 18.6 mg, IC_{50} = 0.37 μg/mL, respectively). Fraction V was separated over an open silica column to yield three fractions with activity weaker than that of the parent fraction (IC_{50} values from 2.2 - 12 μg/mL). Fraction W was separated using a diol HPLC column to afford moderately active fractions with very small quantities of bistramides and long-chain compounds. It was judged that there was only a small possibility for purification and structure elucidation of the bioactive compounds in this fraction, and thus fraction W and fraction V, were not studied further.

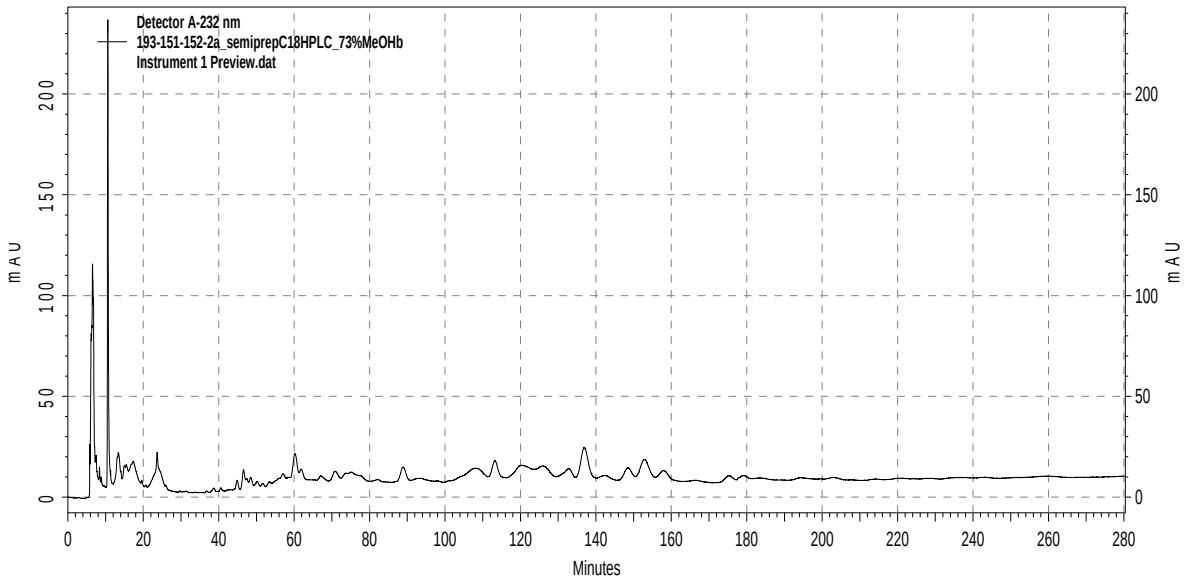

Figure 5.8. *Semi-preparative HPLC chromatogram of fraction U @239 nm*

Despite employing identical fractionation procedures for the two crude marine extracts, it was apparent by the HPLC chromatogram that fraction U contained a few more weakly UV-active non-polar constituents (t_R 180 – 260 min), when compared with fraction G. This greatly lengthened the HPLC run and the separation of this fraction required one month of HPLC time. Though there was excellent reproducibility from fractions G to U, co-elution of the active bistramides with other minor components ultimately prevented successful purification of most of these metabolites, therefore preventing structure elucidation and further bioassay work.

Bistramide A (5.1): light green oil; CD (MeOH, *c* 0.0077) $[\theta]_{215}$ -5.44, $[\theta]_{246}$ 1.87, $[\theta]_{259}$ 2.68; ^{1}H NMR ($CDCl_3$): δ_H 0.80 (3H, d, H-24, J = 6.5 Hz), 0.86 (3H, d, H-10, J = 7.0 Hz), 0.94 (3H, d, H-35, J = 6.5 Hz), 1.24 (3H, d, H-17, J = 6.5 Hz), 1.25 (3H, d, H-40, J

= 7.5 Hz), 1.10 – 1.90 (24H, m, H-7, 8, 9, 20, 21, 23, 25, 26, 28, 29, 30, 32, 33), 1.91 (3H, dd, H-1, *J* = 1.5, 6.5 Hz), 2.19 (1H, m, H_a-12), 2.33 (1H, m, H-24), 2.37 (1H, m, H-16), 2.52 (1H, dd, H_a-5, *J* = 3.0, 16.5 Hz), 2.76 (1H, dd, H_b-12, *J* = 11.5, 15.0 Hz), 2.90 (1H, dd, H_b-5, *J* = 9.0, 17.0 Hz), 3.14 (1H, t, H-22, *J* = 9.5 Hz), 3.25 (1H, m, H_a-14), 3.30 (2H, m, H-19), 3.46 (1H, m, H-31), 3.51 (1H, m, H_b-14), 3.71 (1H, m, H-15), 4.06 (1H, dd, H-11, *J* = 4.5, 11.0 Hz), 4.19 (1H, m, H-6), 5.18 (1H, d, H-36, *J* = 9.0 Hz), 6.12 (1H, dd, H-3, *J* = 1.5, 16.0 Hz), (1H, dd, H-2, *J* = 6.5, 16.0 Hz), 6.96 (1H, t, NH-19, *J* = 5.5 Hz), 7.32 (1H, t, NH-14, *J* = 5.5 Hz); ^{13}C NMR, see Table 5.1; LCEIMS *m/z* 705.5 $[M+H]^+$ (calcd for $C_{40}H_{69}N_2O_8$, 705.5).

Bistramide D (5.2): light green oil; ^{1}H NMR (CD_3OD): δ_H 0.83 (3H, d, H-24, *J* = 6.5 Hz), 0.85 (3H, d, H-10, *J* = 7.0 Hz), 0.95 (3H, d, H-35, *J* = 6.5 Hz), 1.14 (3H, d, H-17, *J* = 7.0 Hz), 1.20 (3H, d, H-40, *J* = 6.5 Hz), 1.25 – 1.95 (22H, m, H-7, 9, 20, 21, 23, 25, 26, 28, 29, 30, 32, 33), 1.35 (2H, m, H-8), 1.38 (2H, m, H-33), 1.43 and 1.65 (2H, m, H-5), 1.61 (3H, s, H-38), 1.67 (d, H-1, *J* = 6.5 Hz), 2.23 (1H, dd, H_a-12, *J* = 4.0, 15.0 Hz), 2.38 (2H, m, H-16, 34), 2.70 (1H, dd, H_b-12, *J* = 11.0, 15.0 Hz), 3.15-3.20 (2H, m, H_a-14, 22), 3.23 (2H, m, H-19), 3.44 (1H, dd, H_b-14, *J* = 4.0, 14.0 Hz), 3.52 (1H, m, H-31), 3.73 (1H, m, H-15), 3.81(1H, m, H-6), 4.11 (1H, m, H-4), 4.14 (1H, m, H-39), 4.27 (1H, ddd, H-11, *J* = 4.0, 6.5, 8.5 Hz), 5.13 (1H, d, H-36, *J* = 9.0 Hz), 5.45 (1H, ddd, H-3, *J* = 1.5, 7.0, 15.5 Hz), 5.64 (1H, dd, H-2, *J* = 7.0, 15.5 Hz). LCEIMS *m/z* 707.6 $[M+H]^+$, 729.5 $[M+Na]^+$ (calcd for $C_{40}H_{71}N_2O_8$, 707.5; calcd for $C_{40}H_{70}N_2O_8Na$, 729.5).

References

1. (a) Murphy, B. T.; Cao, S.; Brodie, P.; Foster, C.; Lazo, J. S.; Kingston, D. G. I. **2007**, Poster presentation, American Society of Pharmacognosy National Meeting, Portland, ME, "Potent antiproliferative bistramides of the ascidian *Tridemnum sp.* from Madagascar"; (b) Murphy, B. T.; Cao, S.; Brodie, P.; Foster, C.; Lazo, J. S.; Kingston, D. G. I. **2007**, Oral presentation, Southeast Regional Meeting of the American Chemical Society, Greenville, SC, "Antiproliferative bistramides of the marine tunicate *Tridemnum sp.* from Madagascar."

2. Sakai, R.; Rinehart, K. L..; Kishore, V.; Kundu, B.; Faircloth, G.; Gloer, J. B.; Karney, J. R.; Namikoshi, N.; Sun, F.; Hughes, R. G.; Grávalos, D. G.; Quesada, G.; Wilson, G. R.; Heid, R. M. Structure-activity relationships of the didemnins. *J. Med. Chem*. **1996**, *39*, 2819-2834.

3. (a) Rinehart, K. L..; Gloer, J. B.; Cook, J. C. Structures of the didemnins, antiviral and cytotoxic depsipeptides from a Caribbean tunicate. *J. Am. Chem. Soc*. **1981**, *103*, 1857-1859. (b) Rinehart, K. L.; Gloer, J. B.; Hughes, R. G.; Renis, H. E.; McGovren, P. J.; Swynenberg, E. B.; Stringfellow, D. A.; Kuentzel, S. L.; Li, L. H. Didemnins: antiviral and antitumor depsipeptides from a Caribbean tunicate. *Science* **1981**, *212*, 933-935.

4. Sakai, R.; Stroh, J. G.; Sullins, D. W.; Rinehart, K. L. Seven new didemnins from the marine tunicate *Tridemnum solidum*. *J. Am. Chem. Soc*. **1995**, *117*, 3734-3748.

5. Boulanger, A.; Abou-Mansour, E.; Badre, A.; Banaigs, B.; Combaut, G.; Francisco, C. The complete spectral assignment of didemnin H, a new constituent of the tunicate *Tridemnum cyanophorum*. *Tetrahedron Lett*. **1994**, *35*, 4345-4348.

6. Abou-Mansour, E.; Boulanger, A.; Badre, A.; Bonnard, I.; Banaigs, B.; Combaut, G. ; Francisco, C. [Tyr5] didemnin **B** and [D-Pro4] didemnin **B**; Two new natural didemnins with a modified macrocycle. *Tetrahedron* **1995**, *51*, 12591-12600.

7. Vervoort, H. ; Fenical, W.; Epifanio, R. Tamandarins A and B: New cytotoxic depsipeptides from a Brazilian ascidian of the family Didemnidae. *J. Org. Chem.* **2000**, *65*, 782-792.

8. Banaigs, B.; Abou-Mansour, E.; Boulanger, A.; Bonnard, I.; Francisco, C. [Hysp2] and [Hap2]didemnin B, two new [Hip2]-modified didemnin B from the tunicate *Tridemnum cyanophorum*. *Tetrahedron* **1999**, *55*, 9559-9574.

9. Maldanado, E.; Lavergne, J. A.; Kraiselburd, E.; Didemnin A inhibits the *in vitro* replication of dengue virus types 1, 2, and 3. *P. R. Health Sci. J.* **1982**, *1*, 22-25.

10. Canonico, P. G. ; Pannier, W.; L.; Huggins, J. W.; Rinehart, K. L. *Antimicrob. Agents Chemother.* Inhibition of RNA viruses *in vitro* and in Rift Valley Fever-infected mice by didemnins A and B. **1982**, *22*, 696-697.

11. National Cancer Institute Clinical Brochure, Didemnin B. NSC325319. IND. Division of Cancer Treatnment, NCI, Bethesda, MD, June 1984.

12. Chun, H. G.; Davies, B.; Hoth, D.; Suffness, M.; Plowman, J.; Flora, K.; Grieshaber, C.; Leyland-Jones, B. Didemnin B. The first marine compound entering clinical trials as an antineoplastic agent. *Invest. New Drugs* **1986**, *4*, 279-284.

13. Dohr, F. A.; Kuhn, J. G.; Phillips, J.; Von Hoff, D. D. Phase I clinical and pharmacokinetic investigation of didemnin B, a cyclic depsipeptide. *Eur. J. Cancer Clin. Oncol.* **1988**, *24*, 1699-1706.

14. Li, L. H.; Timmins, L. G.; Wallace, T. L.; Krueger, W. C.; Prairie, M. D.; Im, W. B. Mechanism of action of didemnin B, a depsipeptide from the sea. *Cancer Lett.* **1984**, *23*, 279-288.

15. Gouiffes, D.; Moreau, S.; Helbecque, N.; Bernier, J. L.; Henichart, J. P.; Barbin, Y.; Laurent, D.; Verbist, J. F. Proton nuclear magnetic study of bistramide A, a new cytotoxic drug isolated from *Lissoclinum bistratum*. *Tetrahedron* **1988**, *44*, 451-459.

16. Biard, J. F.; Roussakis, C.; Kornprobst, J. M.; Gouiffes-Barbin, D.; Verbist, J. F.; Cotelle, P.; Foster, M. P.; Ireland, C. M.; Debitus, C. Bistramides A, B, C, D, and K: A new class of bioactive cyclic polyethers from *Lissoclinum bistratum*. *J. Nat. Prod.* **1994**, *57*, 1336-1345.

17. Gouiffes, D.; Juge, M.; Grimaud, N.; Welin, L.; Sauviat, M. P.; Barbin, Y.; Laurent, D.; Roussakis, C.; Henichart, J. P.; Verbist, J. F. Bistramide A, a new toxin from the urochordata *Lissoclinum bistratum* Sluiter. *Toxicon* **1988**, *26*, 1129-1136.

18. Foster, M. P.; Mayne, C. L.; Dunkel, R.; Pugmire, R. J.; Grant, D. M.; Kornprobst, J. M.; Verbist, J. F.; Biard, J. F.; Ireland, C. M. Revised structure of bistramide A (bistratene A): Application of a new program for the automated analysis of 2D INADEQUATE spectra. *J. Am. Chem. Soc*. **1992**, *114*, 1110-1111.

19. Dunkel, R.; Mayne, C. L.; Foster, M. P.; Ireland, C. M.; Li, D.; Owen, N. L.; Pugmire, R. J.; Grant, D. M. Applications of the improved computerized analysis of 2D INADEQUATE spectra. *Anal. Chem*. **1992**, *64*, 3150-3160.

20. (a) Lowe, J. T.; Wrona, I. E.; Panek, J. S. Total synthesis of bistramide A. *Org. Lett.* **2007**, *9*, 327-330. (b) Yadav, J. S.; Chetia, L. Stereoselective total synthesis of bistramide A. *Org. Lett.* **2007**, *9*, 4587-4589.

21. Bauder, C.; Biard, J. F.; Solladie, G. Synthesis of derivatives of potent antitumor bistramides D and A leading to the first crystal structure of natural bistramide D. *Org. Biomol. Chem*. **2006**, *4*, 1860-1862.

22. Crimmins, M. T.; DeBaillie, A. C. Enantioselective total synthesis of bistramide A. *J. Am. Chem. Soc*. **2006**, *128*, 4936-4937.

23. Wipf, P.; Hopkins, T. D. Total synthesis and structure validation of (+)-bistramide C. *Chem. Comm.* **2005**, *27,* 3421-3423.

24. Lowe, J. T.; Panek, J. S. Proton nuclear magnetic study of bistramide A, a new cytotoxic drug isolated from *Lissoclinum Bistratum* Sluiter. *Tetrahedron* **1988**, *44*, 451-459.

25. Statsuk, A. V.; Liu, D.; Kozmin, S. A. Synthesis of bistramide A. *J. Am. Chem. Soc*. **2004**, *126*, 9546-9547.

26. Wipf, P.; Uto, Y.; Seiji, Y. Total synthesis of a stereoisomer of bistramide C and assignment of configuration of the natural product. *Eur. J. Chem.* **2002**, *8,* 1670-1681.

27. Gallagher, P.O.; McErlean, C. S. P.; Jacobs, M. F.; Watters, D. J.; Kitching, W. Sub-structure syntheses and relative stereochemistry in the bistramide (bistratene) series of marine metabolites. *Tetrahedron Lett.* **2002**, *43*, 531-535.

28. Solladie, G.; Bauder, C.; Biard, J. F. Hemisynthesis of bistramide D by stereoselective reduction of bistramide A. Partial determination of relative and absolute configurations. *Tetrahedron Lett.* **2000**, *41*, 7747-7750.

29. Melville, J. L.; Iain, H.; Baker-Glenn, C.; Shaw, P. E.; Pattenden, G.; Hirst, J. D. The structural determinants of macrolide-actin binding: in silico insights. *Biophys. J.* **2007**, *92*, 3862-3867.

30. Rizvi, S. A.; Tereshko, V.; Kossiakoff, A. A.; Kozmin, S. A. Structure of bistramide A-actin complex at a 1.35 ANG. resolution. *J. Am. Chem. Soc.* **2006**, *128*, 3882-3883.

31. Statsuk, A. V.; Baj, R.; Baryza, J. L.; Verma, V. A.; Hamel, E.; Wender, P. A.; Kozmin, S. A. Actin is the primary cellular receptor of bistramide A. *Nature Chem. Biol.* **2005**, *1*, 383-388.

32. Siavoshian, S.; Jacquot, C.; Biard, J. F.; Briand, G.; Roussakis, C. Subtractive hybridization and differential screening identified two genes differentially expressed after induction of in vitro (atypical) terminal differentiation in the NSCLC-N6 cell line by a marine substance (bistramide K). *Anticancer Res.* **1999**, *19*, 5361-5365.

33. Gautret, P.; Le Pape, P.; Biard, J. F.; Menard, D.; Verbist, J. F.; Marjolet, M. The effect of bistramides on rodent malaria. *Acta Parasitol.* **1998**, *43*, 50-53.

34. Liscia, E.; Riou, D.; Siavoshian, S.; Boesch, S.; Lebert, V.; Tomasoni, C.; Dabouis, G.; Biard, J. F.; Roussakis, C. Terminal differentiation in a non-small-cell

bronchopulmonary carcinoma correlates with increased expression of p53. *Anticancer Res.* **1996**, *16*, 1209-1212.

35. Pusset, J.; Maillere, B.; Debitus, C. Evidence that bistramide A, from the ascidian *Lissoclinum bistratum* Sluiter, has immunomodulating properties *in vitro*. *J. Nat. Tox.* **1996**, *5*, 1-6.
36. Verbist, J. F. Ascidians, an example of the potential value of marine organisms as sources of substances with pharmacological activity. *J. Pharm. Belg.* **1995**, *50*, 98-120.
37. Sauviat, M.P.; Chesnais, J.M.; Diacono, J.; Biard, J.F.; Verbist, J.F. Influence of bistramide A on the twitch tension in rat atrial heart muscle. *Experientia* **1994**, *50*, 926-930.
38. Roussakis, C.; Charrier, J.; Riou, D.; Biard, J. F.; Malochet, C.; Meflah, K.; Verbis, F. Chemotherapeutic inhibition of erb-B2 oncogene expression on a non-small-cell cancer line (NSCLC-N6) by marine substances. *Anti-Cancer Drug Des.* **1994**, *9*, 119-128.
39. Sauviat, M. P.; Verbist, J. F. Alteration of the voltage-dependence of the twitch tension in frog skeletal muscle fibers by a polyether, bistramide A. *Gen. Physiol. Biophys.* **1993**, *12*, 465-471.
40. Riou, D.; Roussakis, C.; Biard, J. F.; Verbist, J. F. A comparative study of the antitumor activity of bistramides A, D and K against a non-small cell broncho-pulmonary carcinoma. *Anticancer Res.* **1993**, *13*, 2331-2334.
41. Riou, D.; Roussakis, C.; Robillard, N.; Biard, J. F.; Verbist, J. F. Bistramide A-induced irreversible arrest of cell proliferation in a non-small-cell

bronchopulmonary carcinoma is similar to induction of terminal maturation. *Biol. Cell* **1993**, *77*, 261-264.

42. Sauviat, M. P.; Chesnais, J. M.; Choukri, N.; Diacono, J.; Biard, J. F.; Verbist, J. F. The polyether bistramide A affects the calcium sensitivity of the contractile proteins in frog atrial heart muscle. *Cell Calcium* **1993**, *14*, 301-309.
43. Sauviat, M. P.; Gouiffes-Barbin, D.; Ecault, E.; Verbist, J. F. Blockade of sodium channels by bistramide A in voltage-clamped frog skeletal muscle fibers. *Biochim. Biophys. Acta Biomem.* **1992**, *1103*, 109-114.
44. Roussakis, C.; Robillard, N.; Riou, D.; Biard, J. F.; Pradal, G.; Piloquet, P.; Debitus, C.; Verbist, J. F. Effects of bistramide A on a non-small-cell bronchial carcinoma line. *Cancer Chemother. Pharmacol.* **1991**, *28*, 283-292.
45. Vaya, N.; Karan, R. S.; Sadanand, S.; Gupta, V. K. Novel dosage form comprising modified-release and immediate-release active ingredients. U. S. Patent cont. in part of U. S. Ser. No. 630, 446, **2006**.
46. Biard, J. F.; Cortadellas, D.; Debitus, C.; Laurent, D.; Roussakis, C.; Verbist, J. F. Biologically active bistramides, process for their production, and their cytostatic applications in therapy, especially against tumors or parasites. PCT Int. Appl. **1994**.
47. Yeung, K. S.; Paterson, I. Actin-binding marine macrolides: Total synthesis and biological importance. *Angew. Chem. Int. Ed.* **2002**, *41*, 4632-4653.
48. Williams, P. G.; Asolkar, R. N.; Kondratyuk, T.; Pezzuto, J. M.; Jensen, P. R.; Fenical, W. Saliniketals A and B, bicyclic polyketides from the marine actinomycete *Salinispora arenicola*. *J. Nat. Prod.* **2007**, *70*, 83-88.

49. Fenical, W; Jenson, P. Developing a new recource for drug discovery: marine actinomycete bacteria. *Nature Chem. Biol*. **2006**, *12*, 666-672.

50. Feling, R. H.; Buchanan, G. O.; Mincer, T. J.; Kauffman, C. A.; Jensen, P. R.; Fenical, W. Salinosporamide A: a highly cytotoxic proteasome inhibitor from a novel microbial source, a marine bacterium of the new genus *Salinospora*. *Angew. Chem., Int*. **2003**, *42*, 355-357.

51. Proksch, P.; Muller, W. E. G. *Frontiers in Marine Biotechnology*; Taylor & Francis, Ltd.: London, 2006; p. 1.

52. Udwary, D. W.; Zeigler, L.; Asolkar, R. N.; Singan, V.; Lapidus, A.; Fenical, W.; Jenson, P. R.; Moore, B. S. Genome sequencing reveals complex secondary metabolome in the marine actinomycete *Salinispora tropica*. *PNAS*, **2007**, *104*, 10376-10381.

53. Lautru, S.; Deeth, R. J.; Bailey, L. M.; Challis, G. L. Discovery of a new peptide natural product by *Streptomyces coelicolor* genome mining. *Nature Chem. Biol*. **2005**, *1*, 265-269.

54. Wilkinson, B.; Micklefield, J. Mining and engineering natural product biosynthetic pathways. *Nat. Chem. Biol*, **2007**, *3*, 379-386.

55. Münchoff, J.; Hirose, E.; Maruyama, T.; Sunairi, M.; Burns, B. P.; Neilan, B. A. Host specificity and phylogeography of the prochlorophyte *Prochloron* sp., an obligate symbiont in didemnid ascidians. *Envir. Microbiol.* **2007**, *9*, 890-899.

56. Shimada, A.; Yano, N.; Kanai, S.; Lewin, R. A.; Maruyama, T. Molecular phylogenetic relationship between two symbiotic photo-oxygenic prokaryotes, *Prochloron* sp. and *Synechocystis trididemni*. *Phycologia* **2003**, *42*, 193-197.

57. Schmidt, E. W.; Sudek, S.; Haygood, M. G. Genetic evidence supports secondary metabolite diversity in *Prochloron* spp., the cyanobacterial symbiont of a tropical ascidian. *J. Nat. Prod.* **2004**, *67*, 1341-1345.

58. Schmidt, E. W.; Nelson, J. T.; Rasko, D. A.; Sudek, S.; Eisen, J. A.; Haygood, M. G., Ravel, J. Patellamide A and C biosynthesis by a microcin-like pathway in *Prochloron didemni*, the cyanobacterial symbiont of *Lissoclinum patella*. *Proc. Nat. Acad. Sci.* **2005**, *102*, 7315-7320.

59. Frank, B.; Knauber, J.; Steinmetz, H.; Scharfe, M.; Blöcker, H.; Beyer, S.; Müller, R. Spiroketal polyketide formation in *Sorangium*: identification and analysis of the biosynthetic gene cluster for the highly cytotoxic spirangienes. *Chem. Biol*., **2007**, *14*, 221-233.

60. Gallimore, A. R.; Stark, C. B. W.; Bhatt, A.; Harvey, B. M.; Demydchuk, Y.; Bolanos-Garcia, V.; Fowler, D. J.; Staunton, J.; Leadlay, P. F.; Spencer, J. B. Evidence for the role of monB genes in polyether ring formation during monensin biosynthesis. *Chem. Biol*. **2006**, *13*, 453-460.

61. Cao S.; Brodie, P. J.; Miller J. S.; Randrianaivo, R.; Ratovoson, F.; Birkinshaw, C.; Andriantsiferana, R.; Rasamison, V. E.; Kingston D. G. I. Guttiferones K and L, Antiproliferative Compounds of *Rheedia calcicola* from the Madagascar Rain Forest. *J. Nat. Prod*. **2007**, *70*, 686-688.

VI. Miscellaneous Plants Studied

6.1 Introduction

Throughout the course of our research, occasionally we are unable to extract any substance of worthy bioactivity or novelty. However, for purposes of building phytochemical libraries, these plants and their constituents will be reported.

6.1.1 Investigation of Ravensara floribunda (MG 1916).

An ethanol extract of the leaves of *Ravensara floribunda* (Lauraceae) displayed an IC_{50} value of 18 μg/mL in the A2780 human ovarian cancer cell assay. Liquid/liquid partitioning of 201 mg of crude material followed by separation of the aqueous fraction over reversed-phase HPLC afforded 22 mg of colorless crystals. The molecule's identity was confirmed by comparison of ^{1}H and ^{13}C NMR data with the literature,[1] in addition to analysis of x-ray diffraction data. The substance was identified as cryptomoscatone D1 (**6.1**), a 6-[ω-arylalkenyl]-5,6-dihydro-pyrone. It displayed an IC_{50} value of 47 μM (8.5 μg/mL).

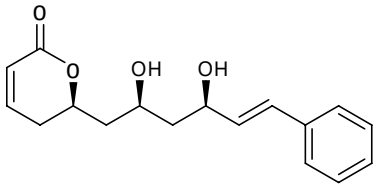

6.1

6.1.2 Investigation of Plagioscyphus sp. (MG 2157)

An ethanol extract of the leaves of *Plagioscyphus* sp. (Sapindaceae) displayed an IC_{50} value of 20 μg/mL in the A2780 human ovarian cancer cell assay. Liquid/liquid partitioning of 1 g of crude material followed by consecutive polyamide and MCI gel columns afforded an impure flavonol glycoside. Purification over reversed-phase C-18 HPLC afforded 2.1 mg of a yellow oil. The compound was identified as kaempferol-3-*O*-α-L-rhamnopyranoside (**6.2**) on the basis of extensive interpretation of one and two-dimensional NMR data. It was inactive in the A2780 assay. Throughout fractionation of MG 2157 activity was continuously lost, thus further fractionation of the plant was stopped.

The crude extract was also active against the Akt enzyme-based assay at an IC_{50} value of 9.3 μg/mL, however further fractionation resulted only in the loss of this activity. Fractionation of the plant was stopped.

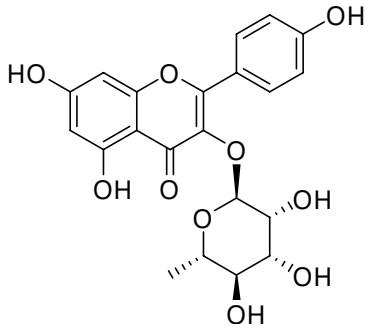

6.2

6.1.3 Investigation of Pemphis acidula (MG 2317)

An ethanol extract of the roots of *Pemphis acidula* (Lythraceae) displayed an IC_{50} value of 9.4 µg/mL in the A2780 human ovarian cancer cell assay. Upon retesting however, the IC_{50} value was determined to be approximately 25 µg/mL. Liquid/liquid partitioning of 116 mg of crude material followed by separation of the aqueous methanol fraction over Sephadex LH-20 led to the collection of seven weakly active fractions (IC_{50} range of 22-24 µg/mL). Reversed-phase HPLC of a fraction containing the bulk of the material afforded 0.95 mg of (+)-catechin (**6.3**). The structure was identified on the basis of interpretation of one and two-dimensional NMR data. It was inactive in the A2780 assay.

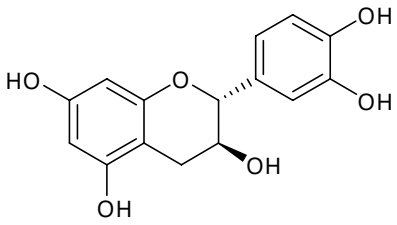

6.3

6.1.4 Investigation of Xylopia sp. (MG 1834, 1835)

An ethanol extract of the leaves of *Xylopia* sp. (Annonaceae) displayed an IC_{50} value of 14 µg/mL in the A2780 human ovarian cancer cell assay. Upon retesting however, the IC_{50} value was determined to be approximately 23 µg/mL. Liquid/liquid partitioning of 1.5 g of crude material followed by phenyl HPLC afforded a number of fractions, one of which displayed weak activity (IC_{50} = 15 µg/mL). By analysis of its ^{1}H

NMR spectrum the fraction was believed to contain a mixture of diterpenes, and further fractionation failed to increase the bioactivity. Further separation was stopped.

An ethanol extract of the wood of *Xylopia* sp. displayed an IC_{50} value of 16 µg/mL in the A2780 assay. Liquid/liquid partitioning of 200 mg of crude followed by separation of the aqueous methanol fraction over a series of C-18 columns failed to increase the bioactivity. Further separation of the plant was stopped.

6.1.5 Investigation of Polyscias sp. (MG 0870)

An ethanol extract of the leaves of *Polyscias* sp. (Araliaceae) displayed an IC_{50} value of 12.9 µg/mL in the A2780 human ovarian cancer cell assay. Liquid/liquid partitioning of 363 mg of crude material followed by separation of the aqueous methanol fraction over Sephadex LH-20 led to the collection of seven fractions. Three of the active fractions (IC_{50} = 6.3, 12, and 14 µg/mL) were screened by ^1H NMR spectroscopy and determined to contain typical resonances of triterpene saponins. Dr. Prakash Chaturvedula, formerly of the Kingston research group, had isolated several bioactive oleanane saponins from *Polyscias amplifolia*.[c] Since it appeared as though the activity of MG 0870 was due to similar triterpene saponins, and since these compounds are unattractive drug candidates, further separation of the plant was stopped.

6.1.6 Investigation of Rhopalocarpus macrorhamnifolius (MG 1813)

An ethanol extract of the fruits of *Polyscias* sp. (Araliaceae) displayed an IC_{50} value of 18 µg/mL in the A2780 human ovarian cancer cell assay. Liquid/liquid partitioning of 260 mg of crude material followed by separation of the aqueous methanol

fraction over consecutive polyamide and C-18 columns failed to increase the bioactivity. The brown flaky texture of most of the fractions in addition to the loss of approximately half of the plant mass on the polyamide column suggested the presence of tannins. Thus, further separation of the plant was stopped.

6.1.7 Investigation of Potameia sp. (MG 1848, 1849)

An ethanol extract of the wood of *Potameia* sp. (Lauraceae) displayed an IC_{50} value of 21.8 µg/mL in the A2780 human ovarian cancer cell assay. Liquid/liquid partitioning of 200 mg of crude material followed by separation of the aqueous methanol fraction over consecutive LH-20 and C-18 columns failed to increase the bioactivity. Activity of all fractions never exceeded the original bioactivity of the crude extract, thus further separation of the plant was stopped.

An ethanol extract of the leaves of *Potameia* sp. displayed an IC_{50} value of 19.4 µg/mL in the A2780 assay. Liquid/liquid partitioning of 120 mg of crude material followed by separation of the aqueous methanol fraction over an SPE diol column failed to increase the bioactivity. Activity of all fractions never exceeded the original bioactivity of the crude extract, thus further separation of the plant was stopped.

6.1.8 Investigation of Rothmannia sp. (MG 1891, 1893)

An ethanol extract of the roots of *Rothmannia* sp. (MG 1891; Rubiaceae) displayed an IC_{50} value of 19.1 µg/mL in the A2780 human ovarian cancer cell assay. Liquid/liquid partitioning of 100 mg of crude material followed by separation of the weakly active chloroform and aqueous methanol fractions (IC_{50} = 15, 22 µg/mL,

respectively) over an MCI gel column failed to produce significant bioactivity. Further separation of the plant was stopped.

An ethanol extract of the fruits and leaves of *Rothmannia* sp. (MG 1893) displayed an IC_{50} value of 29.7 μg/mL in the A2780 human ovarian cancer cell assay. Liquid/liquid partitioning of 100 mg of crude between hexanes and 90% aqueous methanol failed to produce significant bioactivity. Further separation of the plant was stopped.

6.1.9 Investigation of Terminalia sp. *(MG 2182).*

An ethanol extract of the bark of *Terminalia* sp. (Combretaceae) displayed an IC_{50} value of 4.7 μg/mL in the Akt enzyme-based assay. Liquid/liquid partitioning of 200 mg of crude material was followed by a separation of the aqueous fraction over a reversed-phase polyamide column. The resulting fractions all displayed ^{1}H NMR profiles resembling high molecular weight tannins. Consequently, further separation of the plant was stopped.

References

1. Cavalheiro, J. C.; Yoshida, M. *Phytochemistry* **2000**, 53, 811-819.
2. Chaturvedula, P.; Schilling, J. K.; Miller, J. S.; Andriantsiferana, R.; Rasamison, V. E.; Kingston, D. G. I. *Planta Med*. **2003**, *69*, 440-444.

VII. Synthesis and Bioactivities of Simplified Adociaquinone B and Naphthoquinone Derivatives against Cdc25B Phosphatase [1]

7.1 Introduction

Some simplified adociaquinone B analogs and a series of 1,4-naphthoquinone derivatives were synthesized and tested against the three enzymes Cdc25B, MKP1, and MKP2. Cdc25B in particular is an enzyme overexpressed in cancer cells and its inhibition may represent a potential method of chemotherapeutic treatment. A number of analogs exhibited significant inhibitory activity against these enzymes, and the bioassay data in addition to structure–activity relationships of these compounds will be discussed.

7.1.1 Role of Cdc25B in Regulation of the Cell Cycle

The cell cycle is a process that regulates the growth and maintenance of organisms via four stages (G1, S, G2, M), and ultimately results in mitosis. Transition through these stages is regulated by various cyclin dependant kinase (CDK)-cyclin complexes (Figure 7.1), whose activation by a subclass of dual-specificity protein tyrosine phosphatases, namely Cdc25A, B, and C, is a biochemical prerequisite.[2] Studies have linked the oncogenesis of several types of human tumors with the overexpression of Cdc25A and B, thus suggesting that the inhibition of these dual-specificity phosphatases may prove to be a viable and attractive method of cancer treatment.[2-5]

Cdc25B was shown to primarily activate CDK1-cyclin A and CDK1-cyclin B at the G2-M transition of the cell cycle via dephosphorylation of nearby Thr14 and Tyr15 residues,[5-9] though more recent studies have proven that each of the three Cdc25s is involved in the G1-S and G2-M transitions.[10-12] These findings have demonstrated the

difficulty in limiting a Cdc25 enzyme and its corresponding CDK-cyclin complex to one specific cellular role.[13]

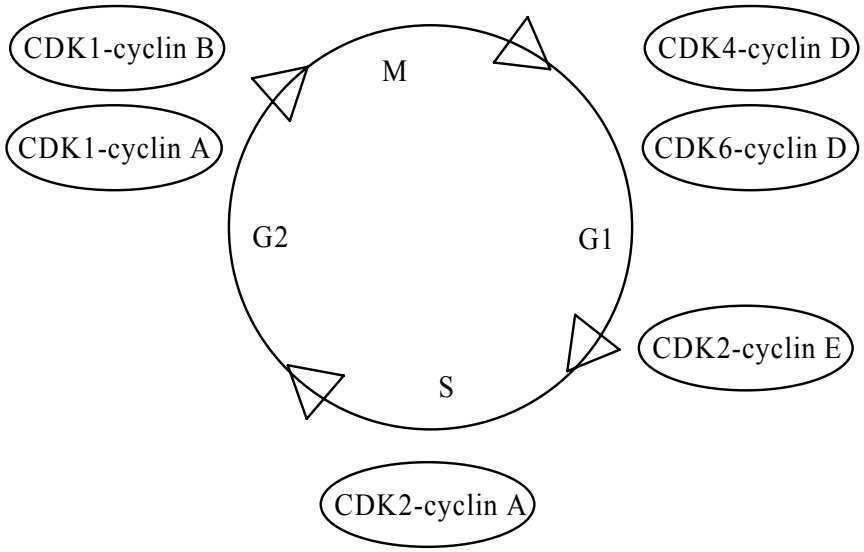

Figure 7.1. *CDK-cyclin complexes and the cell cycle.*[13]

At a chemical level, promotion of the transition between G2-M by CDK1-cyclin A and B is catalyzed via dephosphorylation by a specific cysteine thiolate anion found in a shallow pocket of Cdc25B (Figure 7.2).[14-16] Binding to or oxidation of this thiolate anion prevents activation of the CDK1-cyclin complex, hence triggering cell cycle arrest.[17,18]

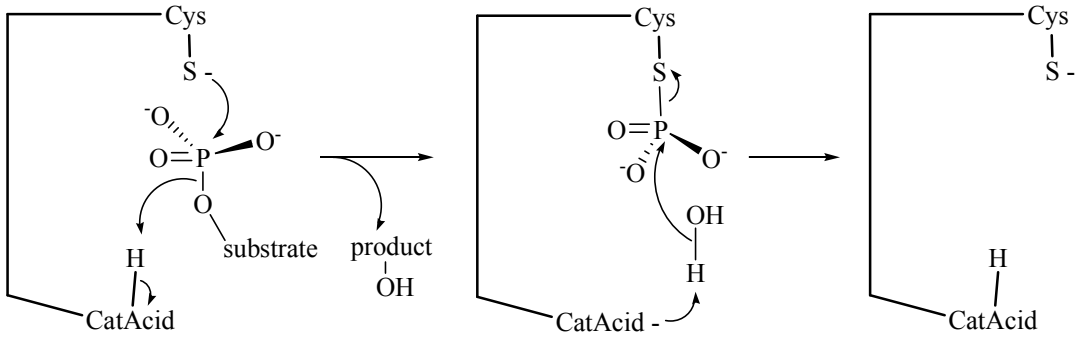

Figure 7.2. *Cdc25B dephosphorylation mechanism.*

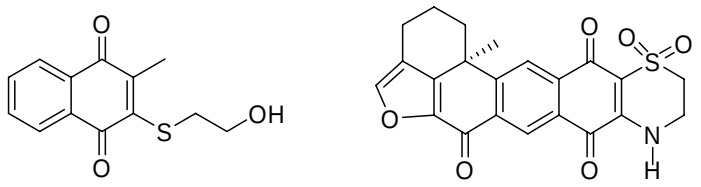

7.1. NSC 672121 **7.2. Adociaquinone B**

Figure 7.3. *Structures of potent Cdc25B inhibitors.*

A majority of the known Cdc25B inhibitors are quinones or quinone-type compounds. Naphthoquinone derivative NSC 672121 (**7.1**; 2.0 μM inhibition of Cdc25B) has received considerable attention after emerging from an activity-based screening of a National Cancer Institute (NCI) chemical repository of 10,070 compounds.[19] Since then, several studies have attempted to improve this scaffold through analog synthesis.[20-25] Furthermore, Dr. Shugeng Cao in the group has previously reported a number of isolates from the Indonesian sponge *Xestospongia* sp., and among them identified what is believed to be the most potent known inhibitor of Cdc25B, adociaquinone B (**7.2**; 0.08-0.11 μM).[26] Reported herein is the design and synthesis of simplified adociaquinone B analogs in addition to several naphthoquinone derivatives, and their subsequent ability to inhibit Cdc25B dual-specificity phosphatase.

7.2 Results and Discussion

7.2.1 Synthesis of Cdc25B Inhibitors

Compounds **7.10**-**7.14** were prepared via coupling reactions of naphthoquinone derivatives with hypotaurine, ethanolamine, and ethanol. Compounds **7.3**-**7.8** were

purchased from commercial entities. Compound **7.9** was synthesized by Dr. Shugeng Cao following the methods in the literature as previously described.[27-30]

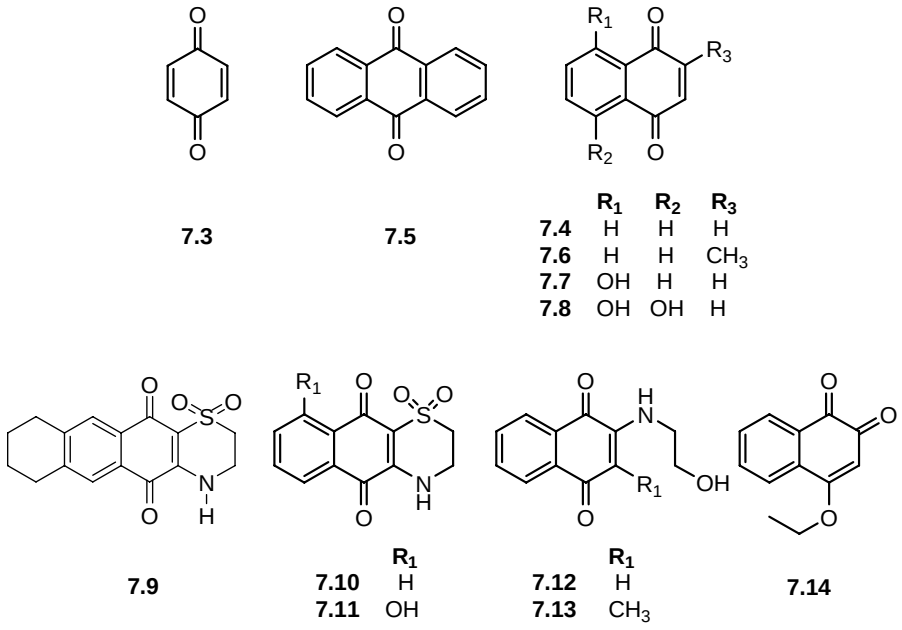

Figure 7.4. *Structures of Cdc25B inhibiting quinones.*

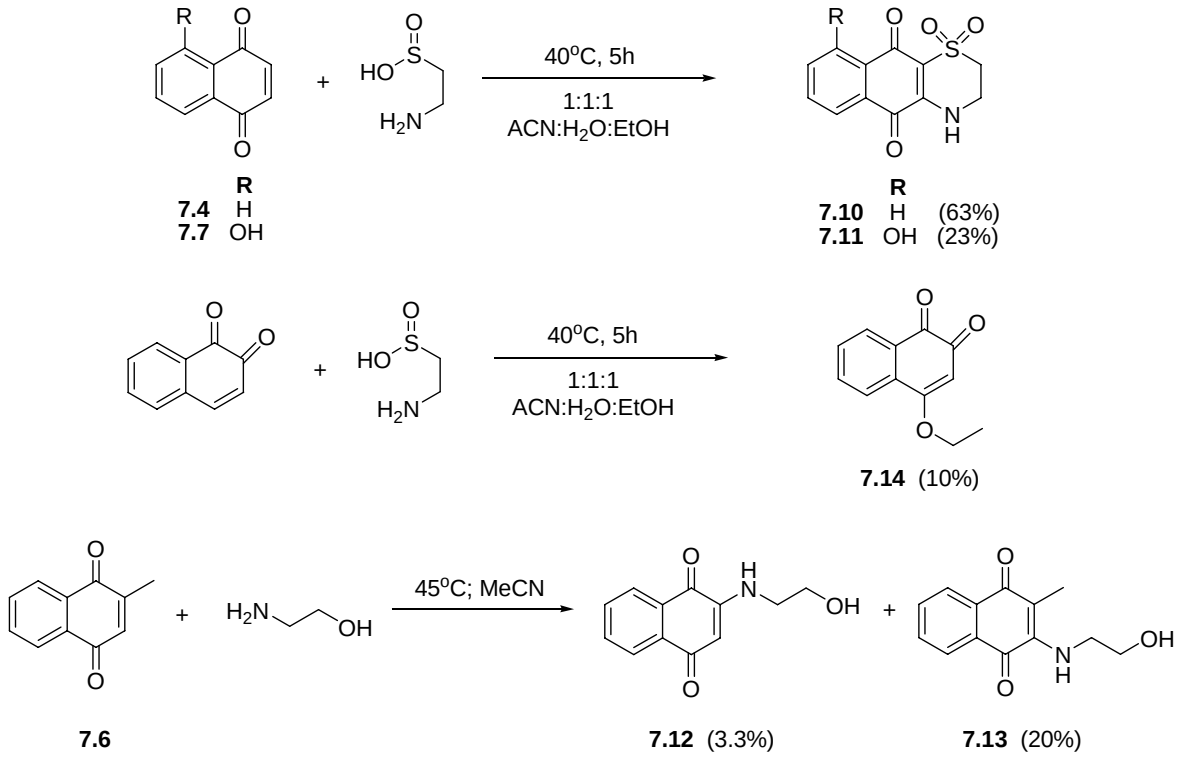

Scheme 7.1. *Synthesis of Cdc25B inhibiting quinones.*

7.2.2 Bioactivity

Table 7.1. Biological Activities of Compounds **7.2 – 7.13** (μM)

Compound	Cdc25B[a]	MKP-1[a]	MKP-2[a]	A2780[b]
Adociaquinone B	0.08/0.11	1.10	1.53	26
7.3	> 50	> 50	> 50	5.7
7.4	2.76	8.45	19.8	2.9
7.5	9.51	> 50	> 50	0.58
7.6	3.38	24.0	20.5	2.4
7.7	1.98	13.0	12.4	2.7
7.8	1.00	9.37	6.90	0.43
7.9	2.3	38.7	> 50	6.9
7.10	0.94	17.8	42.6	6.1
7.11	0.88	33.8	> 50	0.29
7.12	> 50	> 50	> 50	46
7.13	> 50	> 50	> 50	*
7.14	0.27	0.82	1.35	0.40

[a] IC_{50} values (μM), assay was carried out by Caleb Foster at the University of Pittsburgh; [b] antiproliferative activity (IC_{50} μM); growth of the A2780 human ovarian cell line according to the procedure described.[26,31,32] with paclitaxel (IC_{50} 23.4 nM) as the positive control. Assay was carried out by Ms. Peggie Brodie.
* The fluorescence reading was not indicative of the true biological activity of **7.13**. Though fluorescence indicated that **7.13** was not active, microscopic analysis clearly showed that significant inhibition of the growth of A2780 cells occurred.

7.2.3 Discussion

A number of simplified adociaquinone B analogs were synthesized in order to explore the notion of retaining the potent inhibitory activity while reducing some of its structural complexity. Most of the syntheses proceeded as expected, though a few of the reaction products are worthy of further explanation. The first step in the mechanism of formation of **7.10** is postulated to be a Michael-type addition of the amino group on hypotaurine at the 3-position of **7.4**. However, the mechanism of the following cyclization step involving sulfur remains unclear. Similarly, **7.14** is postulated to form

through a Michael-type addition of ethanol at the 4-position of orthoquinone, followed by auto-oxidation to yield the final product. In regard to the formation of **7.12**, an unexpected loss of the C-2 methyl resonance was observed in the ^{1}H NMR spectrum. It is postulated that two molecules of ethanolamine are involved in a reverse-Mannich type reaction, ultimately resulting in loss of methyleneimino-ethanol at the C-2 position (Figure 7.5). Loss of a methyl group from quinones has been reported some time ago, and mechanistic details were described.[33,34]

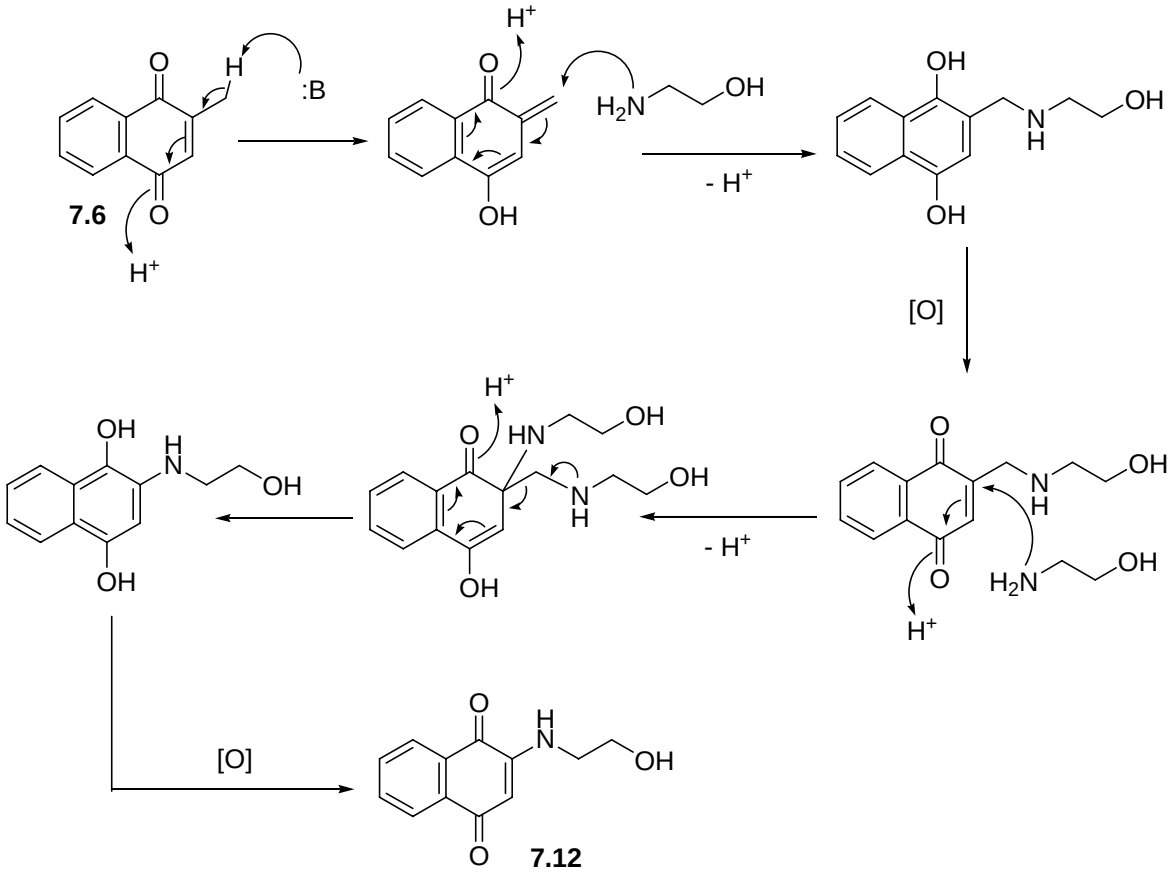

Figure 7.5. *Proposed mechanism for formation of **7.12**.*

Compounds **7.9** and **7.10** were two of the desired synthetic targets. Though **7.9** displayed inhibition of Cdc25B at 2.3 μM, it was still significantly less active than adociaquinone B, thus highlighting the necessity of the tricyclic benzofuranone moiety on the west hemisphere. As opposed to the most potent inhibitor, **7.14** (0.27 μM), **7.10** and **7.11** displayed some promising selectivity toward Cdc25B at 0.94 and 0.88 μM, respectively.

Compounds **7.3** – **7.14** were also tested for activity against two additional enzymes. Mitogen-activated protein kinase phosphatase-1 (MKP-1) and structurally similar MKP-3 are dual specificity phosphatases that are overexpressed in many human tumors and can protect cells from apoptosis caused by DNA-damaging agents or cellular stress. In the case of the current study, assaying against these enzymes assists in the identification of selective Cdc25B inhibitors.

With a few exceptions (**7.12** and **7.13**), the current data clearly support the notion that naphthoquinone-type molecules have the potential to be effective therapeutic agents, though their exact mechanism of Cdc25 inhibition is still a topic of discussion. A few computational studies have attempted to utilize modeling to predict various binding interactions of the Cdc25 dual-specificity phosphatases. The docking orientation of Cdc25B with its Cdk2-CycA protein substrate has previously been reported, and therein the possibility was recognized of targeting several potential small molecule binding pockets to achieve disruption of protein substrate recognition.[35] Additionally, in an effort to postulate a mechanism of enzyme inhibition, attempts were made to dock known small molecule inhibitors of Cdc25B within its shallow active site.[36] One docking program showed hydrogen bonding between the quinone carbonyl oxygens with Arg482 and

Arg544 of the shallow pocket. As previously suggested,[19] this implies that the quinone functionality is necessary for specific enzyme-ligand binding that propagates the observed activity. An alternate docking program bound the inhibitors in such a way that the quinone moiety was in close proximity to the Cys473 thiol residue.[36] Indeed, the structurally similar para-quinolinediones DA3003-1 (**7.15**) and JUN1111 (**7.16**) were shown to engage in redox cycling, thus irreversibly oxidizing the Cys473 thiol to its sulfonic product via production of reactive oxygen species (ROS).[37]

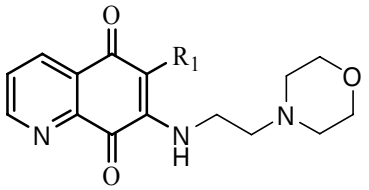

	R_1
7.15	Cl
7.16	H

Figure 7.6. *DA3003-1 and JUN1111.*

In relation to our current study, the simplification of adociaquinone B by deletion of two rings on the west hemisphere may have diminished its ability to effectively bind with residues in the active pocket of Cdc25B, thus reducing its potency. Considering that experimental evidence from the previous study of adociaquinone B[26] allowed us to hypothesize the mechanism of action to be oxidation of the catalytic cysteine, the current bioassay data suggest the fused tricyclic benzofuranone moiety may play a pivotal role in effectively positioning the quinone for Cys473 thiolate oxidation. Furthermore, comparison of **7.9** with **7.10** and **7.11** could suggest that the absence of three ring units on

the west hemisphere of adociaquinone B may grant the resulting small molecule more versatility by allowing increased access to the binding site. And though the aforementioned studies have shown intermolecular hydrogen bonding between Cdc25B residues and polar heteroatoms of small molecules to be crucial, without further experimental evidence our structure activity analysis remains speculation.

The study of Cdc25 dual-specificity phosphatases continues to generate much interest due to their oncogenetic properties, and consequently this class of enzyme may prove to be of great therapeutic value. Their intrinsic relationship with CDKs, subjects essential for the regulation of the cell cycle, has inevitably identified them as potential targets for treatment of various cancers. Recently, Cazales et al. have reported that inhibiting Cdc25 phosphatase activity alters microtubule dynamics and impairs mitotic spindle assembly, resulting in disruption of mitotic process.[38] Furthermore, they observed an enhancement of activity on the proliferation of human HT29 colon cancer cells upon combination of the microtubule-targeting paclitaxel with a Cdc25B inhibitor. This stresses the complex and enduring role of the Cdc25 family in cell cycle regulation and warrants further studies on their mechanism of action so as to pave the road for facile preparation of small molecule inhibitors.

7.3 Experimental Section.

General Experimental Procedures. All of the reagents and solvents received from commercial sources were used without further purification. ^{1}H and ^{13}C NMR spectra were obtained on Varian Unity 400 MHz, Inova 400 MHz, and JEOL Eclipse 500 MHz

spectrometers. Low resolution FAB and EI mass spectra were obtained on a JEOL HX-110 instrument, and a Finnigan LTQ LC/MS, respectively.

Synthesis of compound 7.10. A solution of hypotaurine (60 mg, 550.0 μmol) in water (10 mL) was added to a stirred solution of 1,4-napthoquinone (**7.4**) (60 mg, 379.0 μmol) in 20 mL acetonitrile/ethanol (1:1), and the mixture was stirred at 40°C for four hours. The crude product solution was refrigerated to yield a yellow precipitate, and filtered to afford compound **7.10** (62.6 mg, 63%): ^{1}H NMR (DMSO-d_6) δ 9.16 (1H, br s), 7.99 (2H, dd, J = 4.0, 1.6 Hz), 7.89 (1H, t, J = 7.6 Hz), 7.77 (1H, t, J = 7.6 Hz), 3.85 (2H, br t, J = 5.5 Hz), 3.38 (2H, br t, J = 5.5 Hz); ^{13}C NMR (DMSO-d_6) δ 178.7, 174.6, 146.8, 135.7, 132.9, 132.5, 130.0, 126.4, 125.8, 111.1, 48.26, 39.18; EIMS *m/z* 264.1 $[M+H]^+$ (calcd for $C_{12}H_{10}O_4NS$, 264.03).

Synthesis of compound 7.11. A solution of hypotaurine (9.3 mg, 85.0 μmol) in water (10 mL) was added to a stirred solution of 5-hydroxy-1,4-napthoquinone (**7.7**) (10 mg, 57.0 μmol) in 20 mL acetonitrile/ethanol (1:1), and the mixture was stirred at 40°C for four hours. This specific regioisomer was identified upon comparison of its ^{1}H and ^{13}C NMR data with those in the literature.[41] The crude product was purified over a flash silica column ($CHCl_3$/EtOAc 1:1) to afford yellow needle-like crystals, compound **7.11** (3.6 mg, 23%): ^{1}H NMR (DMSO-d_6) δ 12.83 (1H, s), 9.50 (1H, br s), 7.64 (1H, t, J = 7.2 Hz), 7.55 (1H, dd, J = 7.6, 0.8 Hz), 7.34 (1H, dd, J = 7.6, 0.8 Hz), 3.87 (2H, m), 3.41 (2H, m); ^{13}C NMR (DMSO-d_6) δ 181.5, 177.9, 160.8, 147.8, 135.0, 130.2, 125.8, 119.1, 113.7, 110.0, 48.2, 39.8; EIMS *m/z* 280.1 $[M+H]^+$ (calcd for $C_{12}H_{10}O_5NS$, 280.02).

Synthesis of compound 7.12. Ethanolamine (80.5 µL, 1.34 mmol) was added to a stirred solution of 2-methyl-1,4-napthoquinone (**7.6**) (230 mg, 134 µmol) in 5 mL acetonitrile, and the mixture was stirred at 45°C for two hours. The structure was elucidated by one and two-dimensional NMR methods and subsequently confirmed by X-ray crystallography (Figure 7.7). The crude product was purified by silica gel TLC (EtOAc) to afford orange crystals, compound **7.12** (R_f 0.44, 9.6 mg, 3.3%): ^{1}H NMR (DMSO-d_6) δ 7.98 (1H, dd, J = 8.0, 1.2 Hz), 7.93 (1H, dd, J = 7.6, 1.2 Hz), 7.82 (1H, dt, J = 8.0, 1.2 Hz), 7.72 (1H, dt, J = 7.6, 1.2 Hz), 7.34 (1H, br t, J = 5.6 Hz), 5.72 (1H, s), 4.87 (1H, t, J = 5.6 Hz), 3.58 (2H, q, J = 5.6 Hz), 3.23 (2H, q, J = 5.6 Hz); ^{13}C NMR (DMSO-d_6) δ 181.6, 181.4, 148.7, 134.9, 133.1, 132.2, 130.3, 125.9, 125.3, 99.6, 58.4, 44.6; FABMS *m/z* 199.4 [M–H_2O] (calcd for $C_{12}H_9O_2N$, 199.21).

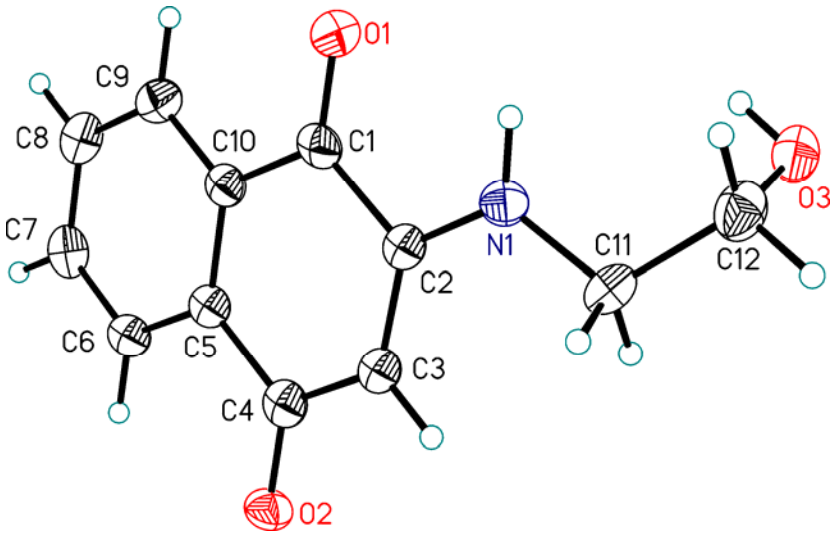

Figure 7.7. Crystal structure of **7.12**.

Synthesis of compound 7.13. Ethanolamine (80.5 μL, 1.34 mmol) was added to a stirred solution of 2-methyl-1,4-napthoquinone (**7.6**) (230 mg, 134 μmol) in 5 mL acetonitrile, and the mixture was stirred at 45°C for two hours. The crude product was purified by silica gel TLC (EtOAc) to afford compound **7.13** as red, needle-like crystals (R_f 0.75, 62.0 mg, 20%): ^{1}H NMR (DMSO-d_6) δ 7.87 (2H, t, J = 6.8 Hz), 7.73 (1H, t, J = 7.6 Hz) 7.64 (1H, t, J = 7.6 Hz), 6.47 (1H, br s), 4.92 (1H, br t, J = 5.2 Hz), 3.57 (4H, m), 2.06 (3H, s); ^{13}C NMR (DMSO-d_6) δ 182.1, 181.7, 146.8, 134.3, 132.7, 132.0, 130.2, 125.6, 125.4, 110.8, 60.5, 46.8, 10.7; FABMS *m/z* 232.1 $[M+H]^+$ (calcd for $C_{13}H_{14}O_3N$, 232.10).

Synthesis of compound 7.14. A solution of 1,2-napthoquinone (30 mg, 190 μmol) in 20 mL acetonitrile/ethanol (1:1) and in the presence of a catalytic amount of DMAP, was stirred at 40°C for five hours. The crude product was purified using silica gel column chromatography ($CHCl_3$/EtOAc 1:1) followed by an open reversed phase C18 column (MeOH/H_2O 3:2) to afford compound **7.14** as yellow needle-like crystals (3.8 mg, 10%): ^{1}H NMR (CD_3CN) δ 8.00 (1H, d, J = 8.4 Hz), 7.91 (1H, d, J = 8.0 Hz), 7.75 (1H, t, J = 8.0 Hz), 7.63 (1H, t, J = 8.4 Hz), 5.94 (1H, s), 4.24 (2H, q, J = 6.8 Hz), 1.49 (3H, t, J = 6.8 Hz); ^{13}C NMR (CD_3CN) δ 180.6, 180.2, 168.5, 135.9, 133.2, 132.3, 131.6, 129.1, 125.4, 104.3, 66.9, 14.2; FABMS *m/z* 203.7 $[M+H]^+$ (calcd for $C_{12}H_{10}O_3$, 203.21).

Antiproliferative bioassay. Determination of antiproliferative activity was performed at Virginia Polytechnic Institute and State University against the A2780 ovarian cancer cell

line as previously described.[31] The A2780 cell line is a drug - sensitive human ovarian cancer cell line.[31,32]

***In vitro* phosphatase assays**. Determination of *in vitro* inhibitory activity against the Cdc25B enzyme was performed at the University of Pittsburgh, using methods previously described.[19,41-43]

References

1. Cao, S.; Murphy, B. T.; Brodie, P.; Foster, C.; Lazo, J. S.; Kingston, D. G. I. Synthesis and activity of simplified adociaquinone B and naphthoquinone derivatives against Cdc25B phosphatase. **2007**, Manuscript in preparation for submission to *Bioorg. Med. Chem.*
2. Lyon, M. A.; Ducret, A. P.; Wipf, P.; Lazo, J. S. Dual-specificity phosphatases as targets for antineoplastic agents. *Nature Rev. Drug Discov*. **2002**, *1*, 961.
3. Cangi, M. G.; Cukor, B.; Soung, P.; Signoretti, S.; Moreira, J. G.; Ranashinge, M.; Cady, B.; Pagano, M.; Loda, M. Role of Cdc25A phosphatase in human breast cancer. *J. Clin. Investig*. **2000**, *106*, 753.
4. Oguri, T.; Singh, S. V.; Nemoto, K.; Lazo, J. S. The carcinogen (7R,8S)-dihydroxy-(9S,10R)-epoxy-7,8,9,10-tetrahydrobenzo[a]pyrene induces Cdc25B expression in human bronchial and lung cancer cells. *Cancer Res*. **2003**, *63*, 771.
5. Galaktionov, K.; Lee, A. K.; Eckstein, J.; Draetta, G.; Meckler, J.; Loda, M.; Beach, D. Cdc25 phosphatases as potential human oncogenes. *Science* **1995**, *269*, 1575.

6. Millar, J. B. A.; Blevitt, J.; Gerace, L.; Sadhu, K.; Featherstone, C.; Russell, P. P55^{Cdc25} is a nuclear protein required for the initiation of mitosis in human cells. *Proc. Natl. Acad. Sci. USA* **1991**, *88*, 10500.

7. Hoffmann, I.; Clarke, P. R.; Marcote, M. J.; Karsenti, E. Draetta, G. Phosphorylation and activation of human Cdc25-C by cdc2-cyclin B and its involvement in the self-amplification of MPF at mitosis. *EMBO J.* **1993**, *12*, 53.

8. Lammer, C.; Wagerer S.; Saffrich R.; Mertens D.; Ansorge W.; Hoffmann I. The Cdc25B phosphatase is essential for the G2/M phase transition in human cells. *J. Cell Science* **1998**, *111*, 2445.

9. Dunphy, W. G.; Kumagai, A. The cdc25 protein contains an intrinsic phosphatase activity. *Cell* **1991**, *67*, 189.

10. Mailand, M.; Podtelejnikov, A. V.; Groth, A.; Mann, M.; Bartek, J.; Lukas, J. Regulation of G(2)/M events by Cdc25A through phosphorylation-dependent modulation of its stability. *EMBO J.* **2002**, *21*, 5911.

11. Chow, J. P. H.; Siu, W. Y.; Ho, H. T. B.; Ma, K. H. T.; Ho, C. C.; Poon, R. Y. C. Differential contribution of inhibitory phosphorylation of CDC2 and CDK2 for unperturbed cell cycle control and DNA integrity checkpoints. *J. Biol. Chem*. **2003**, *278*, 40815.

12. Lindqvist, A.; Kallstrom, H.; Lundgren, A.; Barsoum, E.; Rosenthal, C. K. Cdc25 B cooperates with Cdc25A to induce mitosis but has a unique role in activating cyclin B1-Cdk1 at the centrosome. *J. Cell Biol*. **2005**, *171*, 35.

13. Rudolph, J. Inhibiting transient protein-protein interactions: lessons from the Cdc25 protein tyrosine phosphatases. *Nat. Rev. Cancer* **2007**, *7*, 202.

14. Guan, K. L.; Dixon, J. E. Evidence for protein-tyrosine-phosphatase catalysis proceeding via a cysteine-phos-phate intermediate. *J. Biol. Chem.* **1991**, *266*, 17026.

15. Cho, H.; Krishnaraj, R.; Kitas, E.; Bannwarth, W.; Walsh, C. T.; Anderson, K. S. Isolation and structural elucidation of a novel phosphocysteine intermediate in the LAR protein tyrosine phosphatase enzymatic pathway. *J. Am. Chem. Soc*. **1992**, *114*, 7296.

16. Rudolph, J. Catalytic mechanism of Cdc25. *Biochemistry* **2002**, *41*, 14613.

17. Kar, S.; Lefterov, I. M.; Wang, M.; Lazo, J. S.; Scott, C. N.; Wilcox, C. S.; Carr, B. I. Binding and inhibition of Cdc25 phosphatases by vitamin K analogs. *Biochemistry* **2003**, *42*, 10490.

18. Wang, Q.; Dube, D.; Friesen, R. W.; LeRiche, T. G.; Bateman, K. P.; Trimble, L.; Sanghara, P. R.; Ramachandran, C.; Gresser, M. J.; Pollex, R.; Huang, Z. Catalytic inactivation of protein tyrosine phosphatase CD45 and protein tyrosine phosphatase 1B by polyaromatic quinones. *Biochemistry* **2004**, *43*, 4294.

19. Lazo, J. S.; Nemoto, K.; Pestell, K. E.; Cooley, K.; Southwick, E. C.; Mitchell, D. A.; Furey, W.; Gussio, R.; Zaharevitz, D. W.; Joo, B.; Wipf, P. Identification of a potent and selective pharmacophore for Cdc25 dual specificity phosphatase inhibitors. *Mol. Pharmacol.* **2002**, *61*, 720.

20. Kar, S.; Wang, M.; Ham, S. W.; Carr, B. I. PM-20, a novel inhibitor of Cdc25A, induces extracellular signal–regulated kinase 1/2 phosphorylation and inhibits hepatocellular carcinoma growth *in vitro* and *in vivo*. *Cancer Biol. Ther*. **2006**, *5*, 1340.

21. Kar, S.; Wang, M.; Ham, S. W.; Carr, B. I. Fluorinated Cpd 5, a pure arylating K-vitamin derivative, inhibits human hepatoma cell growth by inhibiting Cdc25 and activating MAPK. *Biochem. Pharmacol*. **2006**, *72*, 1217.

22. Tandon, V. K.; Yadav, D. B.; Singh, R. V.; Vaish, M.; Chaturvedi, A. K.; Shukla, P. K. Synthesis and biological evaluation of novel 1,4-naphthoquinone derivatives as antibacterial and antiviral agents. *Bioorg. Med. Chem*. **2005**, *15*, 3463.

23. Tamura, K.; Southwick, E.; Kerns, J.; Rosi, K.; Carr, B. I.; Wilcox, C.; Lazo, J. S. Cdc25 inhibition and cell cycle arrest by a synthetic thioalkyl vitamin K analogue. *Cancer Res*. **2000**, *60*, 1317.

24. Brun, M.-P.; Braud, E.; Angotti, D.; Mondésert, O.; Quaranta, M.; Montes, M.; Miteva, M.; Gresh, N.; Ducommun, B.; Garbay, C. Design, synthesis, and biological evaluation of novel naphthoquinone derivatives with CDC25 phosphatase inhibitory activity. *Bioorg. Med. Chem*. **2005**, *13*, 4871.

25. Ham, S. W.; Lee, S. Evaluation of sulfone analogs of cpd 5 as Cdc25 inhibitors. *Bull. Korean Chem. Soc*. **2004**, *25*, 1755.

26. Cao, S.; Foster, C.; Brisson, M.; Lazo, J. S.; Kingston, D. G. I. Halenaquinone and xestoquinone derivatives, inhibitors of Cdc25B phosphatase from a *Xestospongia* sp. *Bioorg. Med. Chem*. **2005**, *13*, 999.

27. Baldwin, J. E.; Chang, G. E. C. Synthesis and thermal isomerization of tricycle [4.2.2.01,6] dec-7-ene ([4.2.2] propell-7-ene) to 3,8-dimethylenecyclooctene. *J. Org. Chem.* **1982**, *47*, 848.

28. Lin, C.-T.; Chou, T.-C. 3,4,8,9-Tetramethylene-endo-2,5:endo-7,10-dietheno-cis-decalin. A new exocyclic diene bridged polycyclic hydrocarbon. *J. Org. Chem.* **1990**, *55*, 2252.

29. Thomas, A. D.; Miller, L. L. Repetitive Diels-Alder reactions for the growth of linear polyacenequinoid derivatives. *J. Org. Chem.* **1986**, *51*, 4160.

30. Harada, N.; Sugioka, T.; Soutome, T.; Hiyoshi, N.; Uda, H.; Kuriki, T. Synthesis and absolute stereochemistry of (+)-adociaquinones A and B. *Tetrahedron: Assymetry* **1995**, *6*, 375.

31. Cao, S.; Brodie, P. J.; Randrianaivo, R.; Ratovoson, F.; Callmander, M.; Andriantsiferana, R.; Rasamison, V. E.; Kingston. D. G. I. Guttiferones K and L, antiproliferative compounds of *Rheedia calcicola* from the Madagascar rain forest. *J. Nat. Prod.* **2007**, *70*, 679.

32. Louie, K. G.; Behrens, B. C.; Kinsella, T. J.; Hamilton, T. C.; Grotzinger, K. R.; McKoy, W. M.; Winker, M. A.; Ozols, R. F. Radiation survival parameters of antineoplastic drug-sensitive and -resistant human ovarian cancer cell lines and their modification by buthionine sulfoximine. *Cancer Res.* **1985**, *45*, 2110.

33. Cameron, D. W.; Scott, P. M. Facile loss of C-methyl groups during the amination of quinones. *J. Chem. Soc.* **1964**, 5569.

34. Cameron, D. W.; Samuel, E. L. Reactions of perimidin-4-ones and 6-ones with amines. *Aust. J. Chem.* **1977**, *30*, 2063.

35. Sohn, J.; Parks, J. M.; Buhrman, G.; Brown, P.; Kristjánsdóttir, K.; Safi, A.; Edelsbrunner, H.; Yang, W.; Rudolph, J. Experimental validation of the docking

orientation of Cdc25 with Its Cdk2-CycA protein substrate. *Biochemistry* **2005**, *44*, 16563.

36. Lavecchia, A.; Cosconati, S.; Limongelli, V.; Novellino, E. Modeling of Cdc25B dual specifity protein phosphatase inhibitors: docking of ligands and enzymatic inhibition mechanism. *ChemMedChem* **2006**, *1*, 540.

37. Brisson, M.; Nguyen, T.; Wipf, P.; Joo, B. ; Day, B. W.; Skoko, J. S.; Schreiber, E. M.; Foster, C.; Bansal, P.; Lazo, J. S. Redox regulation of Cdc25B by cell-active quinolinediones. *Mol. Pharmacol.* **2005**, *68*, 1810.

38. Cazales, M.; Boutros, R.; Brezak, M-C.; Chaumeron, S.; Prevost, G.; Ducommun, B. Pharmacologic inhibition of Cdc25 phosphatases impairs interphase microtubule dynamics and mitotic spindle assembly. *Mol. Cancer Ther*. **2007**, *6*, 318.

39. Rice, R. L.; Rusnak, J. M.; Yokokawa, F.; Yokokawa, S.; Messner, D. J.; Boynton, A. L.; Wipf, P.; Lazo, J. S. A targeted library of small-molecule, tyrosine, and dual-specificity phosphatase inhibitors derived from a rational core design and random side chain variation. *Biochemistry* **1997**, *36*, 15965.

40. Wipf, P.; Hopkins, C. R.; Phillips, E. O.; Lazo, J. S. Separation of Cdc25 dual specificity phosphatase inhibition and DNA cleaving activities in a focused library of analogs of the antitumor antibiotic Dnacin. *Tetrahedron* **2002**, *58*, 6367.

41. Anderson, R. A.; Pereira, A.; Huang, X.-H.; Mauk, G.; Vottero, E.; Roberge, M.; Balgi, A. Indoleamine 2,3-dioxygenase (IDO) inhibitors. U. S. Patent No. WO2006005185, **2006**.

42. Kar, S.; Lefterov, I. M.; Wang, M.; Lazo, J. S.; Scott, C. N.; Wilcox, C. S.; Carr, B. I. Binding and inhibition of Cdc25 phosphatases by vitamin K analogues. *Biochemistry* **2003**, *42*, 10490.

43. Lyon, M. S.; Ducruet, A. P.; Wipf, P.; Lazo, J. S. Dual-specificity phosphatases as targets for antineoplastic agents. *Nature Reviews Drug Disc*. **2002**, *1*, 961.

44. Wipf, P.; Hopkins, C. R.; Phillips, E. O.; Lazo, J. S. Separation of Cdc25 dual specificity phosphatase inhibition and DNA cleaving activities in a focused library of analogs of the antitumor antibiotic Dnacin. *Tetrahedron* **2002**, *58*, 6367.

VIII. General Conclusions

Of the fourteen compounds isolated from *Schizolaena hystrix*, six were known substances while eight were reported for the first time. All of the candidates, which were either long chain compounds or flavonoids, were very weakly active in the A2780 human ovarian cancer cell line. None of the isolates represent interesting drug candidates.

From *Artabotrys madagascariensis* was isolated one new cyclohexene derivative, two known butenolides, and one known triterpene. The two butenolide derivatives have a brief history of being cytotoxic, and further testing carried out by the Eisai Research Institute in a panel of cancer cell lines confirmed their generally cytotoxic profile. Despite their interesting structural characteristics and overall simplicity, at this time they do not represent viable drug leads.

Extraction of an unidentified *Malleastrum* species led to the isolation of three novel limonoids with triterpenoid skeletons seldom reported in literature. Two of the three were relatively active in the A2780 cell line, though further testing at the Eisai Research Institute showed a pattern of general toxicity. Whereas they may not be useful in further oncogenic studies, limonoids have a rich history of acting as effective anti-insecticidal agents. Given their high overall yield in the plant, should these agents exhibit said activity, they may be of some commercial interest.

Two known marine metabolites with potent activity against a number of tumor cell lines were isolated from an unidentified species of the marine ascidian *Trididemnum*. A plethora of bioactivity and synthetic studies on the five known analogs of this class of molecule have been published, partly due to their strong therapeutic potential. These

bistramides are actin interacting agents that most likely are the product of a symbiotic microbial relationship. It is highly recommended that further exploration of *Tridemnum* be undertaken in order to isolate new bistramides derivatives, since their presence is plentiful in this particular unidentified species. The prospect of improving their bioactive potential by isolating new derivatives is supported by the difference in toxicity of some known bistramides analogs; upon isolation of bistramide D it was discovered that this analog displayed similar anticancer properties, but was less toxic than bistramide A. Isolation of additional derivatives may provide similar selectivity profiles.

A number of naphthoquinone analogs were synthesized and specially designed to inhibit Cdc25B, an enzyme overexpressed in certain tumors that is responsible for the transition between the G2/M phases of the cell cycle. Based on the most potent known inhibitor, adociaquinone B, these simplified analogs showed much promise as potential therapeutic agents. Despite these promising preliminary results, much work remains in understanding their mechanism of action, particularly to determine whether redox cycling or direct binding to the enzyme's active site is responsible for the observed activity. Design of further simplified naphthoquinone derivatives should take place once the exact mechanism of action is determined. Co-crystallization of some of these inhibitors with Cdc25B would represent an impressive step toward understanding inhibitor-enzyme interactions, though there are currently no plans to attempt such studies.

Table 8.1. Summary of Natural Products Isolated

Compound	Natural Product Class	Plant	IC_{50} (μM)	New / Known
Schizolaenone A	Flavonoid	*S. hystrix*	21	New
Schizolaenone B	Flavonoid	*S. hystrix*	22	New
Schizolaenone C	Flavonoid	*S. hystrix*	21	New
4'-*O*-Methylbonannione A	Flavonoid	*S. hystrix*	40	New
Nymphaeol A	Flavonoid	*S. hystrix*	14	Known
Bonnanione A	Flavonoid	*S. hystrix*	32	Known
Bonnaniol A	Flavonoid	*S. hystrix*	64	Known
Diplacol	Flavonoid	*S. hystrix*	13	Known
Macarangaflavanone B	Flavonoid	*S. hystrix*	43	Known
3'-Prenylaringenin	Flavonoid	*S. hystrix*	29	Known
3-Acetoxy-eicosanoic acid ethyl ester	Long-chain ester	*S. hystrix*	48	New
3*S*-Acetoxy-eicosanoic acid	Long-chain acid	*S. hystrix*	54	Known
3-Acetoxy-doeicosanoic acid	Long-chain acid	*S. hystrix*	63	New
1-Hydroxy-dodecan-2-one	Long-chain alcohol	*S. hystrix*	70	Known
Artabotrene	Cyclohexene derivative	*A. Madagascariensis*	55	New
Melodorinol	Butenolide	*A. Madagascariensis*	12	Known
Acetylmelodorinol	Butenolide	*A. Madagascariensis*	6.9	Known
Polycarpol	Triterpene	*A. Madagascariensis*	41	Known
Malleastrone A	Limonoid	*Malleastrum* sp.	0.49	New
Malleastrone B	Limonoid	*Malleastrum* sp.	0.63	New
Malleastrone C	Limonoid	*Malleastrum* sp.	18	New
Bistramide A	Bistramide	*Trididemnum* sp.	0.19	Known
Bistramide D	Bistramide	*Trididemnum* sp.	n/t	Known
Cryptomoscatone D1	ω- Pyrone	*R. floribunda*	47	Known
Kaempferol-3-*O*-α-L-rhamnopyranoside	Flavonol glycoside	*Plagioscyphus* sp.	N/A	Known
(+)-Catechin	Flavonoid	*P. acidula*	N/A	Known

* n/t = not tested; N/A = not active

APPENDIX

(^{1}H and ^{13}C NMR Spectra)

2.1. Schizolaenone A (in $CDCl_3$)

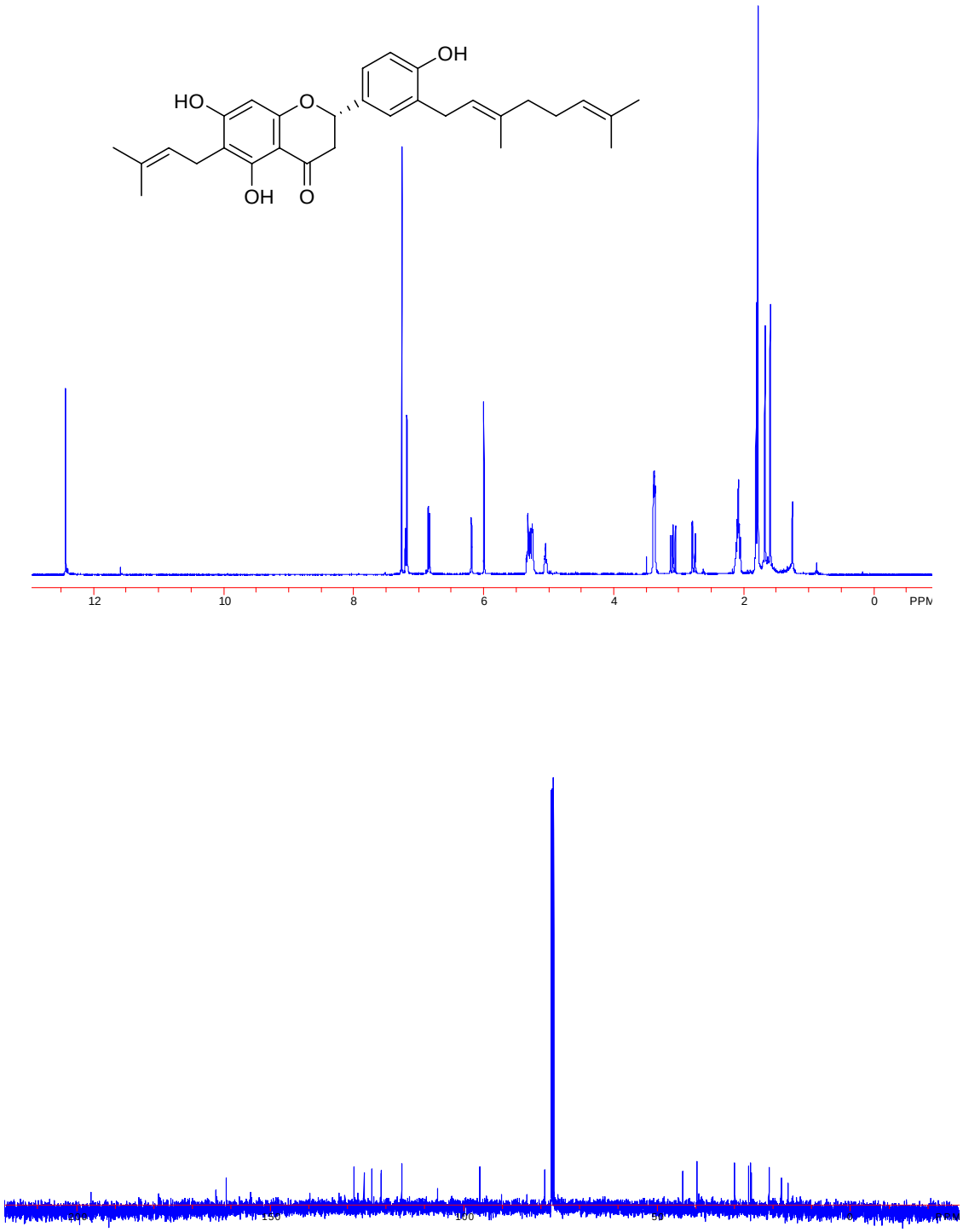

2.2. Schizolaenone B (in $CDCl_3$)

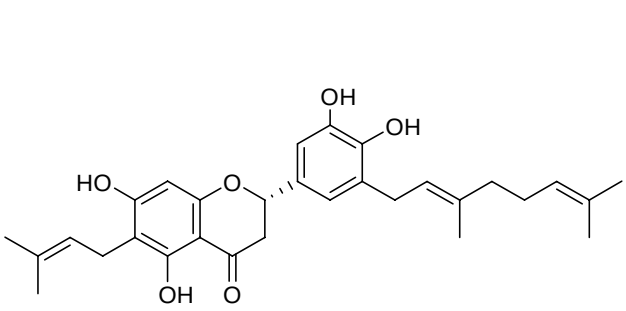

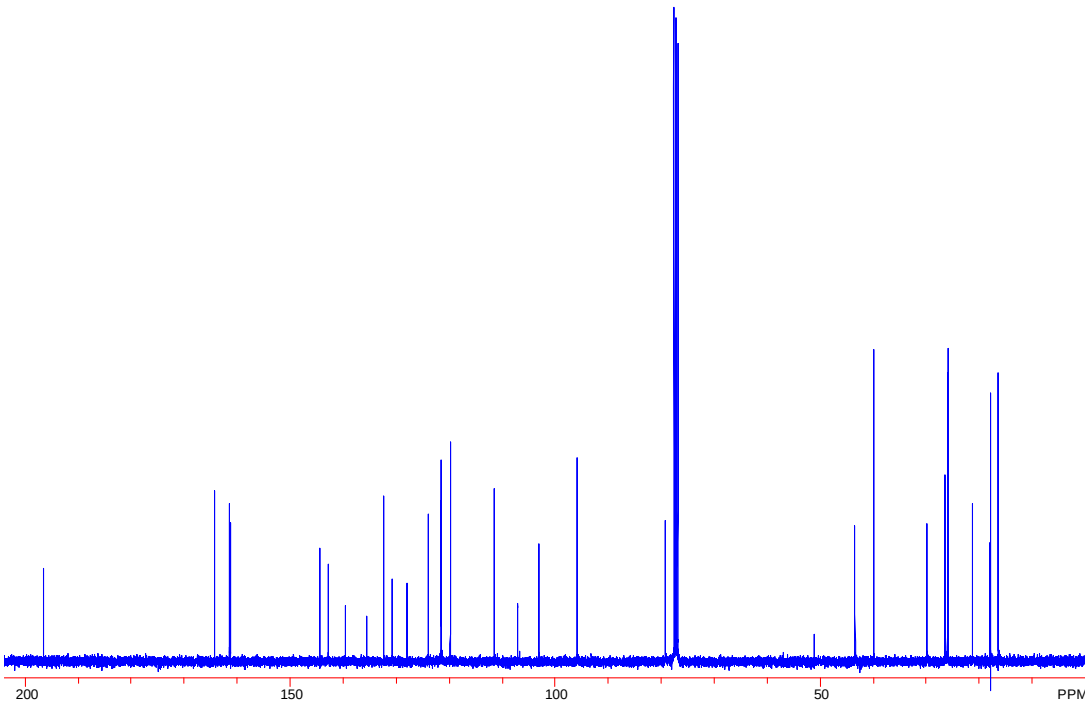

2.3. Schizolaenone C (in CD_3OD)

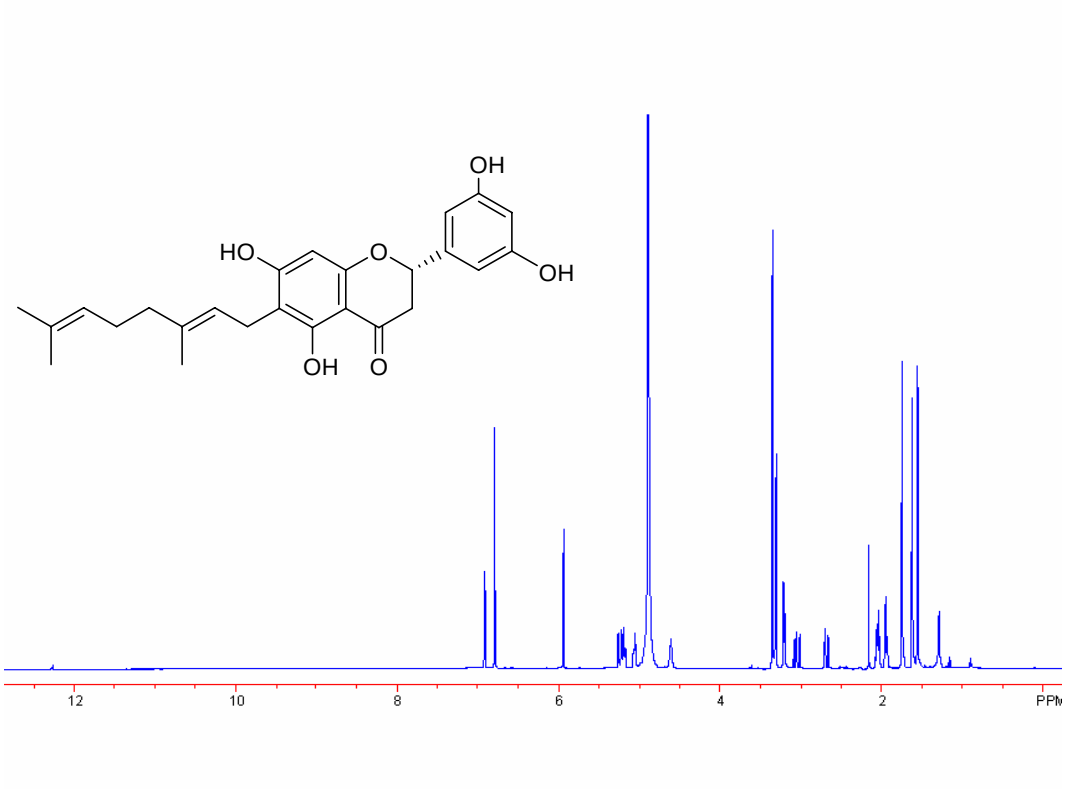

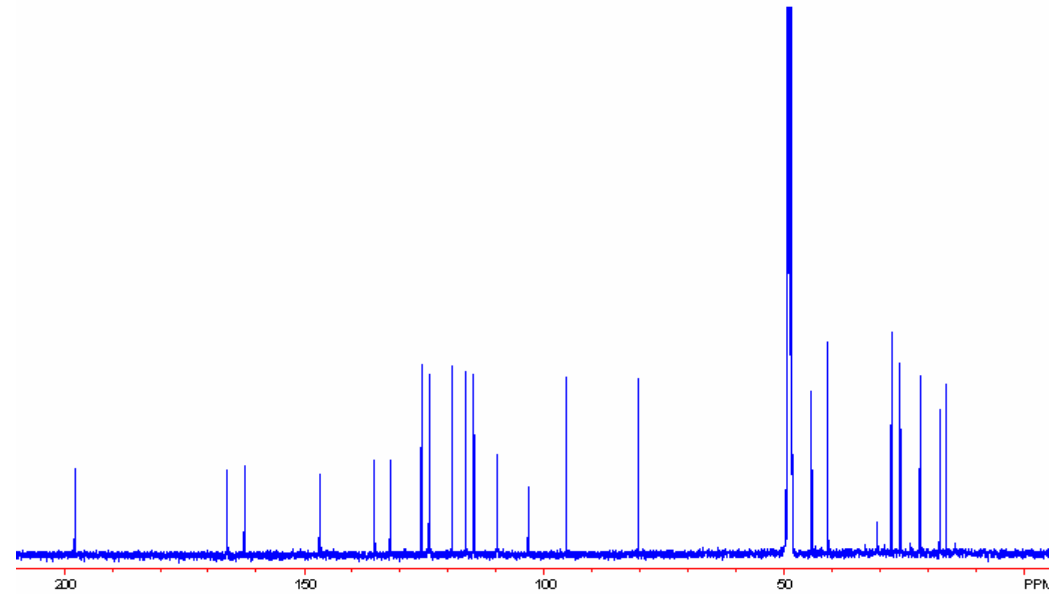

2.4. 4'-O-Methylbonnanione A (in $CDCl_3$)

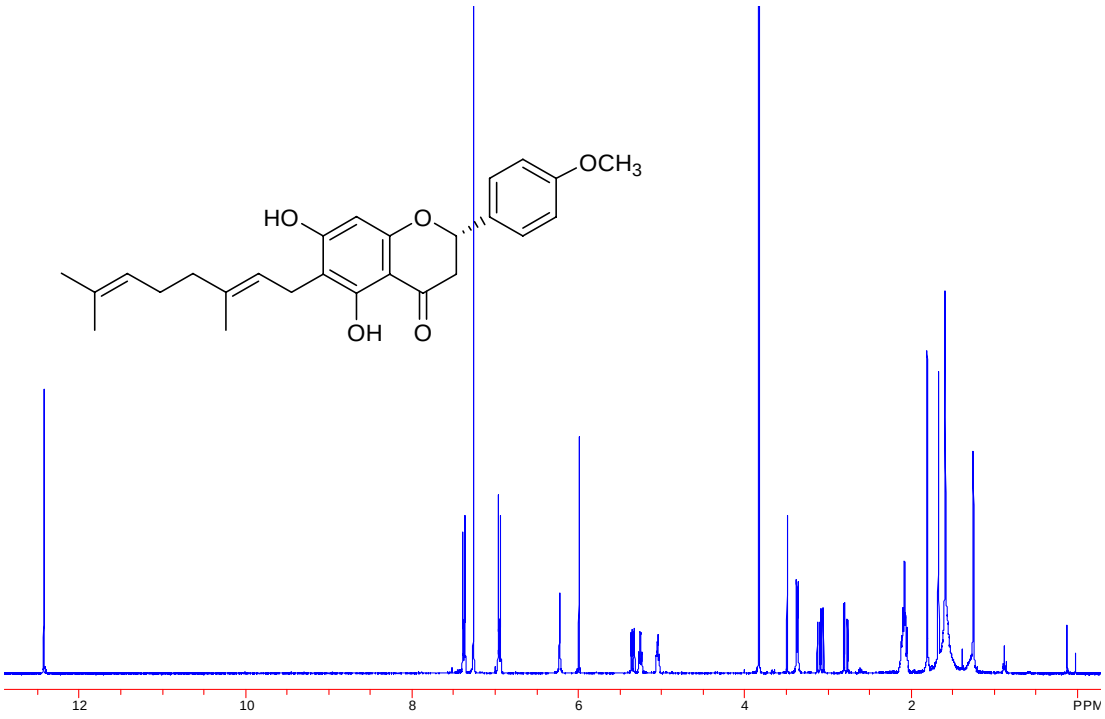

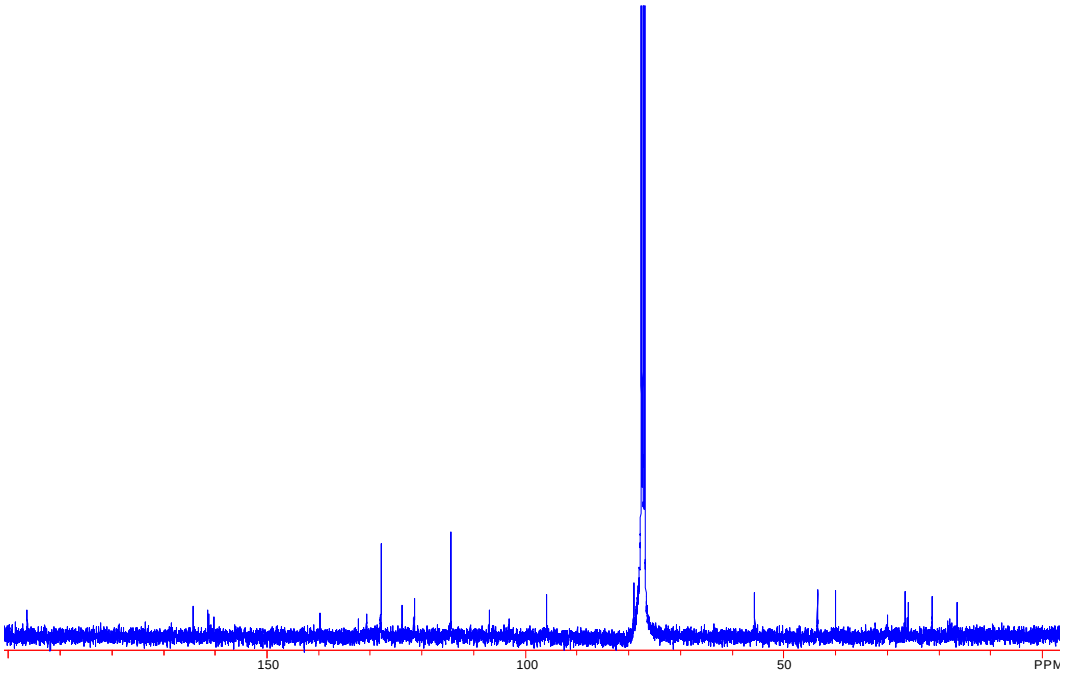

2.5. Nymphaeol A (in CD_3OD)

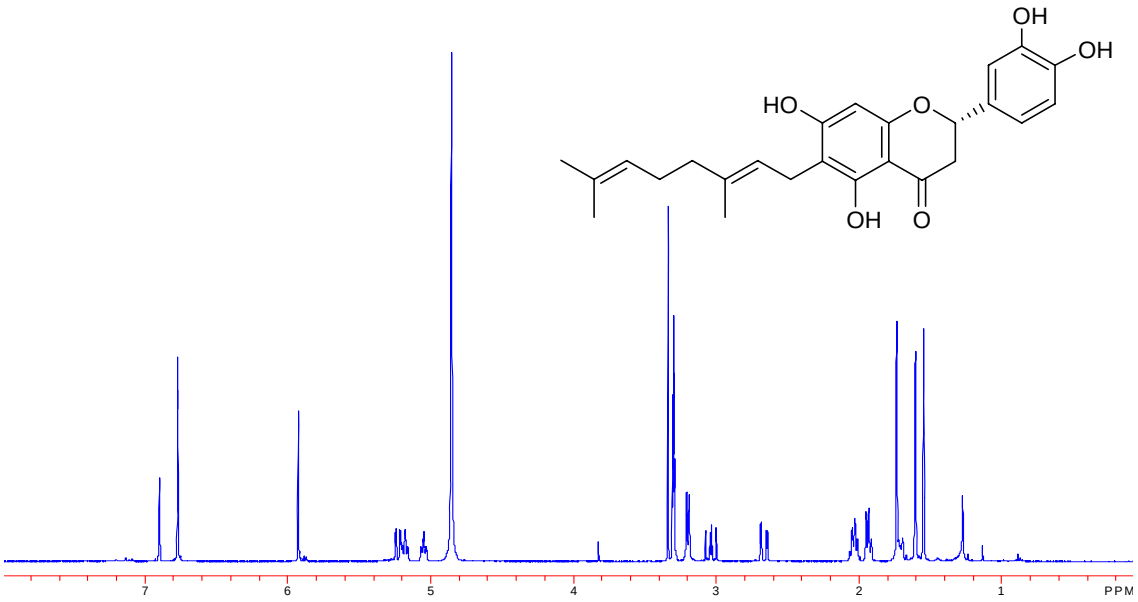

2.6. Bonannione A (in CD_3OD)

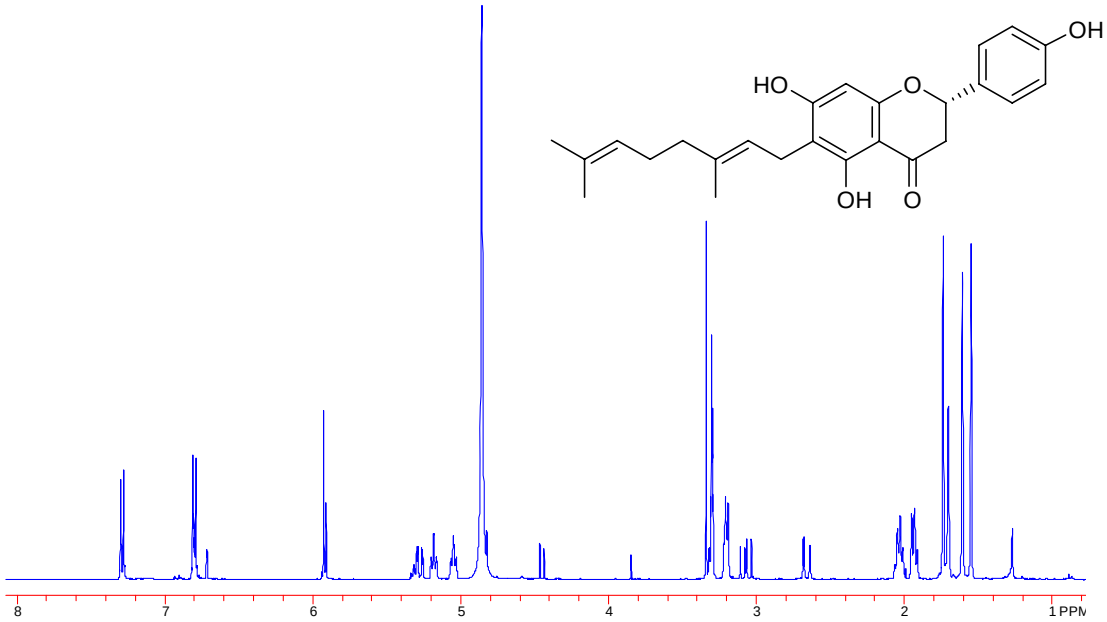

2.7. Bonanniol A (in $CDCl_3$)

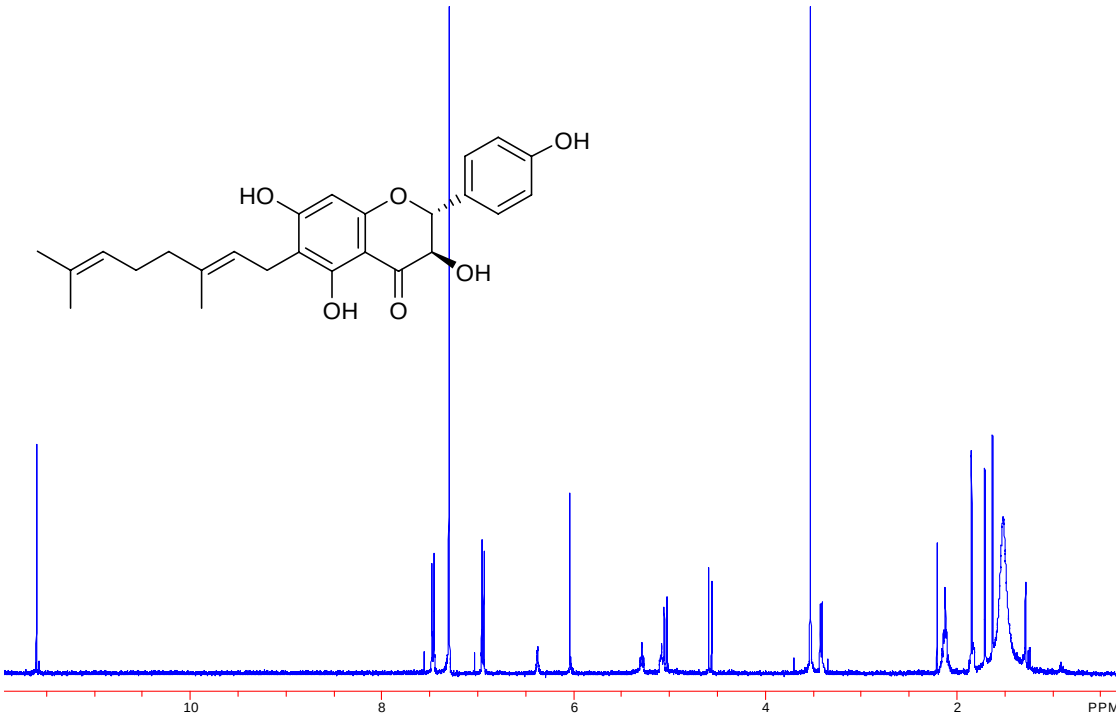

2.8. Diplacol (in CD_3OD)

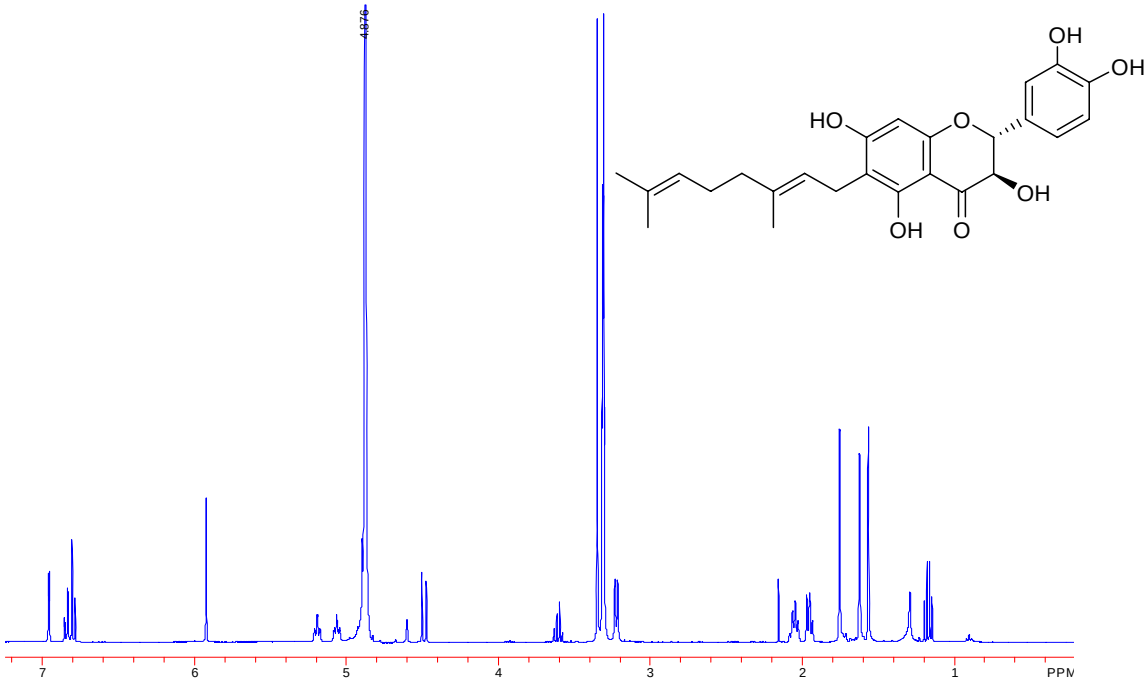

2.9. Macarangaflavanone B (in CD_3OD)

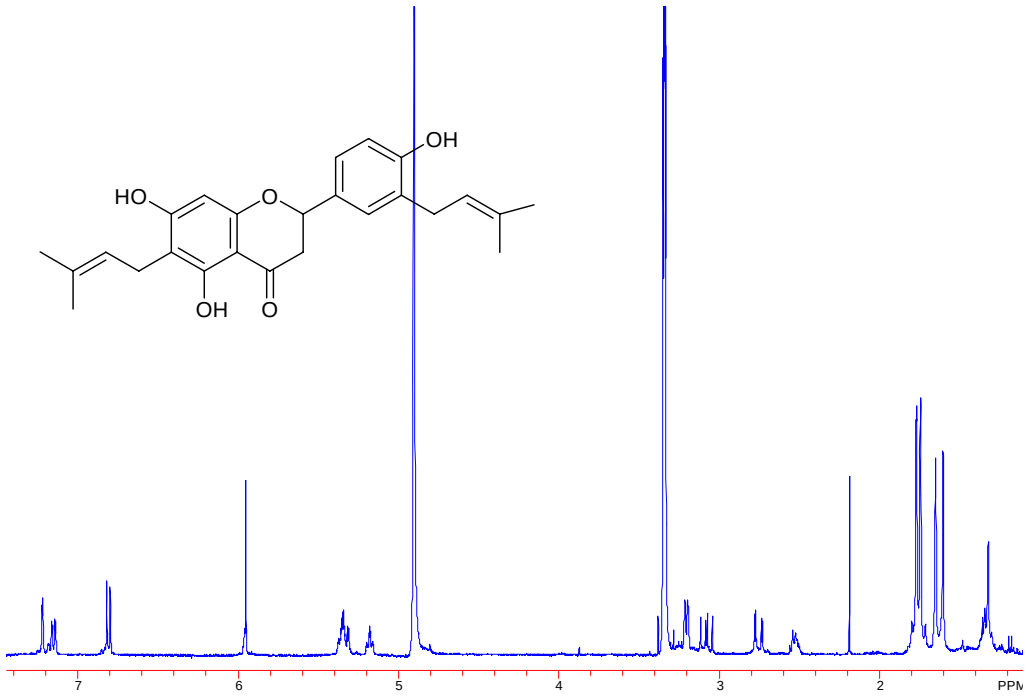

2.10. 3'-Prenylaringenin (in $CDCl_3$)

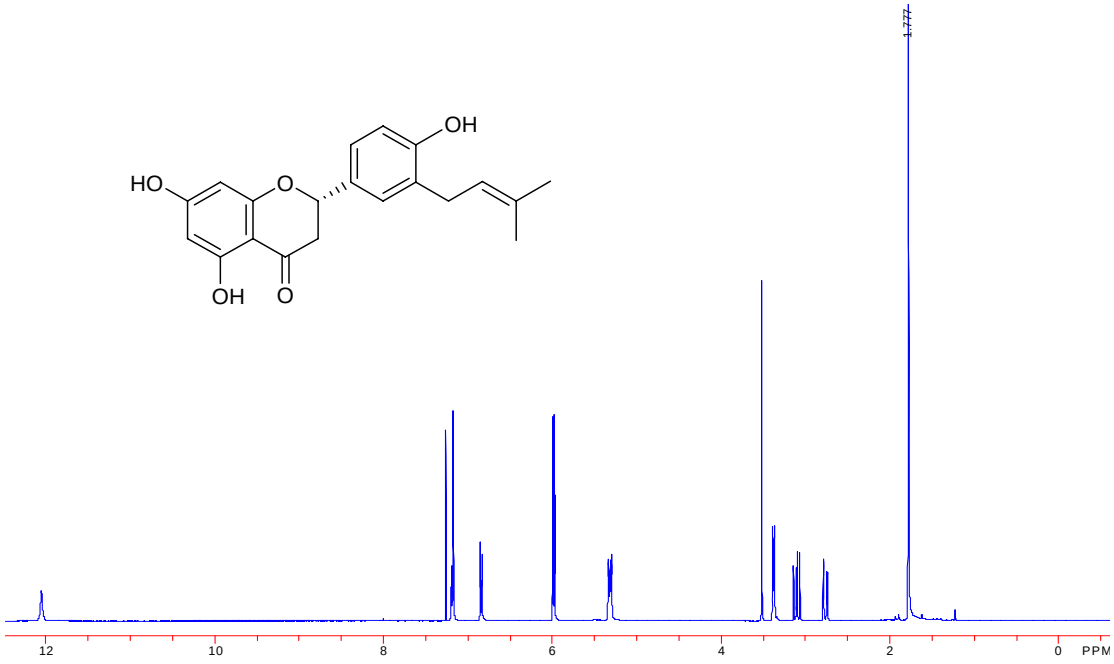

2.11. 3*S*-acetoxy-eicosanoic acid ethyl ester (in C_6D_6)

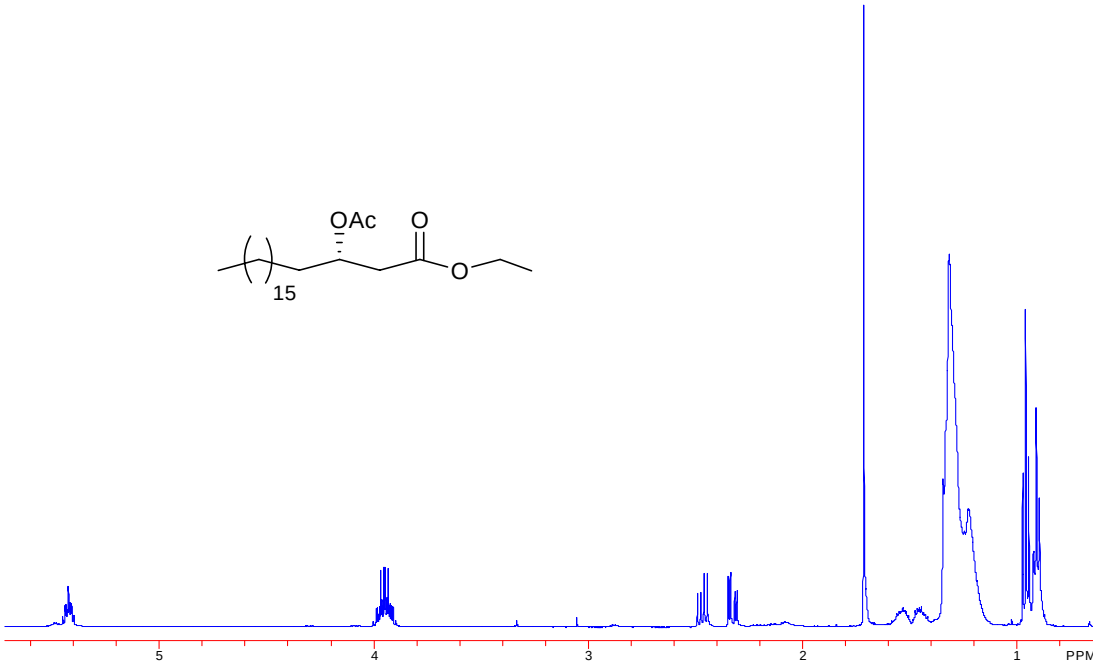

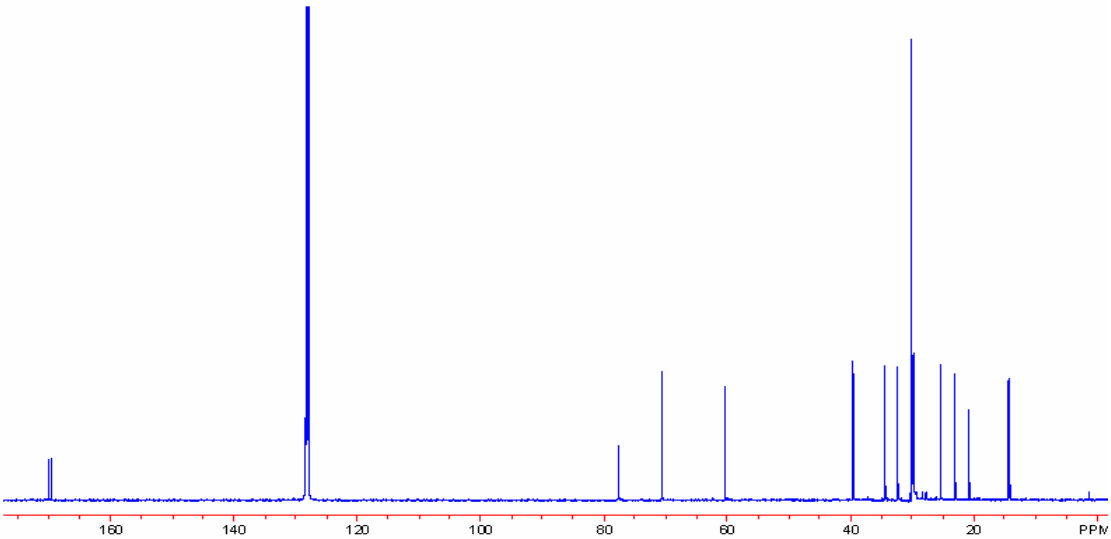

2.12. 3*S*-Acetoxy-eicosanoic acid (in C_6D_6)

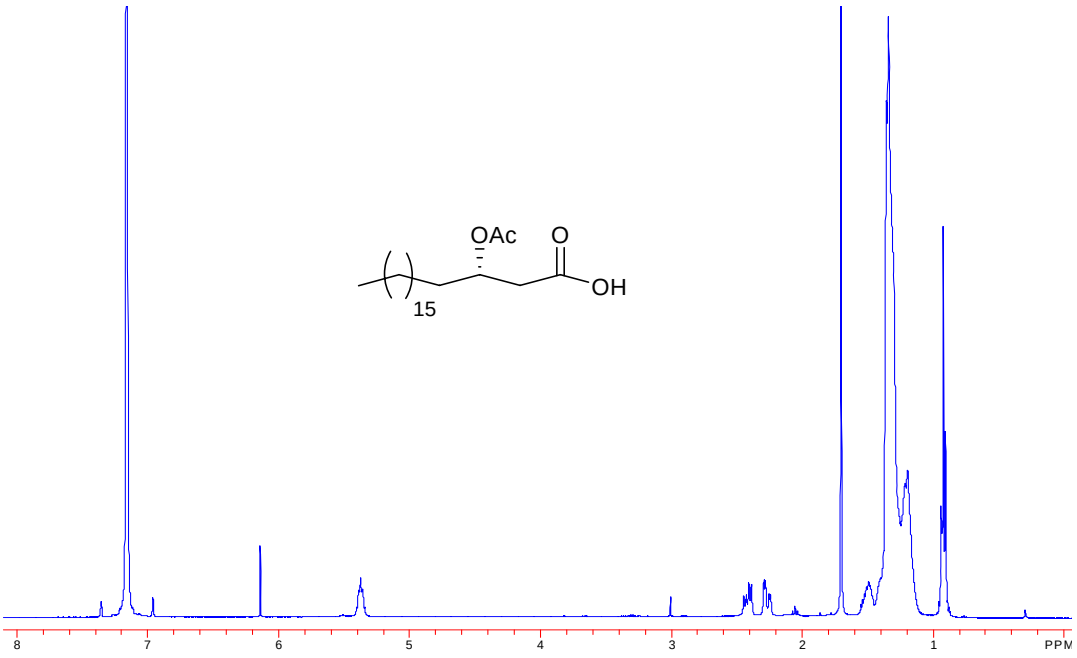

2.13. 3*S*-Acetoxy-eicosanoic acid ethyl ester (in C_6D_6)

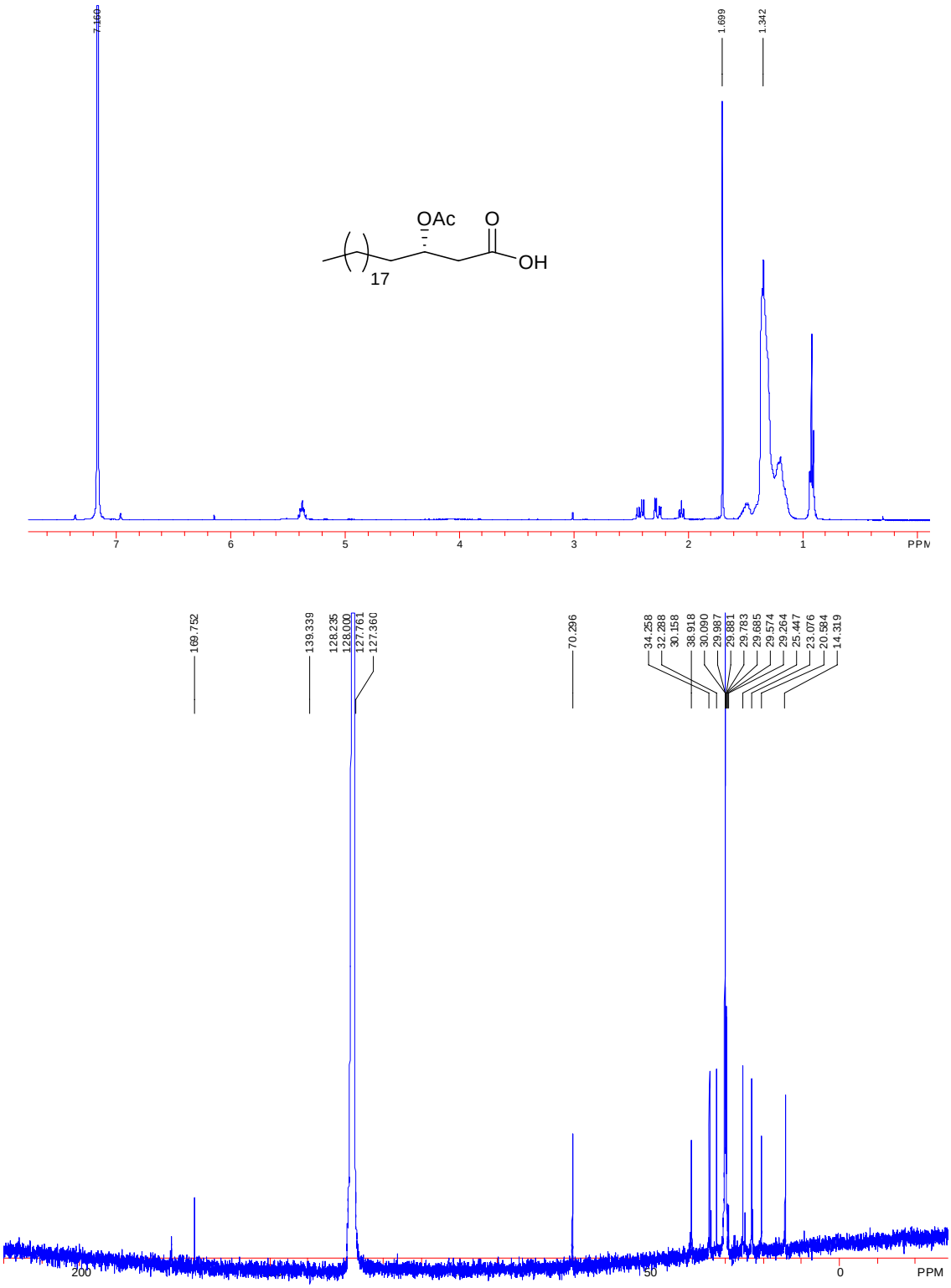

2.14. 1-hydroxy-dodecan-2-one (in $CDCl_3$)

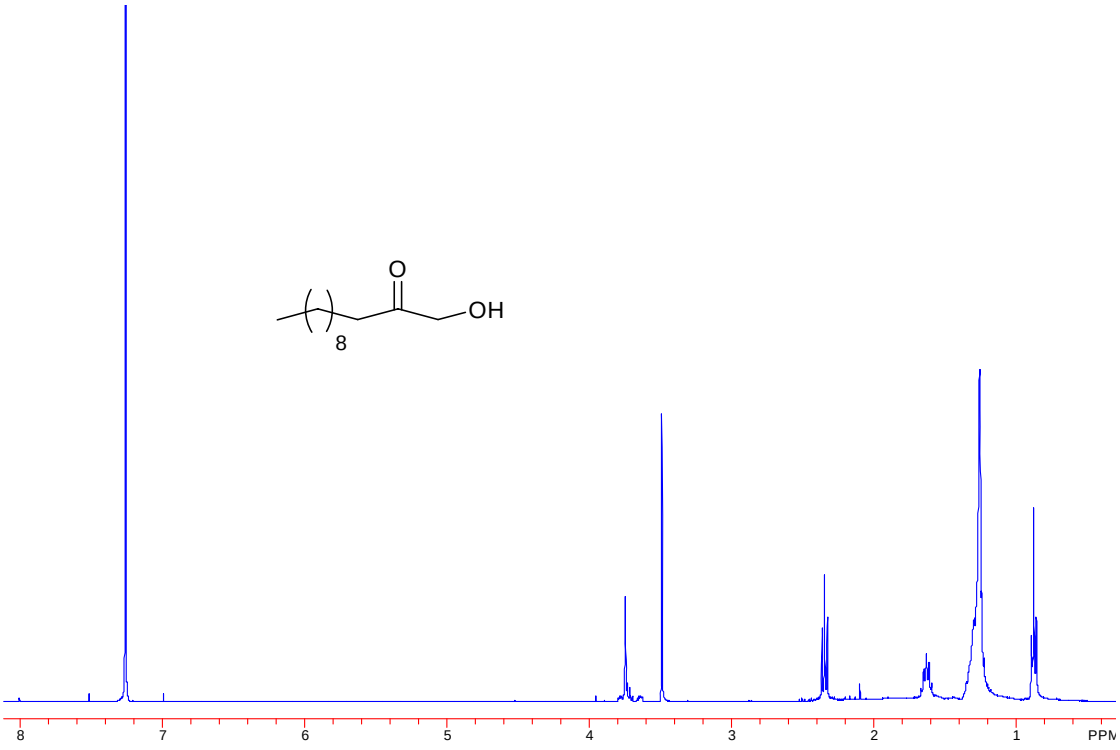

3.1. Artabotrene (in $CDCl_3$)

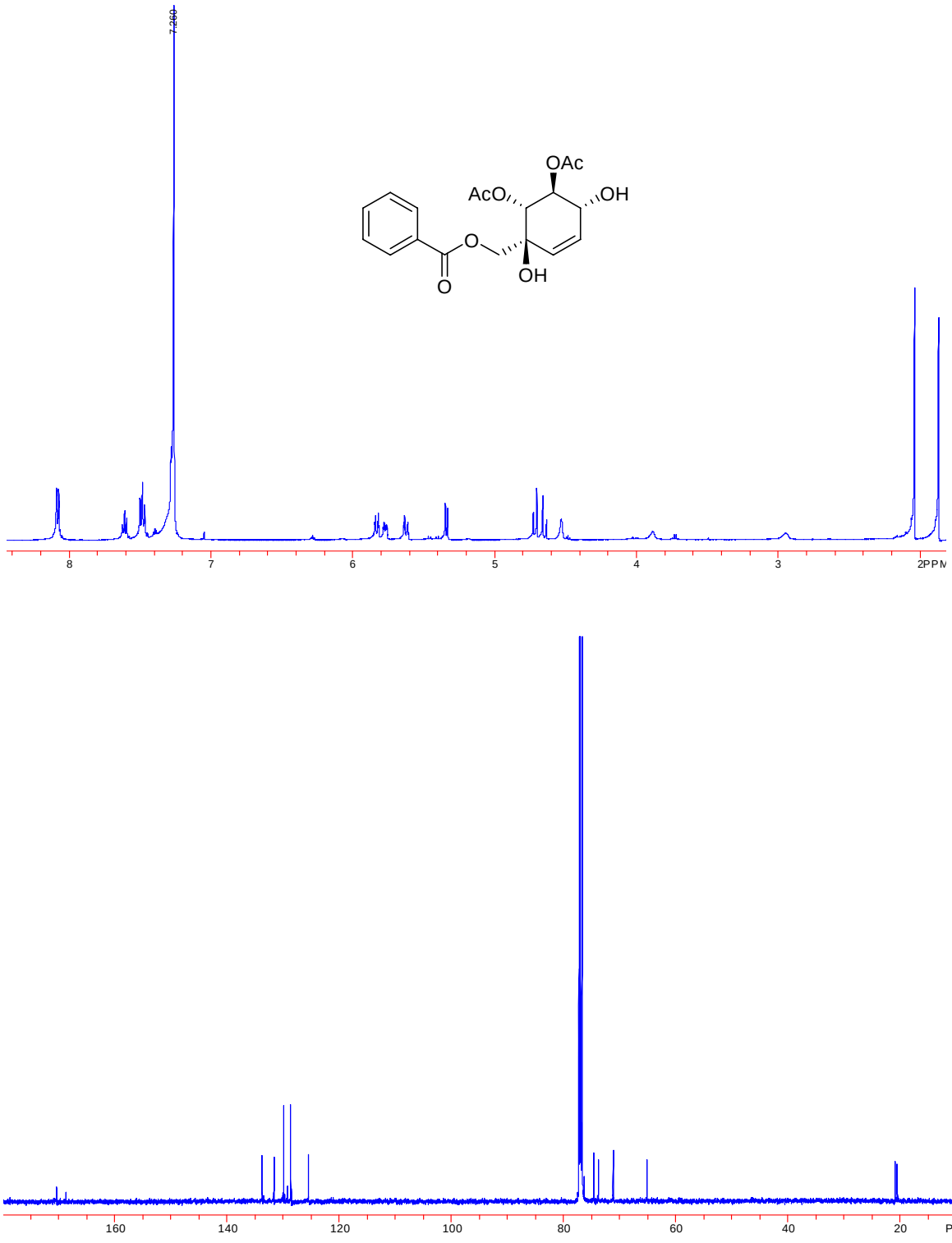

3.2. Melodorinol (in $CDCl_3$)

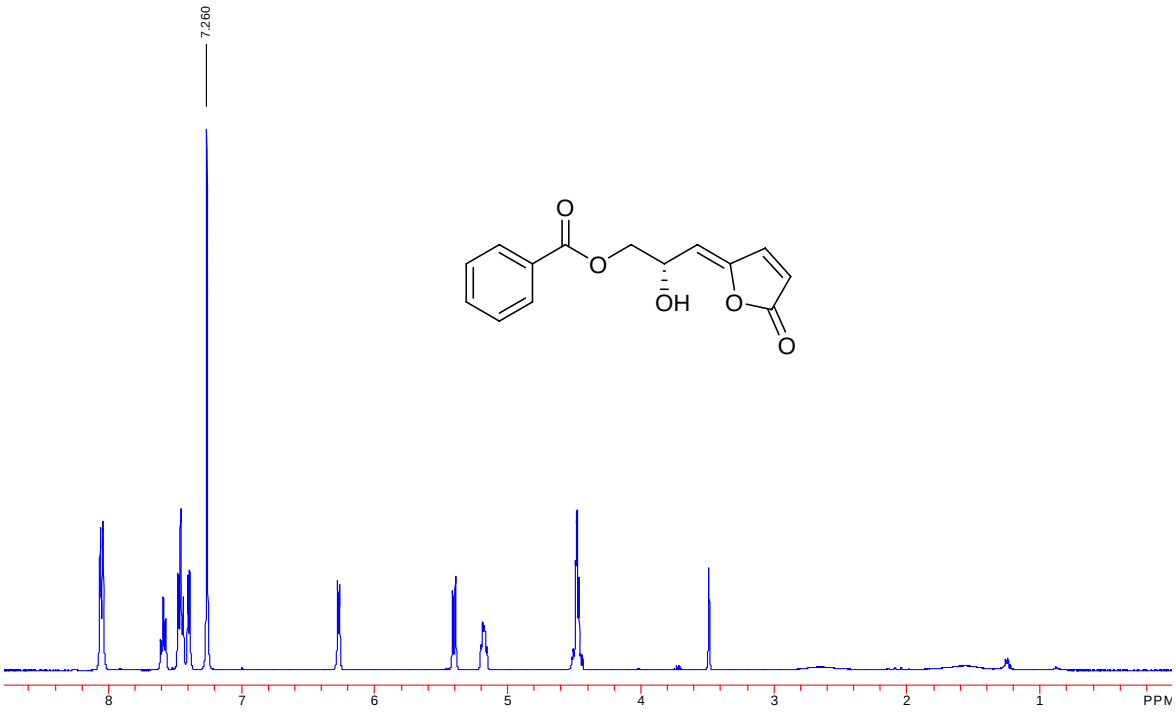

3.3. Acetylmelodorinol (in $CDCl_3$)

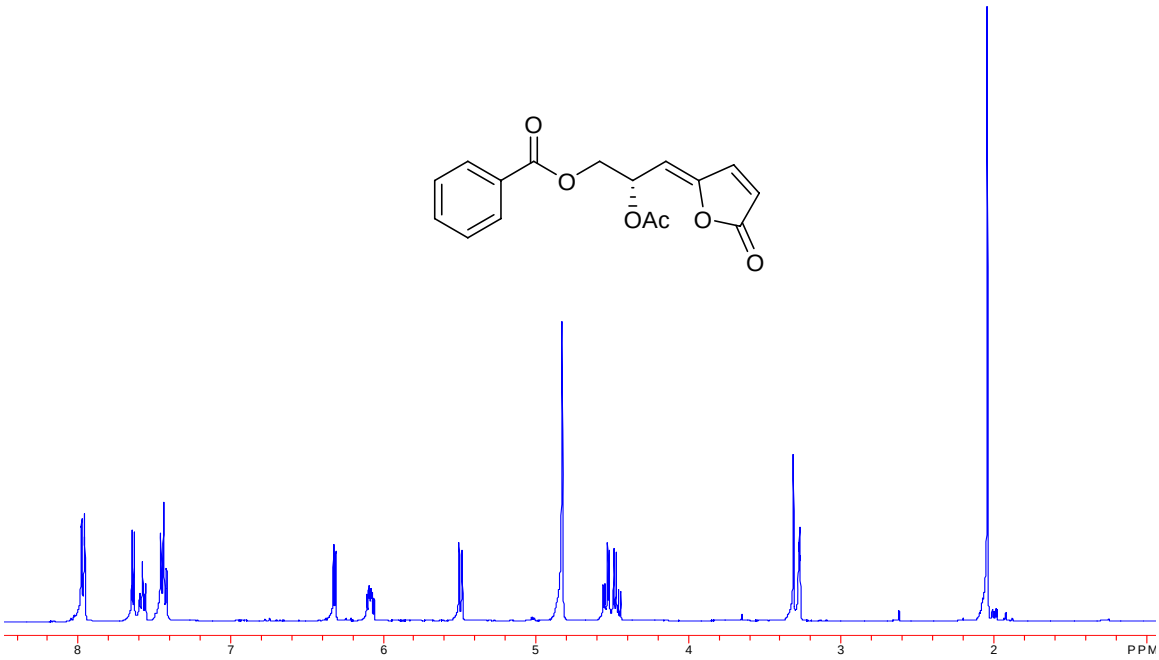

3.4. Polycarpol (in $CDCl_3$)

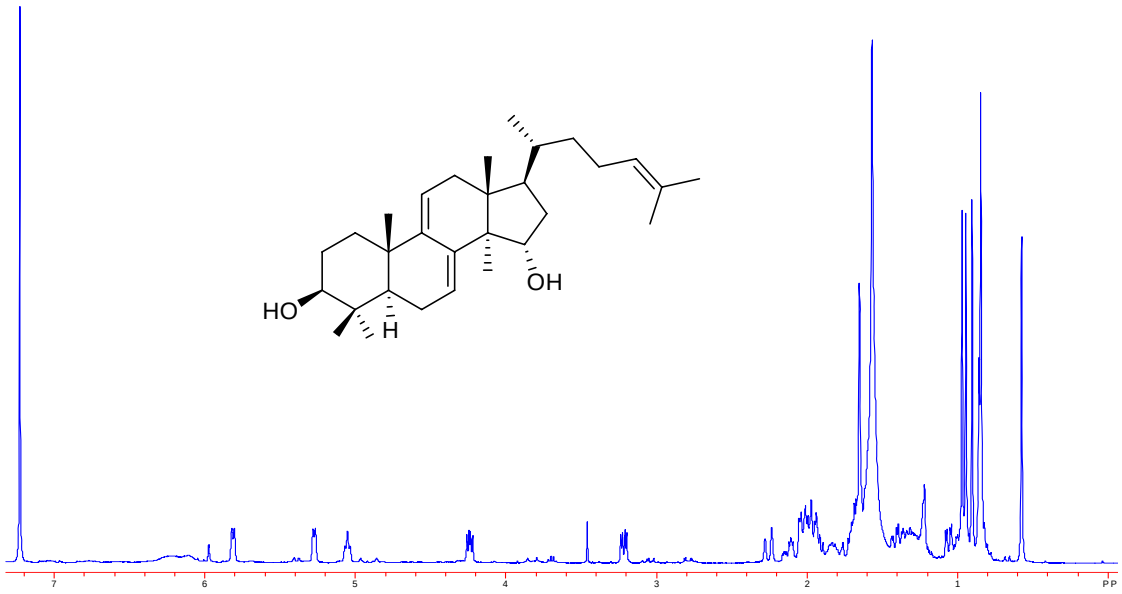

4.1. Malleastrone A (in $CDCl_3$)

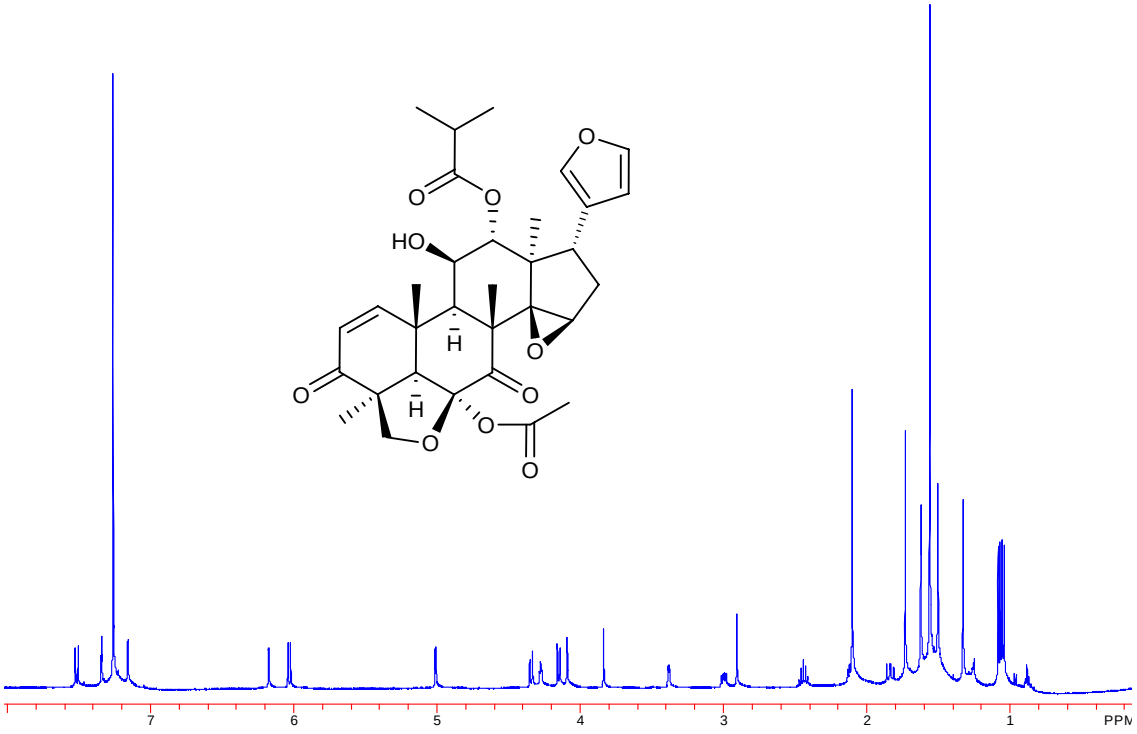

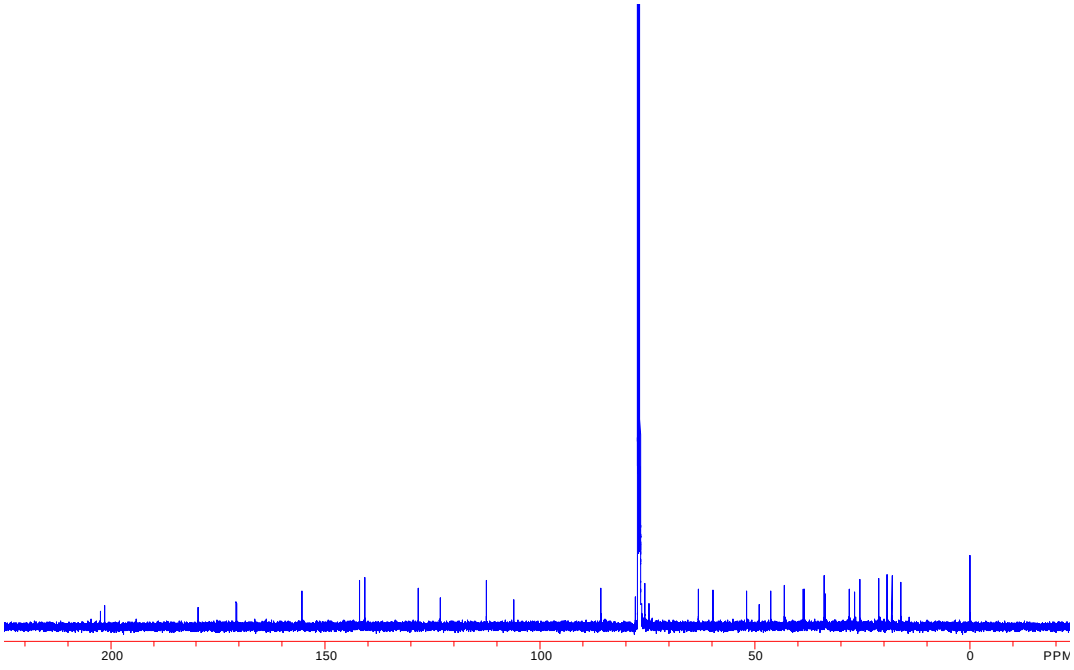

4.2. Malleastrone B (in $CDCl_3$)

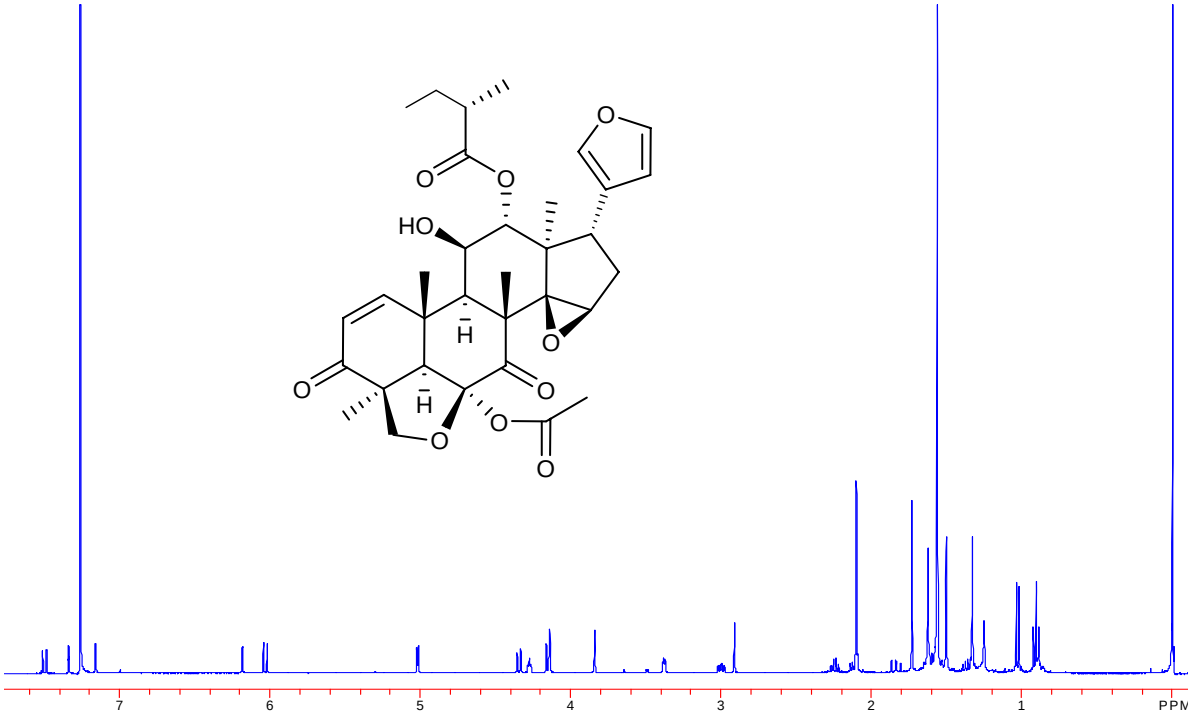

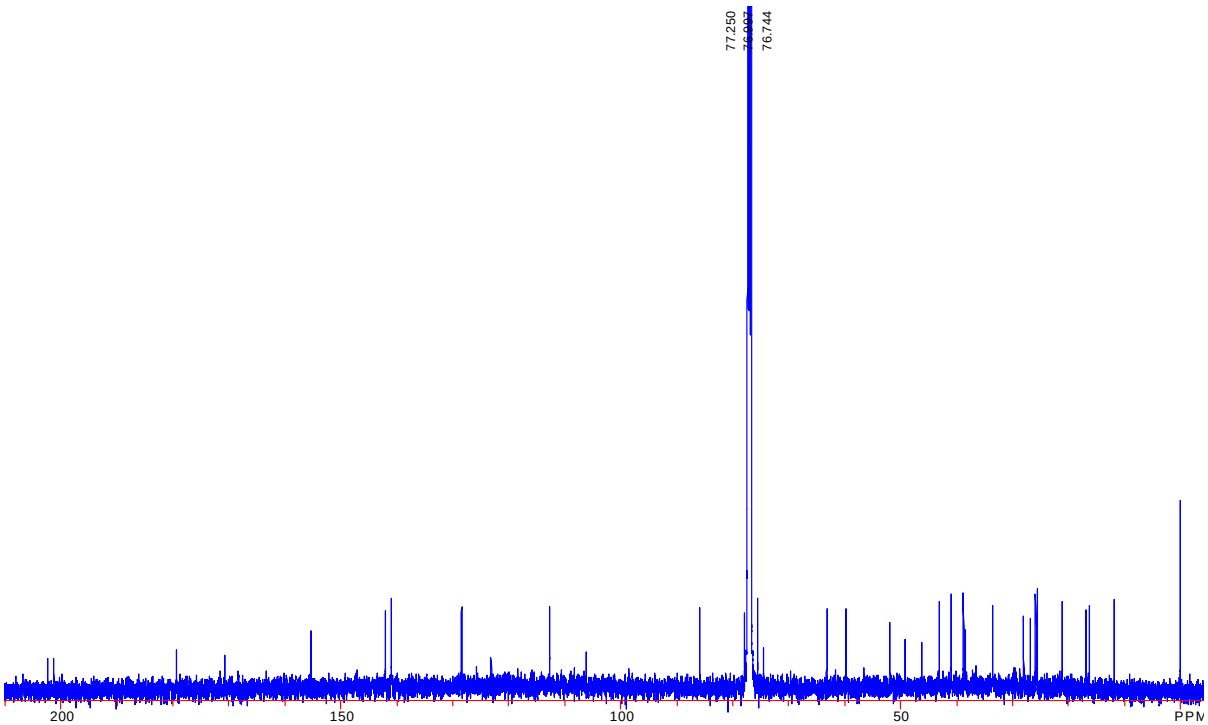

4.3. Malleastrone C (^{1}H in CD_3OD, ^{13}C in $CDCl_3$)

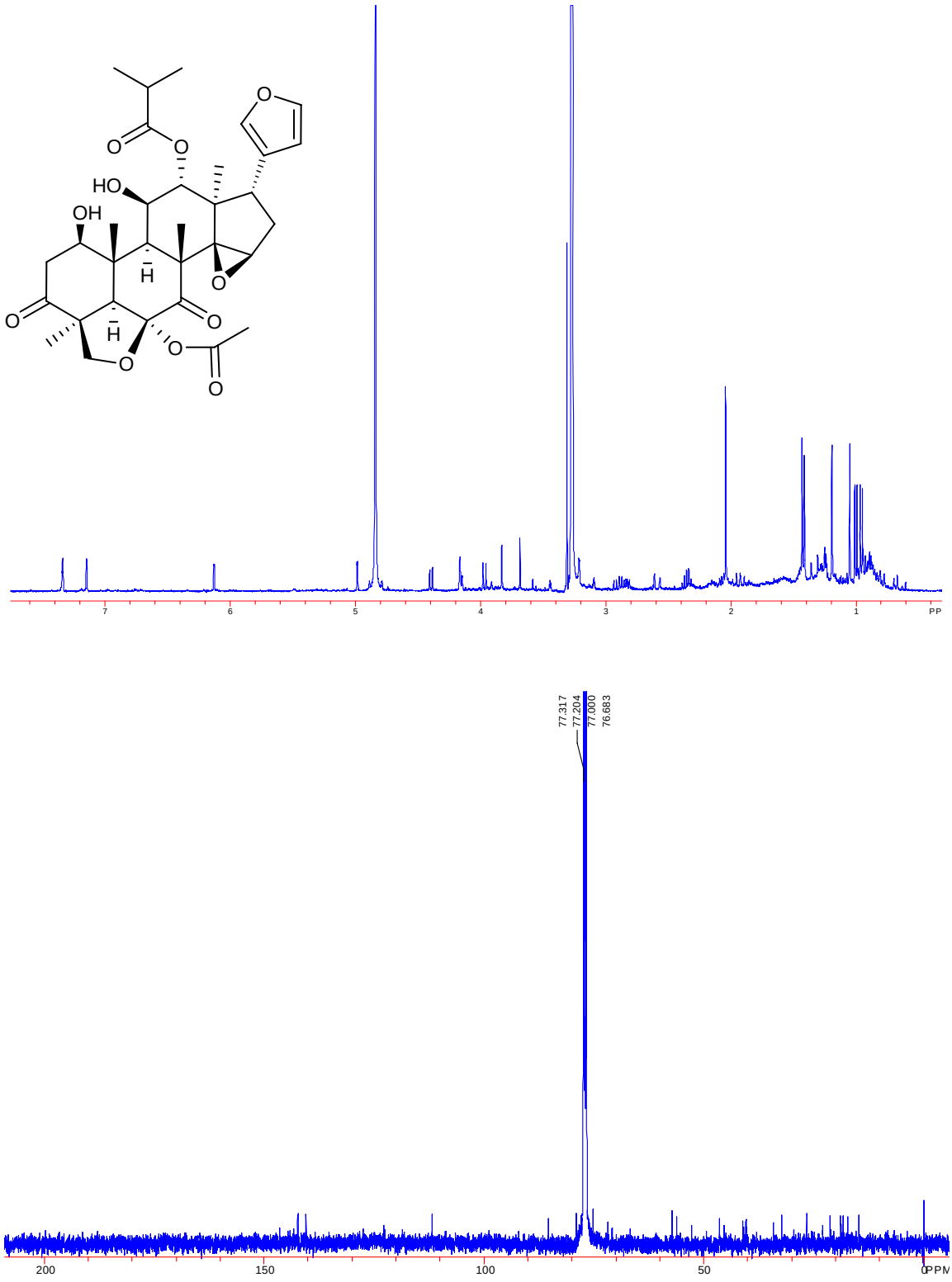

5.1. Bistramide A (in $CDCl_3$)

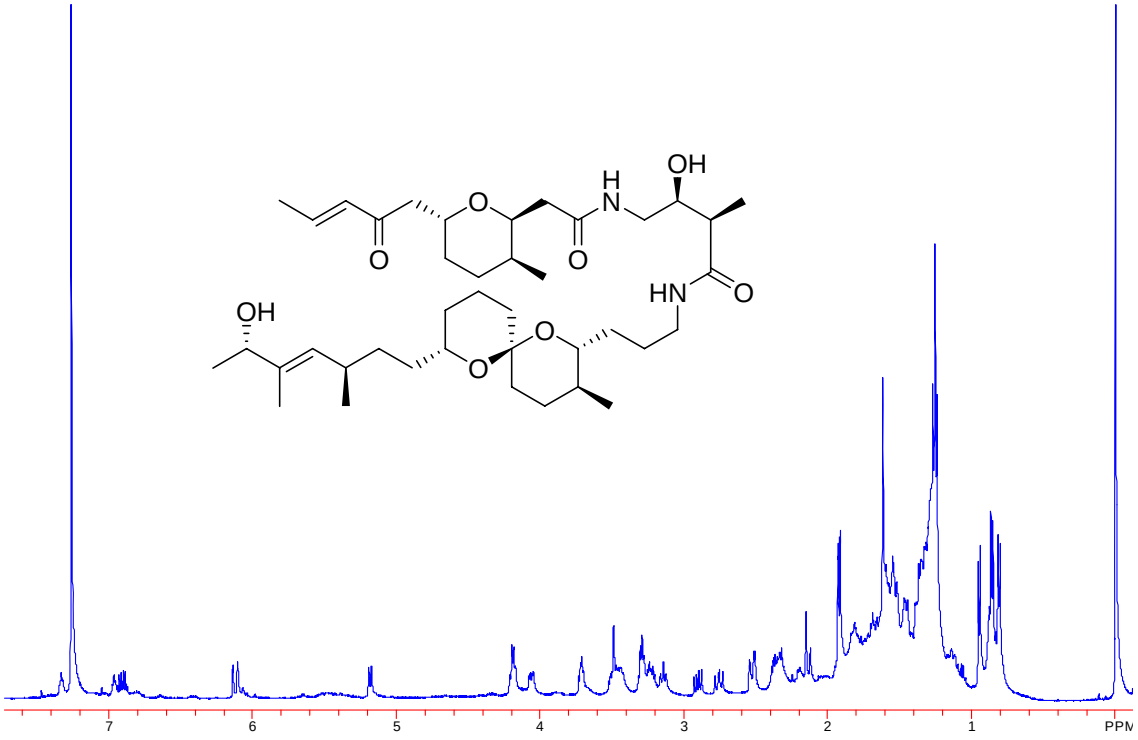

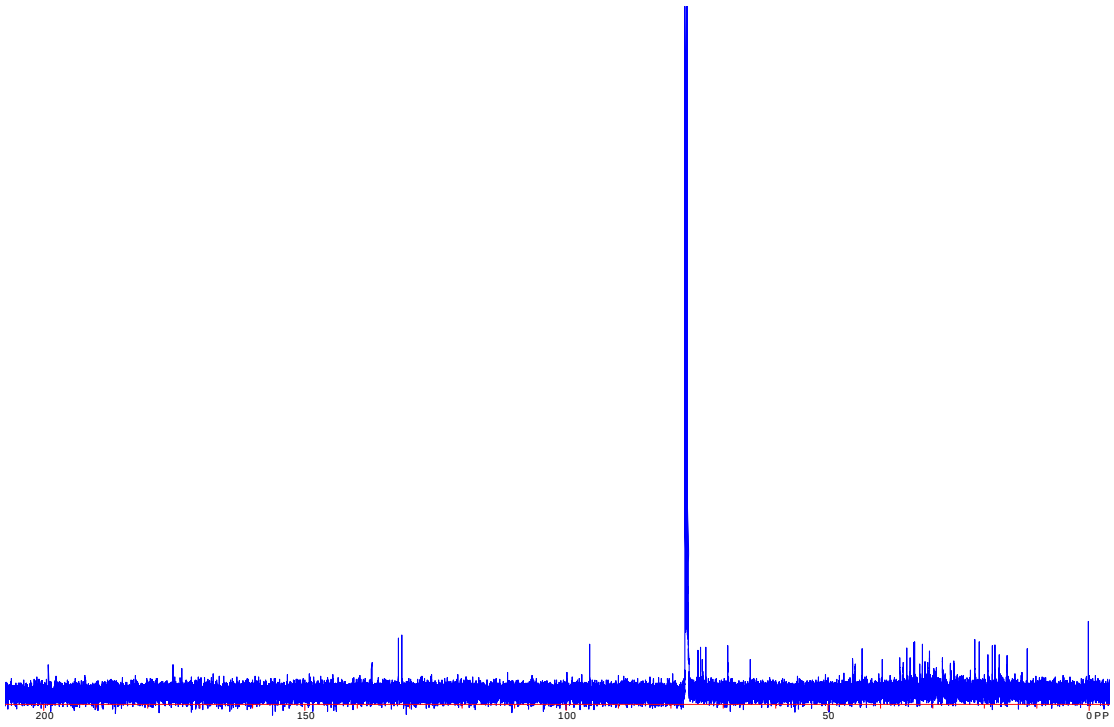

5.2. Bistramide D (in CD_3OD)

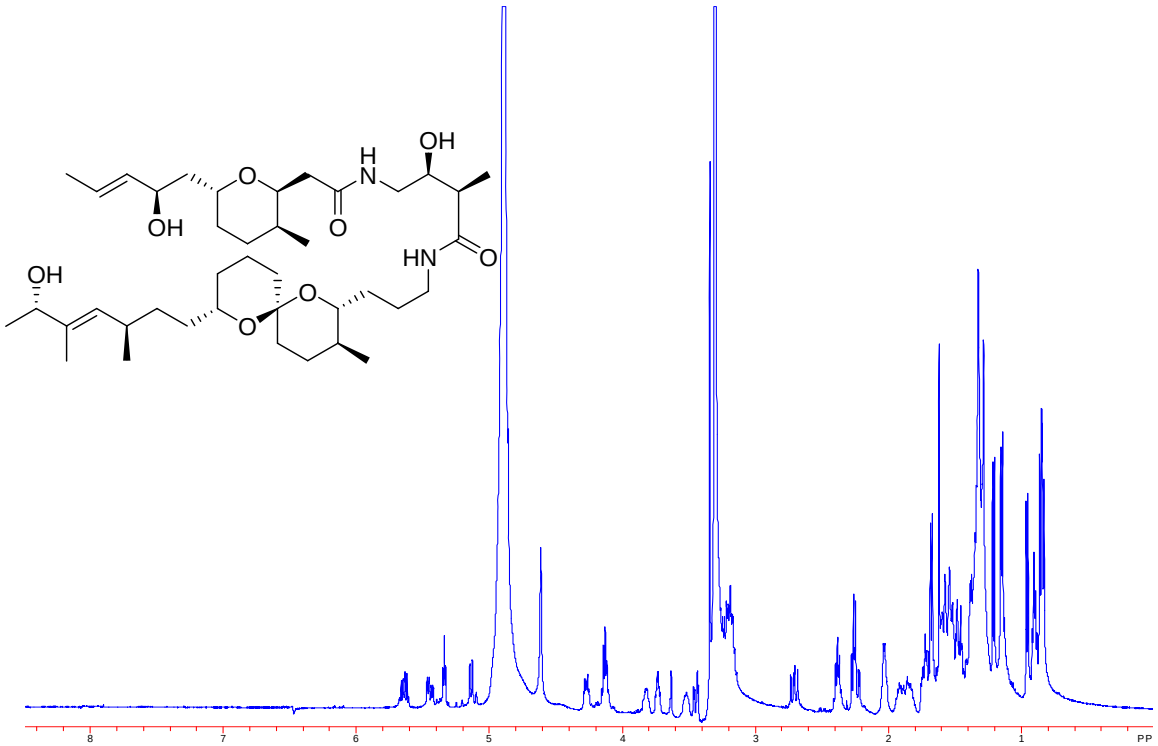

6.1. Cryptomoscatone D1 (in $CDCl_3$)

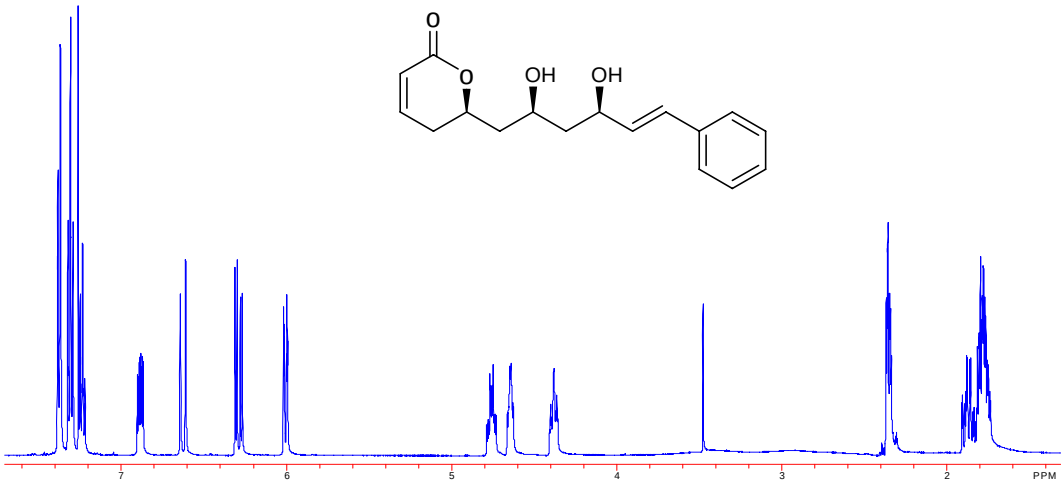

6.2. Kaempferol-3-*O*-α-L-rhamnoside (in CD_3OD)

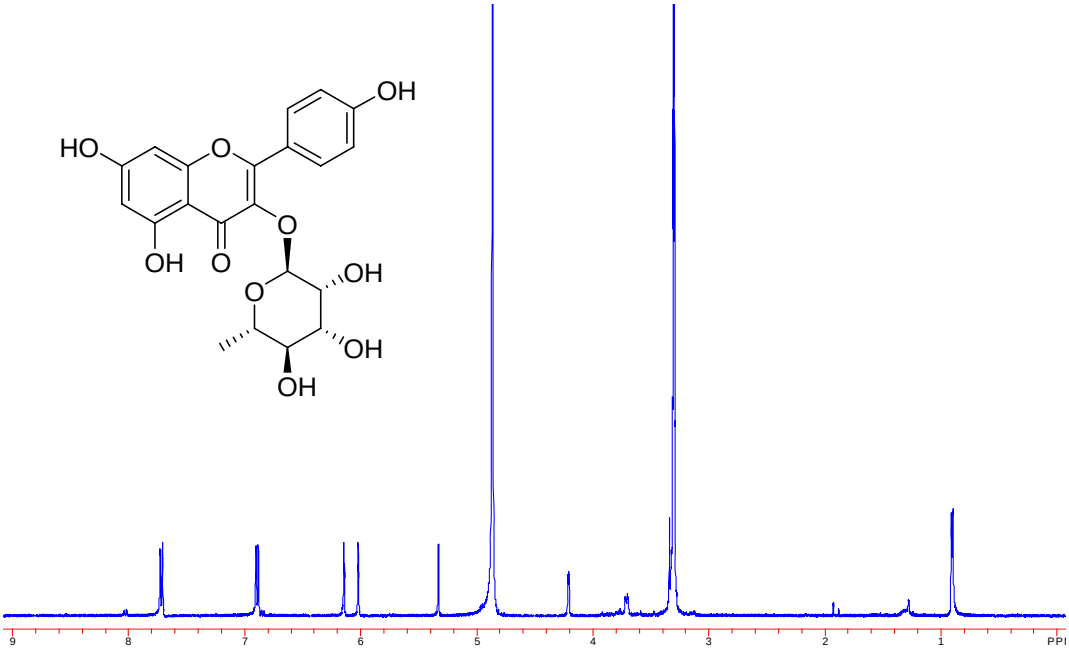

6.3. (+)-Catechin (in CD_3OD)

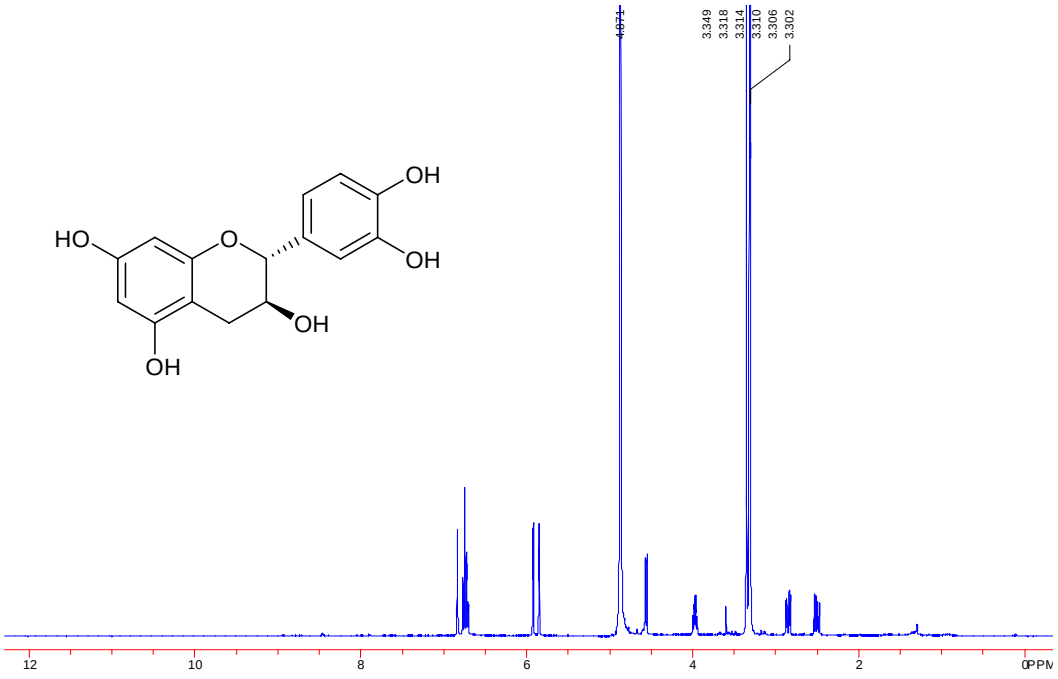

7.3. Benzoquinone (in CD_3OD)

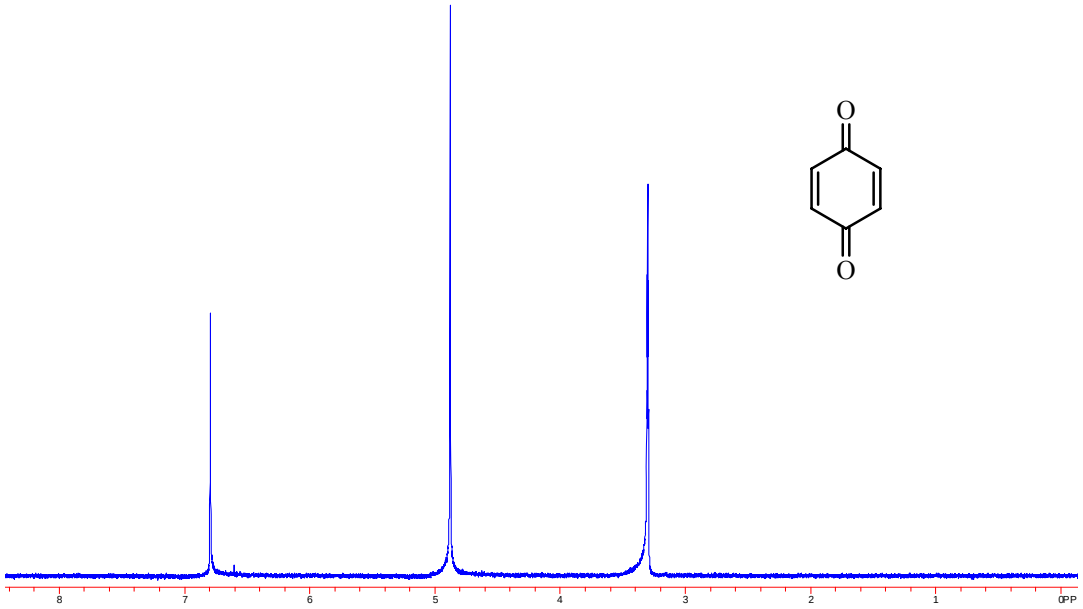

7.4. 1,4-Napthoquinone (in CD_3OD)

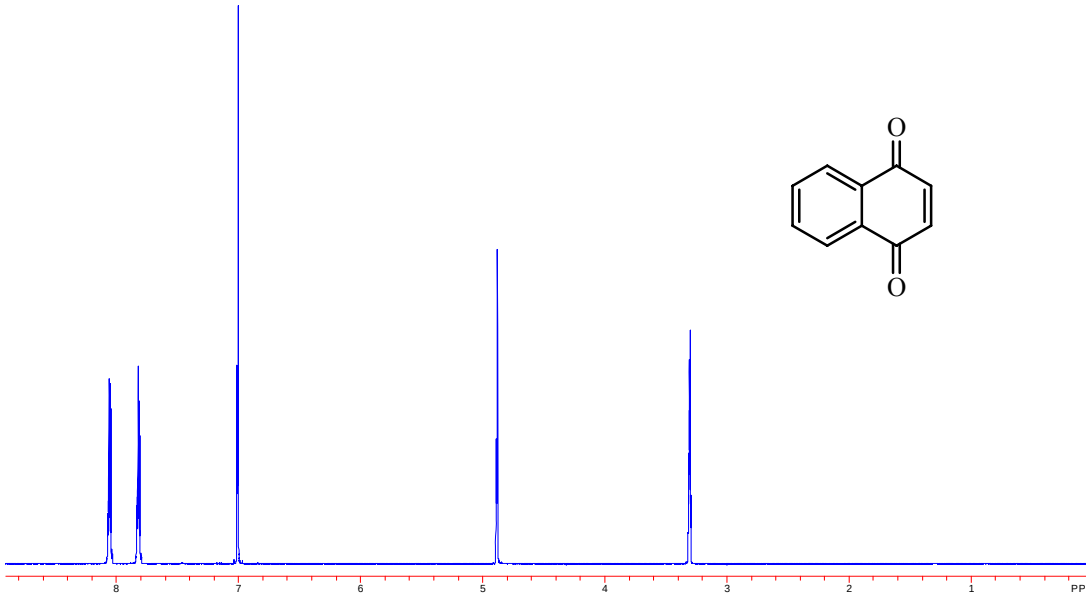

7.5. Anthraquinone (in $CDCl_3$)

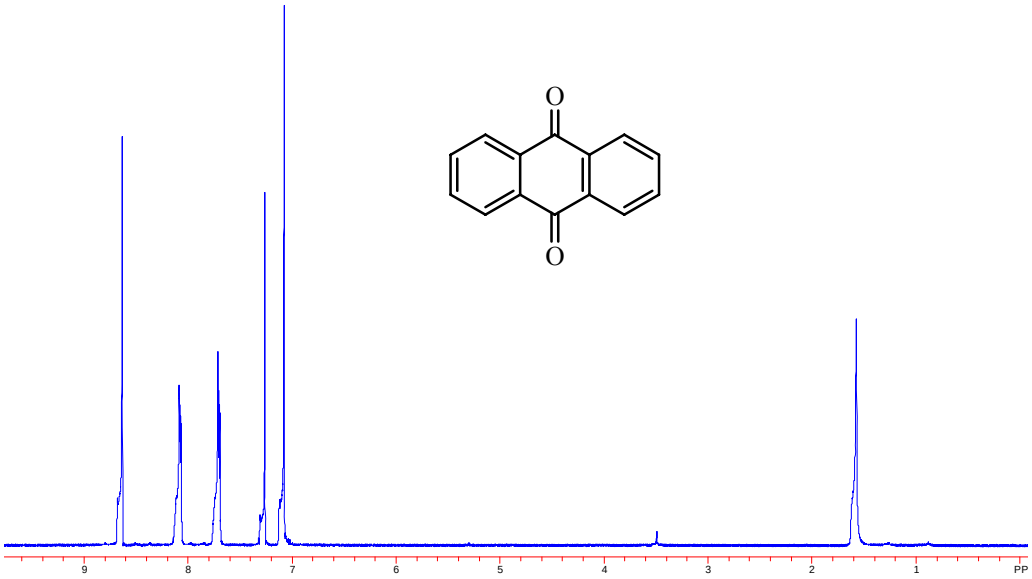

7.6. 2-Methyl-1,4-napthoquinone (in CD_3CN)

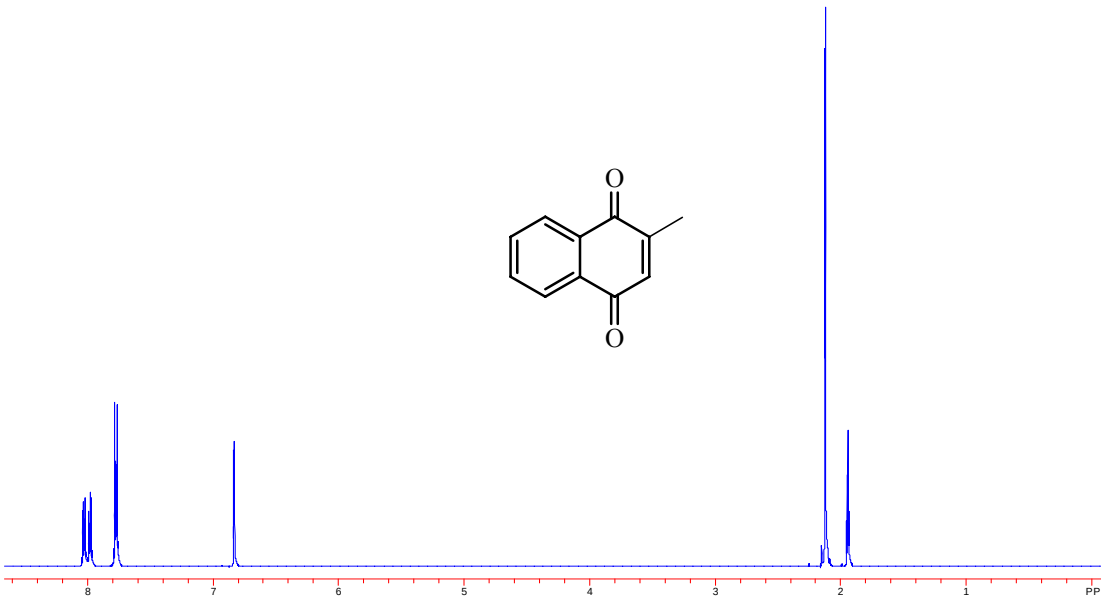

7.7. 5-Hydroxy-1,4-napthoquinone (in CD_3CN)

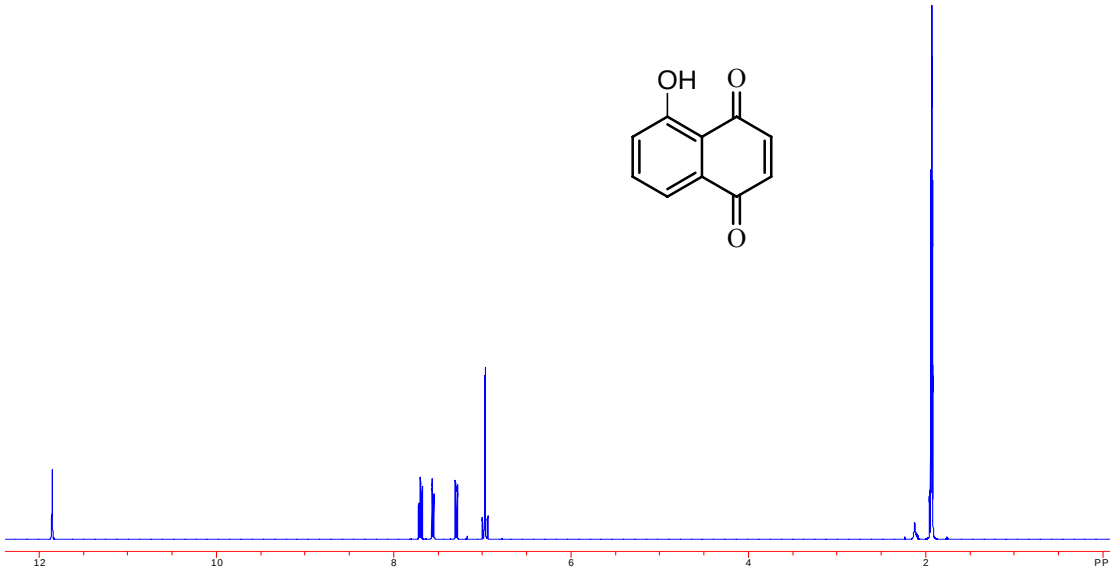

7.8. 5,8-Dihydroxy-1,4-napthoquinone (in CD_3CN)

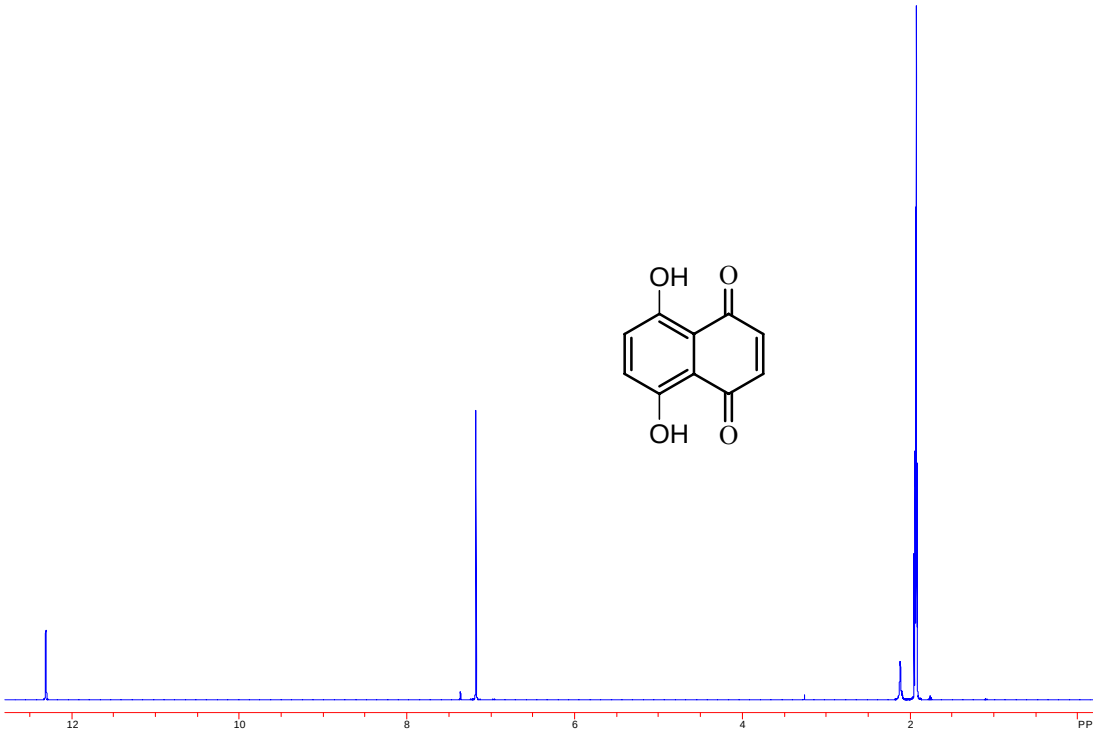

7.10. (in *d*-DMSO)

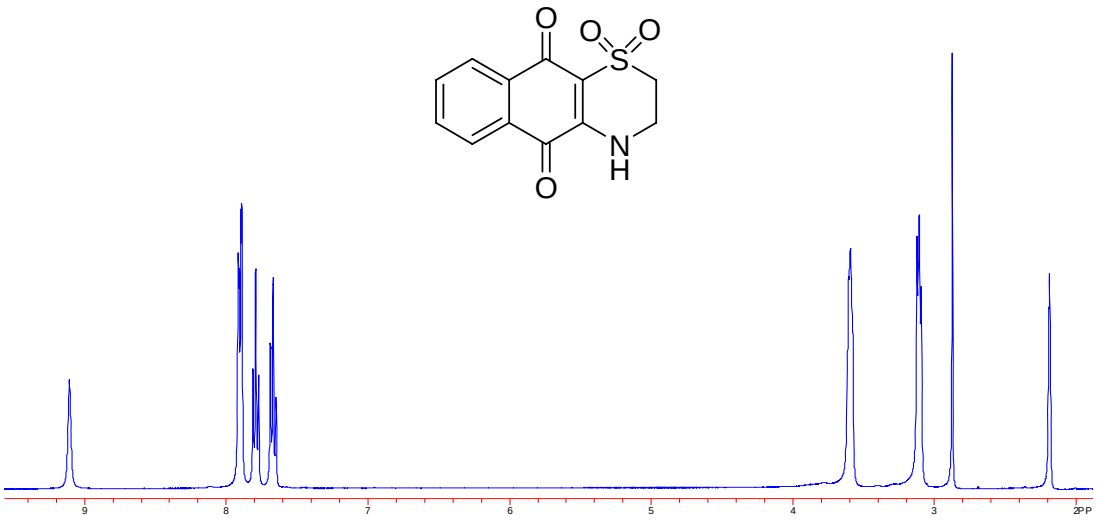

7.11. (in CD_3CN)

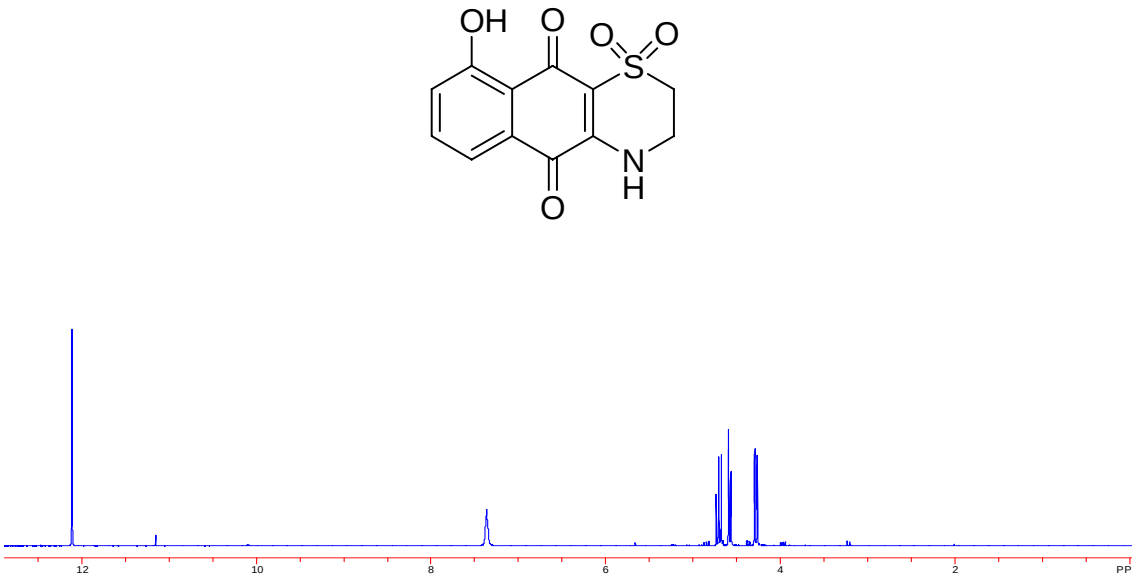

7.12. (in *d*-DMSO)

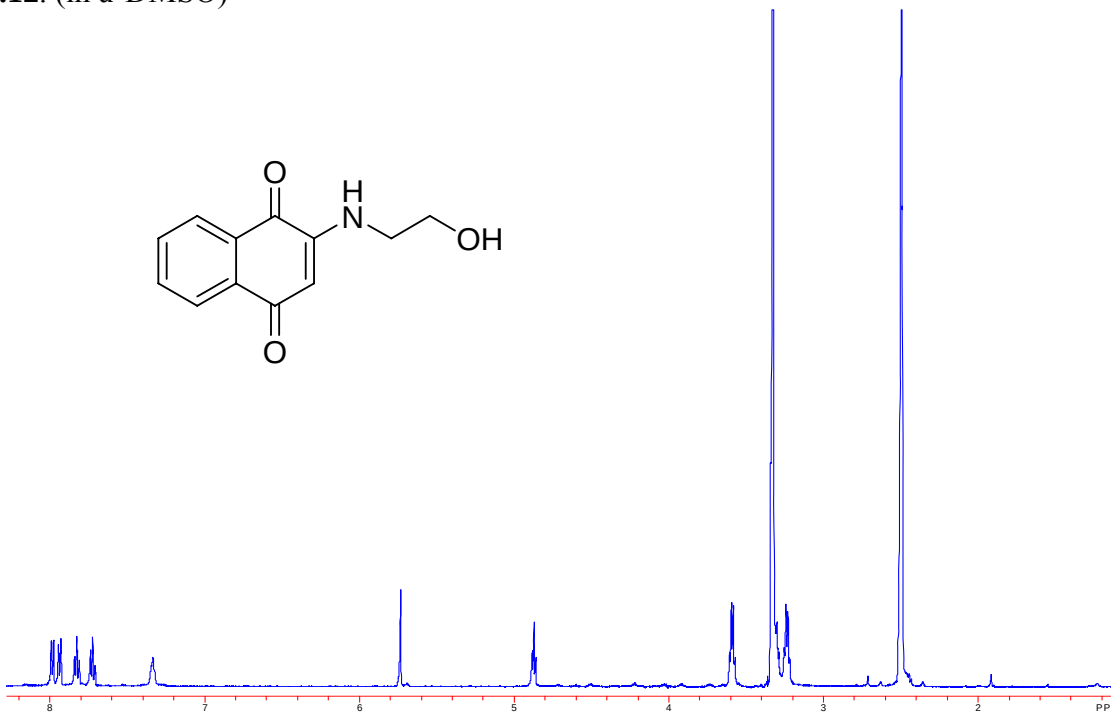

7.13. (in *d*-DMSO)

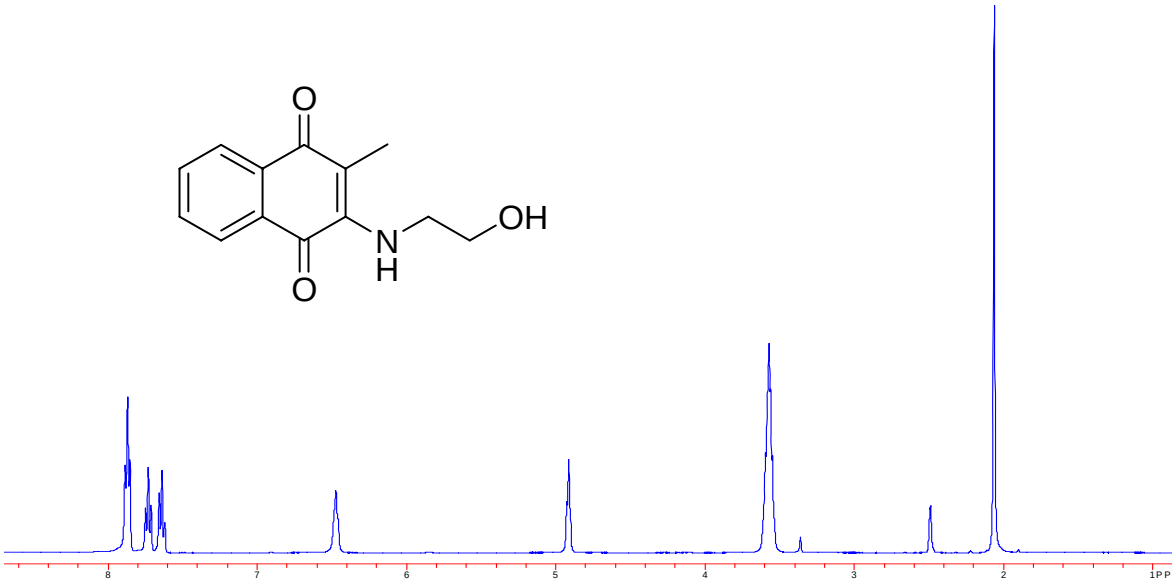

7.14. (in CD_3CN)

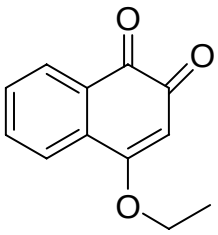

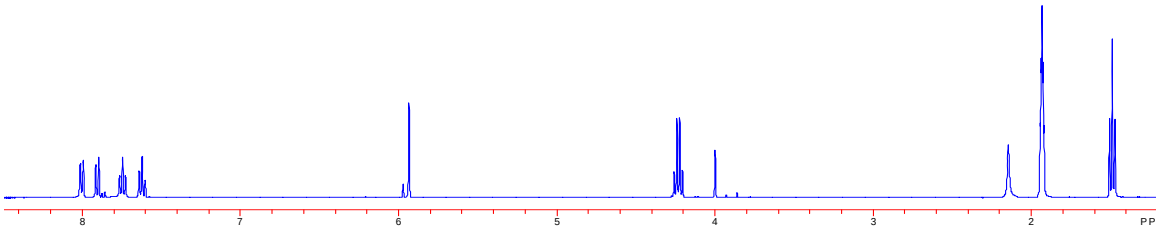

VITA

Brian Thacher Murphy was born in Winthrop, MA. It was in Winthrop by the Sea where he spent his young, adolescent life attending the Winthrop public schools. He was inspired by a chemistry teacher, Mr. Doherty, who taught him how to think beyond traditional means about peculiar substances not visible to the naked eye. In 1998, Brian graduated from Winthrop High School and enrolled in the College of Engineering at the University of Massachusetts, Dartmouth.

After having an outstanding and energetic general chemistry teacher, Brian quickly switched his major to chemistry and shortly thereafter began working for this professor, Dr. Catherine Neto in addition to Dr. Gerald B. Hammond. For three and one-half years his project focused on the isolation and structure elucidation of antioxidants and antitumor agents from *Vaccinium macrocarpon*, or cranberry plant. Such work led to two publications in American Chemical Society (ACS) journals and the contribution of one book chapter in an ACS symposium series book. During this time he received awards from the ACS to present his research at conferences in Orlando, New Orleans, and Dresden, Germany. He was a finalist for the ACS Division of Agriculture and Food Chemistry graduate student research award, and in his final year at UMass Dartmouth was awarded the prestigious Phillip Levins Memorial Prize for excellence in graduate research, sponsored by the ACS. Brian graduated from UMass Dartmouth with his Bachelor's degree in 2002 and Master's degree in 2003.

In an effort to explore his interest in natural products research, in the fall of 2003 Brian began working with Dr. David G. I. Kingston at Virginia Polytechnic Institute and

State University. His project focused on the isolation and structure elucidation of antiproliferative natural products from the rainforests and oceans in Madagascar. Work on several projects led to six publications, four of which he was the first author. He was awarded the Nature's Sunshine travel grant to present his research at an American Society of Pharmacognosy meeting in Corvalis, OR, and gave similar presentations in Arlington (VA), Portland (ME), and Greenville (SC). Through his time at Virginia Tech he was a regular opinions columnist for the newspaper The Collegiate Times, taught free weekly salsa dance lessons to the Virginia Tech community, and avidly sought inspiration through King Ralph and Carlo Rossi. In November of 2007, he received his Ph. D in chemistry.

Brian accepted an offer to do postdoctoral research at the Center for Marine Biotechnology and Biomedicine at the Scripps Institute of Oceanography, under the direction of Professor William Fenical.